

**Molecular Mechanisms of Serotonergic Signaling:
Role in Neuronal Outgrowth and Receptor Oligomerization**

Dissertation

zur Erlangung des mathematisch-naturwissenschaftlichen Doktorgrades

"Doctor rerum naturalium"

der Georg-August-Universität Göttingen

vorgelegt von Fritz Kobe

aus Dresden

Göttingen 2010

This thesis has been written independently and with no other aids and sources than quoted.

Fritz Kobe

Göttingen, March 2010

Referent: Prof. Dr. Michael Hörner

Koreferent: Prof. Dr. Erwin Neher

Tag der mündlichen Prüfung: 30.04.2010

Contents

1 INTRODUCTION	1
1.1 G-Protein coupled receptors.....	1
1.2 G-protein mediated signaling.....	4
1.3 Post-translational modifications of the receptors.....	6
1.4 Serotonin (5-Hydroxytryptamine) receptors.....	7
1.5 Oligomerization of G-protein coupled receptors.....	12
1.6 Aims of the study.....	14
2 EXPERIMENTAL PROCEDURES	16
2.1 Materials.....	16
2.1.1 Chemicals.....	16
2.1.2 Vectors.....	17
2.1.3 Buffers and Solutions.....	17
2.1.4 Antibodies.....	18
2.2 Methods.....	19
2.2.1 Protein Analysis.....	19
2.2.2 Cell culture and transfection.....	21
2.2.3 Electrophysiology.....	24
2.2.4 Behavioral tests.....	26
2.2.5 Confocal imaging and FRET analysis.....	30
3 RESULTS	36
3.1 Functional role of 5-HT7/G12 signaling.....	36
3.1.1 5-HT7 Receptor activation induces formation of dendritic filopodia and new synapses.....	36
3.1.2 Morpho- and synaptogenic effects of the 5-HT7 receptor are mediated by the G α 12 Protein.....	39
3.1.3 Effect of 5-HT7/G12 signaling on EPSCs and spike frequency.....	41
3.1.4 Effects of 5-HT7R/G12 signaling on neuronal morphology in organotypic cultures.....	43
3.1.5 5-HT7R/G12 signaling leads to changes in miniature postsynaptic currents (mPSCs) in organotypic hippocampal slices.....	45
3.1.6 5-HT7R/G12 Signaling modulates neuronal excitability and LTP in organotypic cultures.....	46
3.1.7 In vivo effects of treatment with 5-HT7 receptor antagonist.....	50
3.1.8 Expression of 5-HT7 and G12 proteins is decreased during postnatal development.....	55
3.2 Oligomerization of the 5-HT1A receptor.....	57
3.2.1 Biochemical analysis of 5-HT1A receptor oligomerization.....	57
3.2.2 Acceptor photobleaching analysis of 5-HT1A receptor oligomerization.....	59

3.2.3	Analysis of receptor oligomerization by fluorescence lifetime FRET measurements.	63
3.2.4	Spectrometric detection of FRET between 5-HT _{1A} receptors in living cells.	64
3.2.5	Specificity of 5-HT _{1A} receptor oligomerization.	65
3.2.6	Quantitative analysis of oligomerization dynamics in living cells.....	67
3.2.7	Agonist stimulation and lipid rafts localization of the 5-HT _{1A} receptor.	73
4	DISCUSSION	75
4.1	Role of 5-HT ₇ /G ₁₂ signaling in morpho- and synaptogenesis	75
4.1.1	Early structural and functional changes are modulated via the 5-HT/G ₁₂ pathway	75
4.1.2	Possible function of 5-HT ₇ /G ₁₂ signaling during early postnatal development .	78
4.2	Oligomerization of 5-HT ₁ receptor.....	80
4.2.1	Verification of oligomerization specificity by a novel FRET-based approach.....	81
4.2.2	Regulation of oligomerization by agonist; role of lipid rafts and receptor palmitoylation	83
5	SUMMARY	86
6	REFERENCES	88
7	APPENDIX	100
7.1	Abbreviations	100
7.2	Curriculum vitae.....	102

Acknowledgements

This work would not have been possible with the help and support of many people, teachers, colleagues, friends and family - I owe them a great debt of gratitude.

Foremost I would like to thank my supervisor Professor Evgeni Ponimaskin, who introduced me to the “serotonergic world” and gave me the opportunity to work in this department. He patiently supported, guided and encouraged me throughout the past couple of years. I would also like to take the opportunity to thank Professor Michael Hörner and Professor Erwin Neher who, as members of my thesis committee, provided valuable input and reflections on the progress of my work. I am also grateful to Professor Diethelm W. Richter for having given me the opportunity to continue my work at this institute.

I am indebted to all my collaborators in the department for their invaluable contributions to this work, special thanks go to Dietmar Hess, Lucian Medrihan, Mingyue Zhang, Ute Renner, Andrew Woehler, Jakub Wlodarczyk, Peter Salonikidis, Bao Guobin, Konstantin Glebov, Katja Papoucheva, Michael Müller and Weiqi Zhang. I also would like to thank my external collaborators Konstantin Radyushkin and Ahmed El-Khordi and Hannelore Ehrenreich as well as Sören Westerholz.

Scientific work requires also a big team of people in the background helping to provide the basics to carry out research. We often take this for granted but here I take the opportunity to thank them all for their indispensable work. I thank Gaby Klaehn, Dagmar Crzan, Regina Sommer-Kluß, Peter Funk, Wayne Sidio, and especially the people from the animal facility, Axel, Uwe and Susi.

Very special thanks go to Peter Salonikidis, Andrew Woehler, Bao Guobin, Jakub Wlodarczyk, Ivan Manzini, André Zeug and Matthew Holt who I not only call colleagues but friends and who made lab and life often nicely indistinguishable.

Most of all, I am deeply grateful to my parents, Jutta-Maria and Eberhard, my brother Martin and my sister Katharina for their encouraging and loving support during all this time.

1 INTRODUCTION

One of the most striking phenomena of life is the ability of all organisms to communicate internally as well as externally giving them the opportunity to respond to their environment. This is mostly achieved by cellular receptors, which detect, transduce and signal inside the organism as well as between other cells. These processes are very complex, highly regulated and function in a well-orchestrated manner in order to exert their function. Generally, receptors are classified in five distinct classes (Bockaert and Pin, 1999). The first class combines receptors responsible for the interaction between cells (tyrosine receptors). Communication between cells and the extracellular matrix (e.g. integrin receptors) is realized by second class receptors. The third class comprises tyrosine kinase receptors used as receptors for growth factors. Class four contains the ligand gated ion channels and their task relies on transporting ions across the plasma membrane. However, the most common class of receptors are G-protein coupled receptors (GPCRs). They are the largest family of signaling proteins and represent the best-studied class of receptors due to their importance as a target for the development of therapeutic drugs. GPCRs mediate a wide range of responses predominantly via their interaction with the heterotrimeric guanine nucleotide-binding regulatory protein, termed G-protein. G-proteins exert their action through the modulation of activity of diverse second messengers.

1.1 G-Protein coupled receptors

GPCRs are the largest family of membrane proteins (Lander et al., 2001) and mediate most cellular responses to a variety of ligands, including hormones and neurotransmitters, many other proteins and peptides as well as mechanical stimuli and light. They also play a major role for vision, olfaction and taste (Lindemann, 1996; Hoon et al., 1999; Nelson et al., 2001; Filipek et al., 2003). At the most basic level, all GPCRs are characterized by the presence of seven membrane spanning α -helical segments separated by alternating intracellular and

extracellular loop regions. Both physiological and structural features have been used to classify GPCRs. The most frequently used classification system is based on differences in sequence and divides GPCRs, into four distinct sub-classes: A, B, C and F/S (Horn et al., 1998; Horn et al., 2003). Despite many similarities, individual GPCRs have unique combinations of signal-transduction activities involving multiple G-protein subtypes, as well as G-protein-independent signaling pathways and complex regulatory processes. Hence, it would be more correct to term this super-family “seven transmembrane (TM) receptors,” but the GPCR terminology is more established (Pierce et al., 2002).

The A-family (rhodopsin-like receptors) is the largest and most diverse GPCR family, and its members are characterized by conserved sequence motifs that imply shared structural features and activation mechanisms (Bockaert and Pin, 1999). The common features of this family include the NSxxNPxxY motif in transmembrane domain 7, the DRY motif or D(E)-R-Y(F) at the border between TM3 and intra cellular loop (IL) 2. The structures of the rhodopsin receptors differ from those of adhesion, secretin, frizzled, and glutamate receptors as they have generally a short N-terminus. Now it is widely accepted that receptor ligands bind in a cavity between the TM regions, in contrast to receptors from the other families, where the N-terminus has a key role for the involved ligand binding. However, in several glycoprotein binding receptors (i.e. LH, FSH, TSH, and LG), the ligand-binding domain is localized at the N-terminus. The A family can be divided into four subgroups (Fredriksson et al., 2003) which are named α , β , γ and δ . The α -group includes the amine binding GPCRs, several peptide binding and prostaglandin receptors. The β -group includes the receptors that bind peptides as ligands. The γ -group contains many peptide-binding receptors, such as the chemokine receptors, some receptors that bind neuropeptides such as somatostatins, galanin, and opioids. The δ -group includes the olfactory receptors, purin receptors and glycoprotein receptors.

The receptors of the **B-family (secretin)** have a long N-terminus, which comprises 60-80 amino acids and contains conserved cysteine bridges. The N-terminus is important for the binding of the ligand to these receptors. The secretin receptors bind large peptide ligands that act in a paracrine manner. There are 15 such receptors in the human genome and it

appears that receptors from this family are found in considerable numbers in all vertebrates. Prominent examples of the B type family are secretin, calcitonin, parathyroid hormone/parathyroid hormone-related peptides and vasoactive intestinal peptide receptors, they all activate adenylyl cyclase and the phosphatidyl-inositol-calcium pathway (Gether, 2000).

The C family is composed of eight metabotropic glutamate (mGlu1-8) receptors, two heterodimeric γ -aminobutyric acid B (GABA_B) receptors, a calcium-sensing receptor (CaR), three taste (T1R) receptors, a promiscuous L- α -amino acid receptor (GPRC6A), and five orphan receptors (Bräuner-Osborne et al., 2007). All these receptors, apart from the orphan receptors are characterized by a large amino-terminal domain, which binds the ligands. The eight mGlu receptor subtypes identified to date are divided into three subgroups based on amino acid sequence similarity, agonist pharmacology and G-protein coupling property. Two GABA_B receptors are cloned to date, one is the GABA_{B1} and the other the GABA_{B2}. The C family of GPCRs plays an important role in to the overall synaptic transmission of the major excitatory and inhibitory neurotransmitters in the body. The mGlu receptors are localized almost exclusively in the CNS, whereas the other C family receptors can be found both centrally and in peripheral tissues (Bräuner-Osborne et al., 2007).

The F Family (frizzled/taste 2 receptors) is a more recently identified group of GPCRs. The frizzled receptors control cell fate, proliferation, and polarity during metazoan development by mediating signals from the secreted glycoproteins Wnt. The frizzled receptors have about 200 amino acid long N-termini with conserved cysteins that are likely to participate in Wnt binding. The role and function of the taste 2 (TAS2) receptors is not very well understood, but it is known that they are expressed in the tongue and palate epithelium and they are likely to function as bitter taste receptors (Chandrashekar et al., 2000)

In vertebrates, GPCRs plays a wide and pivotal role in organism functioning and are often involved in many disorders such as allergies, depression, cancer, obesity, pain, diabetes and many others (Lundstrom, 2005; Tang and Insel, 2005; Thompson et al., 2005). Therefore, they serve as major pharmacological targets to treat pathophysiological conditions (Bockaert and Pin, 1999; Angers et al., 2001; McCudden et al., 2005; Thompson et al., 2005). Three

quarters of therapeutic drugs on the market target GPCRs and have therefore an enormous importance and economic potential for the pharmaceutical industry (Lundstrom, 2005).

1.2 G-protein mediated signaling

Heterotrimeric G proteins play an important role as molecular switches in signal transduction pathways mediated by GPCRs. Heterotrimeric G proteins are composed of three subunits, α , β and γ . The $G\alpha$ are divided into four main classes based on the similarity of the primary sequence: $G\alpha_s$, $G\alpha_i$, $G\alpha_q$ and $G\alpha_{12}$. The molecular weight of $G\alpha$ subunits varies between 39 and 45 kDa. All $G\alpha$ subunits, excluding the $G\alpha_t$ or transducin, also contain palmitate, which is reversibly attached to a cysteine at the N-terminus. Fatty acid modifications are essential for $G\alpha$ subunit membrane localization (Peitzsch and McLaughlin, 1993). Depending on their α subunits, G-proteins activate different second messenger cascades.

The switching function of heterotrimeric G proteins depends on the ability of the G protein α -subunit ($G\alpha$) to cycle between an inactive GDP-bound conformation that is set for interaction with an activated receptor, and an active GTP-bound conformation that can modulate the activity of downstream effector proteins. In practical terms, after ligand binding, the receptor undergoes conformational change. This promotes the coupling with heterotrimeric G proteins ($G\alpha\beta\gamma$) and catalyzes the exchange of GDP by GTP on the α -subunit, leading to dissociation and conformational changes between α - and $\beta\gamma$ -subunits. Now the GTP-bound $G\alpha$ -subunit and the $G\beta\gamma$ -dimer can modulate the activity of various effectors.

$G\alpha_s$ -proteins activate adenylyl cyclase, which then produces cAMP, which further activates cAMP-dependent protein kinases (Sutherland and Rall, 1958).

$G\alpha_i$ -proteins inhibit adenylyl cyclase, leading to a decrease in intracellular cAMP levels (Emerit et al., 1990; Barnes and Sharp, 1999).

$G\alpha_q$ -proteins activate phospholipase C (PLC) (Blank et al., 1991). PLCs hydrolyze the phosphoester bond of the plasma membrane lipid phosphatidylinositol 4,5-bisphosphate, generating the ubiquitous second messengers inositol 1,4,5-trisphosphate (Ins(1,4,5)P₃) and diacylglycerol (DAG).

Gα12/13 proteins. The G12-protein family consists of the ubiquitously expressed G12 and G13 subunits (Strathmann and Simon, 1991). Prominent downstream effectors in G12-mediated signaling are the members of the Rho family of small GTPases (Rho, Rac, and Cdc42), which regulate a variety of cellular activities by controlling the actin cytoskeleton or gene expression (Hall, 1998). In this study we have analyzed effects modulated by G12/13 proteins. Previous research being done in our lab demonstrated that the serotonin receptor 5-HT7 can activate heterotrimeric G12 protein, leading to the selective activation of small GTPases RhoA and Cdc42 changing morphology and cytoarchitecture of the cells (Kvachnina et al., 2005; Ponimaskin et al., 2007).

βγ-subunits: So far more than 5 different β and 12 γ subunits have been described, (McCudden et al., 2005). The variation of the Gβ/γ subunits is wider than in Gα, ensuring a higher number of potential combinations of Gβ/γ dimers. It is known that all γ subunits are post-translationally modified by prenylation of the C-terminus (Wedegaertner et al., 1995), acting as a membrane anchor attached to the cell membrane. Previously, it has been suggested that Gβ/γ dimers serve as adaptors to promote coupling of G-protein heterotrimers to GPCRs, in addition to its function as Gα inhibitor. The role of Gβ/γ dimers as adaptors is well documented but they can also directly activate many effectors. One of the first described partner for the Gβ/γ dimer was the G-protein regulated inward rectifier K⁺ channels (GIRK) (Logothetis et al., 1987) and until now there is evidence that Gβ/γ dimers regulate Ca²⁺ channels, PLCβ, p38 mitogen activated protein kinases (MAPKs), MAPK scaffold proteins, as well as involvement in membrane attachment of the small GTPases Rho and Rac. It has also been shown that adenylyl cyclases are not only governed by Gα, but also by Gβ/γ heterodimer (Faure et al., 1994; Coso et al., 1996; Harhammer et al., 1996; Akgoz et al., 2002; Sunahara and Taussig, 2002; Woehler and Ponimaskin, 2009).

1.3 Post-translational modifications of the receptors

Like many proteins, GPCRs are subject to a variety of post-translational modifications that are an essential part in regulating their activities. These post-translational modifications include:

glycosylation, is the addition and processing of an oligosaccharide to either asparagine, hydroxylysine, serine, or threonine, resulting in a glycoprotein. This is an important prerequisite for proteins to fold correctly.

phosphorylation, describes the reversible process of adding a phosphate group to protein, usually to serine, tyrosine, threonine or histidine residues within the cytoplasmic receptor domains. Phosphorylation is a key mechanism leading to conformational changes of proteins turning receptors from an activated into an inactivated state.

methylation, this is a process where a methyl group is added to lysine or arginine residues. Methylation plays a role in the regulation of gene expression, regulation of protein function and RNA metabolism.

palmitoylation, is the addition of palmitate through a thioester linkage to cysteine located within the receptor terminus (Towler et al., 1988). Most commonly palmitoylation is linked to membrane association of otherwise soluble proteins (Smotrys and Linder, 2004). However, the function of palmitoylation ranges far beyond that of membrane anchoring. Palmitoylation together with other lipid modifications and protein motifs also facilitate protein targeting to appropriate cellular destinations (Brown and London, 1998). Interestingly, palmitoylation is the only reversible lipid modification, suggesting that palmitoylation and depalmitoylation of proteins could have important functional consequences for signaling (Linder and Deschenes, 2003; Smotrys and Linder, 2004). In G-proteins coupled receptors (GPCRs) palmitoylation plays an important role in processes ranging from coupling to G-proteins and regulated endocytosis to receptor phosphorylation and desensitization (Ross, 1995; Mumby, 1997; Dunphy and Linder, 1998). Moreover, palmitoylation of several GPCRs has been shown to play a central role in the regulation of receptor function. Recent studies on rhodopsin indicate that its depalmitoylation enhances light-dependent GTPase activity of G_t and strongly decreases the light-independent activity of opsin (Mulheron et al., 1994; Garnovskaya et al.,

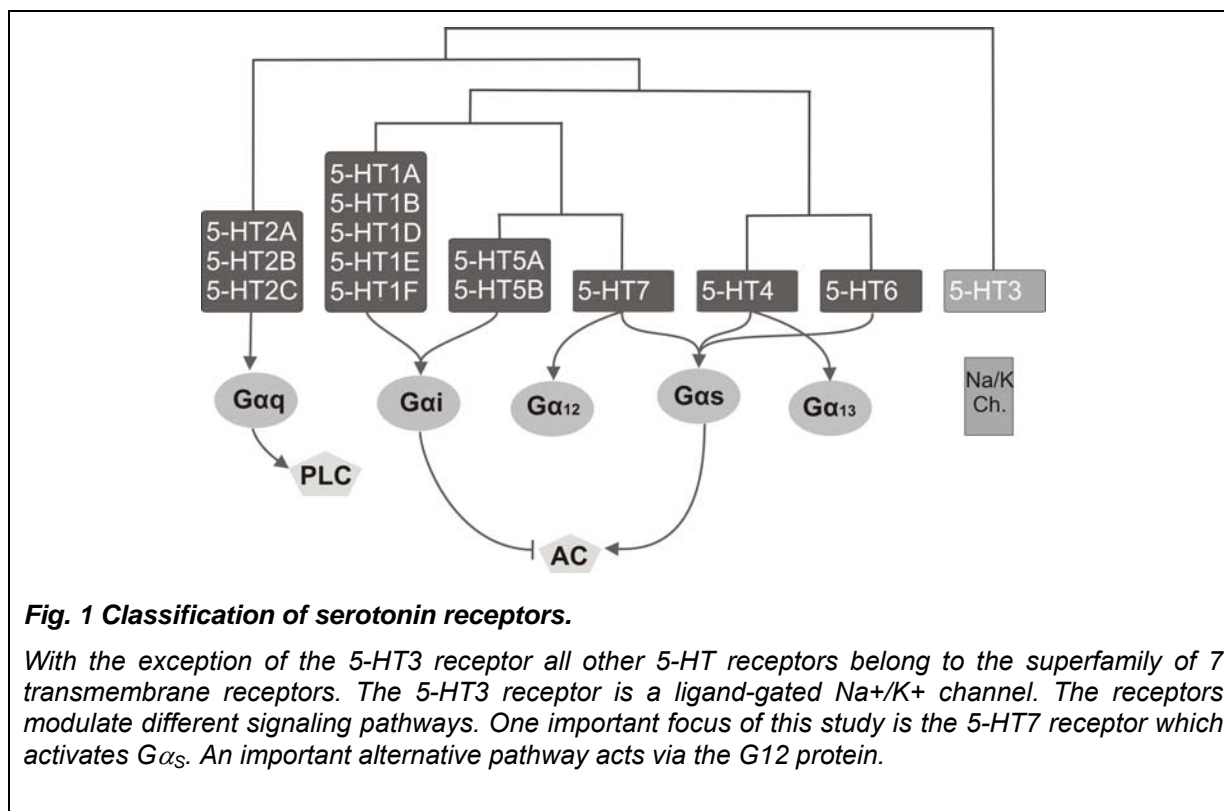
1996). The functional characterization of non-palmitoylated β 2-adrenergic and endothelin-B (ET_B) receptors has revealed that palmitoylation is essential for agonist-stimulated coupling to G_S and to both G_{q-} and G_i proteins, respectively. Analysis of the non-palmitoylated ET_A receptor mutant demonstrated that ligand-induced stimulation of G_S was unaffected by the lack of palmitoylation, whereas signaling through G_q was prevented. Recent data on chemokine CCR5 and prostacyclin receptors also demonstrated that receptor palmitoylation is involved in the activation of intracellular signaling pathways.

1.4 Serotonin (5-Hydroxytryptamine) receptors

Serotonin (5-hydroxytryptamine; 5-HT) is a neurotransmitter acting via membrane receptors in the central nervous (CNS) and the peripheral nervous system (PNS), as well as in non-neuronal tissues (e.g. blood, gastro-intestinal, endocrine, sensory and cardiovascular systems). 5-HT is one of the oldest neurotransmitter in evolution, and its receptors are estimated to have appeared 700–800 million years ago in eukaryotes (Hoyer et al., 2002). The major classes of 5-HT receptors must have diverged about 750 millions years ago, long before cholinergic, adrenergic or dopaminergic receptors (Hoyer et al., 2002).

Serotonin was first described as enteramine and was isolated from the gut in the 1930s by Erspamer et al. (Erspamer and Asero, 1952) and showed to cause contraction of the uterus. 5-HT was rediscovered in the 1940s by Irvin Page's group in the circulation and called serotonin, based on its vasoconstrictor features (Rappport et al., 1948). Maurice Rappport purified, crystallized and characterized the molecule from blood. Rappport also found that enteramine and serotonin were in fact the same, namely 5-hydroxytryptamine (Rappport et al., 1948).

Serotonin acts via specific receptors which belong, with the exception of the 5-HT₃ receptors (ligand gated ion channels), to the GPCR superfamily. Serotonin receptors are classified into 7 classes and are then further subdivided into 14 subtypes based on their pharmacology, transduction, sequence and structure (Kroeze et al., 2002; Kroeze et al., 2003; Meneses, 2008; Kamiyama and Chiba, 2009).



The 5-HT1 receptor class is to date the best characterized 5-HT receptor which consists of five receptors isoforms (5-HT1A, 5-HT1B, 5-HT1D, 5-HT1 and 5-HT1F). They share 40-63 % overall sequence identity in humans and preferentially couple to G_{i/o} to inhibit the formation of cAMP. It has been shown that the 5-HT1 receptor plays a major role in the pathophysiology of anxiety and depression (Delgado et al., 2005; Fricker et al., 2005; Dawson et al., 2006).

There are 3 types of **5-HT2 receptors**, 5-HT2A, 5-HT2B and 5-HT2C receptors. These receptors couple preferentially to G_{q/11} proteins and modulate intracellular inositol phosphates and Ca²⁺ concentrations (Canton et al., 1996), 1996). They are best known for their role in muscle contraction and temperature control (Barnes and Sharp, 1999).

The **5-HT3 receptor** belongs to the ligand-gated ion channel superfamily, similarly to the nicotinic acetylcholine, glycine or GABA-A receptors. The receptor is located on central and peripheral neurons and triggers rapid depolarization due to opening of non-selective cation channels (Na⁺, Ca²⁺ influx, K⁺ efflux (Blier and Bouchard, 1993). The 5-HT3 receptors can be found in different brain regions, such as the CA1 pyramidal cell layer in the hippocampus, the dorsal motor nucleus of the solitary tract and the area postrema (Laporte

et al., 1992). Peripherally, they have also been identified on pre- and postganglionic autonomic neurones and on neurones of the sensory nervous system. Additionally 5-HT₃ receptor activation throughout the GI tract regulates both motility and intestinal secretion (De Ponti and Tonini, 2001).

The **5-HT₄** receptors are preferentially coupled to G_s and promote cAMP formation by activation of various isoforms of adenylyl cyclases. For the 5-HT₄ receptor, at least 8 splice variants are known. In addition to coupling to the G_s, the 5-HT₄(b) receptor is also associated with the G_{i/o} protein. The 5-HT₄(a) receptor is also known to activate G13 signaling pathway leading to activation of the RhoA small GTPase (Ponimaskin et al., 2002a). In the CNS, 5-HT₄ receptors modulate neurotransmitter (acetylcholine, dopamine, serotonin and GABA) release and enhance synaptic transmission, whereas in the GI tract the receptor acts as modulator on motility. Furthermore the 5-HT₄ receptor is also involved in mediating secretory responses to 5-HT in intestinal mucosa. The 5-HT₄ receptor plays a role in learning and memory as well as in the respiratory cycle (Barnes and Sharp, 1999; Manzke et al., 2003; King et al., 2008).

The function of the **5-HT₅ receptor** remains unclear. Within the CNS the 5-HT_{5A} receptor shows a relatively broad distribution, while the 5-HT_{5B} receptor has a very restricted distribution. The 5-HT_{5A} receptor has been demonstrated to couple to G proteins, and the primary coupling appears to be through G_{i/o} inhibiting adenylyl cyclase activity. The 5-HT_{5B} receptor is expressed in mice and rats, but not humans, where the coding sequence is interrupted by stop codons.

The **5-HT₆ receptor** is positively coupled to adenylyl cyclase via the G_s protein. It is located in the striatum, amygdala, nucleus accumbens, cortex and the olfactory tubercle. However, it can also be found in the stomach and in the adrenal glands. Functionally the 5-HT₆ receptor is involved in regulating cognition (Barnes and Sharp, 1999; Ballaz et al., 2007; Svenningsson et al., 2007; Wesolowska and Nikiforuk, 2007).

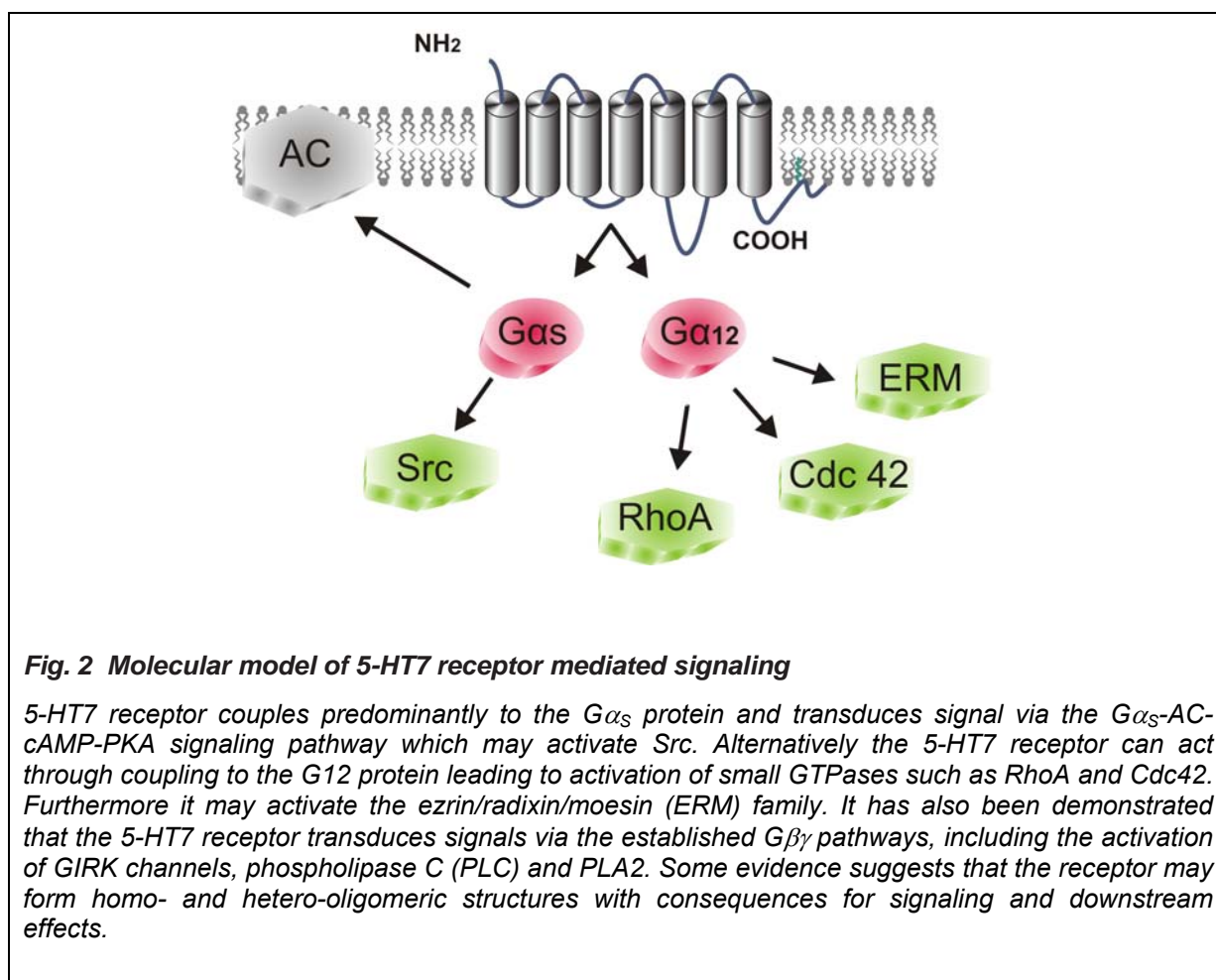
The **5-HT₇ receptor** consists of at least four splice variants (5-HT₇(a), 5-HT₇(b), 5-HT₇(c), 5-HT₇(d)). All these 5-HT₇ receptor isoforms are known to couple to adenylyl cyclase via the heterotrimeric G_s protein leading to an increase of intracellular cAMP levels (Adham et al.,

1998; Heidmann et al., 1998). Recently it was shown that $G_{\alpha 12}$ can also be activated by the 5-HT₇ receptor, leading to the activation of small GTPases of the RhoA family changing the morphology and cytoarchitecture of neuronal cells (Kvachnina et al., 2005; Ponimaskin et al., 2007). The 5-HT₇ receptors can be found in the central nervous system, the thalamus, the hippocampus, the hypothalamus and the cortex of the brain. However, the receptors are also present at the periphery, especially in smooth muscles of blood vessels and in the gastrointestinal tract. Functionally, the 5-HT₇ receptor has been associated with a number of physiological and pathophysiological phenomena, such as 5-HT-induced phase shifting of the circadian rhythm or age-dependent changes in circadian timing (Lovenberg et al., 1993; Duncan et al., 2004). A large amount of experimental data suggests that 5-HT₇ receptors are involved in the induction of sleep and the development of hypothermia (Hedlund et al., 2003; Thomas et al., 2003).

Serotonin and the regulation of neuronal morphology. In addition to their well-established role in neuronal communication, serotonin has been shown to be involved in many aspects of neural development, such as neurite outgrowth, regulation of neuronal morphology, growth cone motility and dendritic spine shape and density, (Azmitia, 2001; Kvachnina et al., 2005; Udo et al., 2005; Ponimaskin et al., 2007; Manzke et al., 2009). Although several serotonin receptors, including 5-HT_{1A}, 5-HT₂ and 5-HT₄ have been proposed to modulate morphogenic events elicited by 5-HT (Fiorica-Howells et al., 2000; Azmitia, 2001), the molecular downstream mechanisms remain poorly understood.

Reorganization of the actin cytoskeleton is one of the critical steps in regulation of neuronal morphology and activity-dependent synaptic modification (Jontes and Smith, 2000). Dynamic changes of the actin cytoskeleton in many cell types are under control of small GTPases of the Rho family, including RhoA, Rac1 and Cdc42 (Hall, 1998). Over the past years it has become evident that members of the Rho family are widely expressed in multiple neural tissues and appear to function as key mediators that link the extracellular signals to cytoskeletal rearrangements (Yamamoto et al., 1989; Olenik et al., 1999). Marked changes in morphology, motility and guidance of axons have been observed in response to activation of Rho family GTPases both *in vitro* and *in vivo* (Zipkin et al., 1997; Ng et al., 2002). The

combined studies suggest that Rac1 and Cdc42 are positive regulators promoting neurite extension and growth cone protrusion. Conversely, activation of RhoA induces stress fiber formation, leading to growth cone collapse and neurite retraction (Lee et al., 2000; Li et al., 2000). As key regulators of both actin and microtubule cytoskeleton, the Rho GTPases have also emerged as important regulators of dendrite and spine structural plasticity (Newey et al., 2005), and appear to be a part of the initial molecular cascade required for the growth of new synapses associated with long-term memory (Udo et al., 2005). Although the importance of Rho GTPases in neuronal morphogenesis is widely accepted, the upstream signaling components including extracellular ligands and receptors involved in regulation Rho-mediated pathways through the lifetime of a neuron are not fully characterized.



We have recently demonstrated that the serotonin receptor 5-HT7 is coupled to the heterotrimeric G12 protein, which in turn selectively activates small GTPases RhoA and

Cdc42 (Kvachnina et al., 2005). Agonist-dependent activation of the 5-HT₇ receptor induced pronounced filopodia formation via a Cdc42-mediated pathway paralleled by RhoA-dependent cell rounding in neuroblastoma cells. Stimulation of 5-HT₇ receptor in hippocampal neurons resulted in marked extension of neurite length. In the present study, using cultured hippocampal neurons, we found that activation of the 5-HT₇R/G₁₂ signaling pathway promotes both dendritic branching and synaptogenesis, leading to the enhancement of spontaneous synaptic activity. By establishing and analysis of organotypic preparations from the hippocampus of juvenile mice, we demonstrated that 5-HT₇R/G₁₂ signaling potentiated the formation of dendritic spines, increased the basal neuronal excitability and lead to robust changes in long-term potentiation (LTP). While prominent in neuronal preparations from juvenile mice, the effects of 5-HT₇/G₁₂ signaling on synaptic plasticity in adult mice were abolished. Accordingly, the behavior of adult animals was also not significantly influenced upon chronic 5-HT₇ receptor inhibition. Such discrepancies in the effects of 5-HT₇R/G₁₂ signaling obtained in juvenile and adult animals may be explained by the fact that expression of both 5-HT₇ receptor and G_α12 protein was significantly reduced during development. Thus, regulated expression of both 5-HT₇ receptor and G_α12 protein may represent a molecular mechanisms by which serotonin differentially regulates neuronal morphology and function during development.

1.5 Oligomerization of G-protein coupled receptors

“Until recently, G-protein coupled receptors were assumed to exist and function as monomeric entities that interact with the corresponding G-protein at a 1:1 stoichiometry. However, biochemical, structural and functional evidence obtained in the last decade suggests that some GPCRs can form homo- and hetero-oligomers (Devi, 2001). Initial clues for the existence of receptor dimers and oligomers came from the appearance of high molecular weight SDS-resistant complexes on SDS-PAGE (Javitch, 2004). In addition, trans-complementation assays not only confirmed the existence of receptor–receptor interactions but also specified their functional implications. In these experiments, it was demonstrated that co-expression of two mutant receptors, which were not able to transduce signals

individually, restored signal transduction (Maggio et al., 1993; Monnot et al., 1996). Recently, GPCR dimers were directly visualized under physiological conditions when rhodopsin dimers in murine rod outer segments were imaged by atomic force microscopy (Liang et al., 2003). Dimers were also found in crystal structure of rhodopsin (Salom et al., 2006).

Although there is evidence suggesting that oligomeric complexes may represent the preferred state of GPCRs (Chabre and le Maire, 2005), no general principle defining the regulation of oligomerization has been elucidated. There are two general models describing the mechanisms of GPCR oligomerization. One model proposes that GPCR oligomers are formed early after receptor synthesis and that oligomeric state does not change upon ligand treatment (Bulenger et al., 2005). A well-known example of such constitutive oligomerization is the GABA_B receptor, for which oligomerization between GABA_BR1 and GABA_BR2 has been shown to be necessary for the proper trafficking and functioning at the cell surface (Malgaroli and Tsien, 1992; Jones et al., 1998; Kaupmann et al., 1998; White et al., 1998). The other model, which has been documented for several GPCRs by using biochemical as well as biophysical approaches, describes receptor oligomerization as a ligand-dependent process (Angers et al., 2002; Pflieger and Eidne, 2005; Yamazaki et al., 2005).

In the second part of this study, we examined the oligomerization state of the serotonin 5-HT_{1A} receptor and analyzed its dynamics in living cells. As mentioned before the 5-HT_{1A} receptor can couple to a variety of effectors via the pertussis-toxin sensitive heterotrimeric G-proteins of the G_{i/o} families and is the most extensively characterized member of the serotonin receptor family. Activation of the 5-HT_{1A} receptor results in the inhibition of adenylyl cyclase and subsequent decrease of intracellular cAMP levels. In addition to the effects mediated by the G_{αi/o} subunit, activation of the 5-HT_{1A} receptor leads to a G_{βγ}-mediated activation of a K⁺ current, inhibition of a Ca²⁺ current, stimulation of the phospholipase C, as well as an activation of the mitogen-activated protein kinase Erk2 (Andrade et al., 1986; Fargin et al., 1989; Clarke et al., 1996; Garnovskaya et al., 1996). With respect to its physiological functions, it is noteworthy that the 5-HT_{1A} receptor is involved in manifold processes including the regulation of neurogenesis (Radley and Jacobs, 2002), respiratory control (Manzke et al., 2003; Richter et al., 2003) cardiovascular control (Saxena

and Villalón, 1990), neuroendocrine regulation (Burnet et al., 1996), temperature control (Overstreet, 2002) and regulation of sleep (Bjorvatn and Ursin, 1998). Considerable interest in this receptor has been raised due to its involvement in regulation of depression and anxiety states (Parks et al., 1998; Overstreet, 2002; Gordon and Hen, 2004). Previously, we have demonstrated that the 5-HT_{1A} receptor is stably palmitoylated at its C-terminal cysteine residues Cys417 and Cys420. Characterization of acylation-deficient 5-HT_{1A} mutants revealed that palmitoylation of the 5-HT_{1A} receptor is critical for G_i protein coupling and effector signaling as well as for the localization in lipid rafts (Papoucheva et al., 2004). Therefore in addition to providing evidence for oligomerization of wild-type 5-HT_{1A} receptors, we investigate whether a palmitoylation state of 5-HT_{1A} receptor may affect its oligomerization (Kobe et al, 2008).

1.6 Aims of the study

This work attempts to analyze the molecular mechanisms and functional consequences of serotonergic signaling mediated by two physiological important receptors, the 5-HT_{1A} and the 5-HT₇ receptor.

The first part the study is based on the current knowledge that the neurotransmitter serotonin (5-hydroxytryptamine) modulates different aspects of early neuronal differentiation, such as neurite outgrowth and synaptogenesis. However, it remains unclear by what mechanisms these actions are achieved by the 5-HT receptors. This part will focus on the 5-HT₇/G₁₂ pathway in respect to the regulation of morphology and synaptogenesis as well as functional consequences (e.g. synaptic plasticity).

The second part is building on the recent evidence that GPCRs can form homo- and hetero-oligomers. The goal of the study was to determine the oligomerization state and the oligomerization dynamics of the serotonin 5-HT_{1A} receptor in living cells as well as the role of receptor palmitoylation in this process.

2 EXPERIMENTAL PROCEDURES

2.1 Materials

2.1.1 Chemicals

Applied Biosystems	<i>GeneAmp Gold RNA PCR Reagent Kit, TaqMan Universal PCR Master Mix, Gene Expression Assays</i>
Calbiochem	<i>transferrin</i>
Invitrogen	<i>gentamicin, Lipofectamine2000 Reagent, glutamax I, L-glutamine, b-FGF, B-27 supplement, Neurobasal-A-Medium, TRIzol Reagent, PureLink Micro-to-Midi Total RNA Purification System</i>
Millipore	<i>0.4 µm Millicell-CM</i>
Nunc	<i>cell culture plastic</i>
Peqlab	<i>AceGlow detection kit</i>
Pierce	<i>1,11-bis-maleimidotriethyleneglycol (BM[PEO]₃)</i>
Qiagen	<i>Plasmid DNA purification Maxi Kit</i>
Roche	<i>laminin</i>
Roth	<i>HCl, Aceton, NaHCO₃, NaCl, KCl, Na₂HPO₄, ampicillin, TEMED, acrylamide, bis-acrylamide, 2-mercaptoethanol, glycine, kanamycin, bromphenole blue</i>
Sigma	<i>poly-L-lysine, Hanks balanced salt solution, HEPES, glucose, bovine albumin, MgSO₄, trypsin, DNase, trypsin inhibitor, MEM Earle's, insulin, Dulbeccos's modified Eagle's medium (DMEM), horse serum, cytosine arabinoide, 5-hydroxytryptamine, ethidiumbromide, penicillin/streptomycin solution, PMSF, Optiprep™ gradient medium, protein A-sepharose,</i>
Smith Kline Beecham	<i>SB656104-A</i>
Tocris	<i>WAY 100135, SB 269970. 5-carboxamidotryptamine maleate</i>

2.1.2 Vectors

Plasmids encoding for G α i2, G β 1 and G γ 2 subunits of heterotrimeric G-protein from mice were kindly provided by Dr. Tatyana Voyno-Yasenetskaya (University of Illinois, Chicago).

To visualize the dendritic structures we used a plasmid encoding for cytosolic GFP (pEGFP from Clontech). Plasmids previously constructed in the lab (Papoucheva et al., 2004; Renner et al., 2007) were used: HA-tagged 5-HT1A and 5-HT1A receptors fused to different spectral variants of the green fluorescence (CFP/ YFP) proteins as well as their palmitoylation-deficient counterparts.

2.1.3 Buffers and Solutions

1x TE buffer:	0.01 M Tris-HCl, pH 8.0, 7.6 or 7.4, 1 mM Na ₂ EDTA (pH 8.0)
50x TAE-buffer:	2 M Tris-HCl, 0.05 M Na ₂ EDTA (pH 8.0), 1 M glacial acetic acid
Antibody incubation buffer:	PBS / 0.05% Tween
Artificial cerebrospinal fluid (ACSF):	130 mM NaCl, 3.5 mM KCl, 1.25 mM NaH ₂ PO ₄ , 24 mM NaHCO ₃ , 1.2 mM CaCl ₂ , 1.2 mM MgSO ₄ , and 10 mM dextrose; aerated with 95%O ₂ , 5% CO ₂ to adjust pH to 7.4
Blocking solution:	5% (w/v) ECL blocking reagent in PBS-Tween
Blot buffer:	25 mM Tris/HCl, pH 8.3, 192 mM glycine, 20% (v/v) methanol
Digestion solution:	137 mM NaCl, 5 mM KCl, 7 mM Na ₂ HPO ₄ , 4.2 mM NaHCO ₃ , pH 7.4
Extracellular solution:	118 mM NaCl, 2 mM KCl, 10 mM glucose, 10 mM HEPES, 2 mM CaCl ₂ , 1 mM MgCl ₂
Fixation solution:	4.0% w/v formaldehyde in PBS
Hanks balanced salt solution with supplements:	4.2 mM NaHCO ₃ , 10 mM HEPES, 30 mM glucose, albumine bovine (0.72 g/l), 12 mM MgSO ₄ , gentamicin (0.5 μ l/ml)
Intracellular solution:	1 mM NaCl, 125 mM K-gluconate, 10 mM HEPES, 0.5 mM CaCl ₂ , 1 mM MgCl ₂ , 11 mM EGTA, 1 mM ATP, 0.3 mM GTP, pH adjusted to 7.4 using KOH
PBS:	150 mM NaCl, 20 mM NaH ₂ PO ₄ , pH 7.4

Permeabilization solution:	0.5% v/v Triton-X-100, 0.5 M NaCl, 50 mM PBS, pH 7.4
Protein-loading-gel buffer (3x):	93.7 mM Tris/HCl (pH 6.8), 30% Glycerin, 9% SDS, 1.5 % bromphenolblue.
RIPA-buffer:	20 mM Tris/HCl pH 7.4, 150 mM NaCl, 10 mM EDTA, 10 mM iodacetamide, 1% Triton X-100, 1% deoxycholic acid, 0.1% SDS, 1 mM PMSF, 5 µg/ml aprotinin, 2 µg/ml leupeptin.
SDS-Gel electrophoresis buffer:	25 mM Tris/HCl (pH 8.3-8.5), 192 mM Glycin, 0.1% SDS.
TNE buffer:	25 mM Tris/HCl, pH7.4, 150 mM NaCl, 5 mM EDTA, 1 mM DTT, 10% sucrose, 1% Triton X-100, 1 mM PMSF, 10 µM Leupeptin, 2 µg/ml Aprotinin NaHCO ₃ , 1 mM NaH ₂ PO ₄ , 5 mM glucose, pH 7.4
Tris-HCl/SDS buffer for protein gel electrophoresis (4x):	0.5 M Tris-HCl, pH 6.8, 14 mM SDS.
Tris-HCl/SDS buffer for protein gel electrophoresis (4x):	1.5 M Tris-HCl, pH 8.8, 140 mM SDS

2.1.4 Antibodies

Abcam:	anti-GFP antibody
Eusera:	anti-GFP
Invitrogen:	Alexa Fluor® 488 rabbit anti-goat IgG (H+L), rabbit anti-HA antibody
Jackson ImmunoResearch:	Cy TM 3-conjugated AffiniPure goat anti-mouse IgG
Santa Cruz:	PSD-95, mouse monoclonal anti-HA-tag
Sigma:	synaptophysin, mouse monoclonal

2.2 Methods

2.2.1 Protein Analysis

2.2.1.1 SDS-polyacrylamide gel electrophoresis

Proteins can be separated by their molecular weight by applying an electrical field within the continuous, cross-linked polymer matrix (SDS-PAGE). For this proteins need to be solubilized in sample buffer and loaded onto a gel together with a molecular weight marker in order to define the size of the protein.

2.2.1.2 Immunoprecipitation and immunoblotting

“Twenty-four hours post-transfection cells were washed in PBS and lysed in 500 μ l RIPA-buffer for 30 min on ice. The lysate was cleared by centrifugation at 13.000 rpm for 20 min at 4°C. The receptors were immunoprecipitated from the supernatant by incubation with rabbit anti-HA antibody (Santa Cruz) or anti-GFP antibody (Abcam) for 4 h at 4°C, followed by incubation of lysates with protein A-sepharose (Sigma) for 2 h. The immunoprecipitation-sepharose complexes were washed with RIPA buffer, eluted with 40 μ l Laemmli loading buffer, and 15 μ l of each sample were separated by 10% SDS-PAGE under reducing conditions. Proteins were transferred to Hybond nitrocellulose membrane (Amersham) and probed either with antibodies against HA-tag (Santa Cruz; 1:5000 diluted in PBS/Tween20) or against GFP (Eusera; diluted 1:20.000 in PBS/Tween20). Proteins were detected using AceGlow detection reagents (Peqlab).

2.2.1.3 Chemical cross-linking

Transiently transfected cells were resuspended in PBS and mixed with the indicated concentrations of cross-linker 1,11-bis-maleimidotriethyleneglycol (BM[PEO]₃) diluted in PBS for 10 min at room temperature. The reaction was stopped by addition of dithiothreitol to a final concentration of 10 mM followed by incubation on ice for 10 min. After two washes with PBS, cells were lysed and proteins were immunoprecipitated and subjected to the SDS-PAGE and immunoblot analysis.

2.2.1.4 Gradient centrifugation

Separation of detergent-resistant membranes derived from transfected N1E-115 cells (1×10^6) growing on 35 mm dishes was performed as recently described (Harder et al., 1998). Cells were lysed in TNE buffer and lysates (1.2 mg protein/ml) were mixed with the double volume of 60% Optiprep™ gradient medium. The resulting 40% Optiprep™ mixture was transferred into the ultracentrifuge tube and overlaid with steps of each 35%, 30%, 25%, 20% and 0% Optiprep™ in TNE. The gradients were centrifuged for 5 h at 50.000 rpm in the TLS-55 rotor of the ultracentrifuge TL-100 (Beckman). Six fractions were collected from the top of the gradient and TCA-precipitated. The protein pellets were analyzed by SDS-PAGE followed by immunoblot analysis with appropriate antibodies. In several experiments chemical cross-linking with BM[PEO]₃ together with 5-HT treatment (10 μM) was performed before ultracentrifugation.

2.2.1.5 RT-PCR for receptor and G-protein mRNA expression

RNA Isolation: Immediately following the preparation of hippocampus total RNA was isolated using TRIzol Reagent. Briefly, 0,5 ml TRIzol was used to prepare homogenates from 50-100 mg brain tissue. After homogenization, 100 μl of chloroform were added and the tubes were shaken vigorously by hand for 15 seconds. Emulsions were centrifuged at 12,000 rpm/4°C/15 min. The aqueous phase containing the RNA was transferred into a fresh tube and mixed with an equal volume of 70% ethanol. RNA was purified from the samples using PureLink Micro-to-Midi Total RNA Purification System according to the manufacturers' instructions. RNA was bound to a silica-based membrane in the spin-cartridge and impurities were removed by washing. Potential contaminating DNA was removed by treatment with DNaseI. The purified RNA was eluted in water and stored at -80°C.

Reverse transcription of mRNA: Reverse transcription was carried out using the GeneAmp Gold RNA PCR Reagent Kit (Applied Biosystems). Concentration of RNA was determined in a photometer at 260 nm. A measure of 5 μg of total RNA was subjected to first strand cDNA synthesis using random hexamer primers. The obtained cDNAs were stored at -20°C.

Quantitative real time PCR: The amplification was carried out on a ABI PRISM7000 Sequence Detector (Applied Biosystems) using TaqMan Universal PCR Master Mix (Applied

Biosystems). For the detection of 5-HT1A-, 5-HT7-, G α s- and G α 12-mRNA the corresponding Gene Expression Assays (Applied Biosystems) containing gene-specific primers and FAM-probes were used. For normalization, Eukaryotic 18S RNA was also quantified (Kobe et al, 2008).

2.2.2 Cell culture and transfection

Cells lines

N1E-115 neuronal cells from mouse neuroblastoma

Animals

Naval Medical Research Institute mice

C57BL/6NCrl (Charles River Laboratories, Sulzfeld, Germany)

2.2.2.1 Adherent cell culture and transfection

Mouse N1E-115 neuroblastoma cells from the American Type Culture collection (ATCC) were grown in Dulbecco's modified Eagle's medium (DMEM) containing 10% fetal calf serum (FCS) and 1% penicillin/streptomycin at 37 °C under 5% CO₂. For transient transfection, cells were seeded at low-density in 60-mm dishes (1×10^6) or on 10-mm cover-slips (5×10^5) and transfected with appropriate vectors using Lipofectamine2000 Reagent according to manufacturer's instruction. Four hours after transfection, cells were serum starved over night before analysis.

2.2.2.2 Culture of primary hippocampal neurons

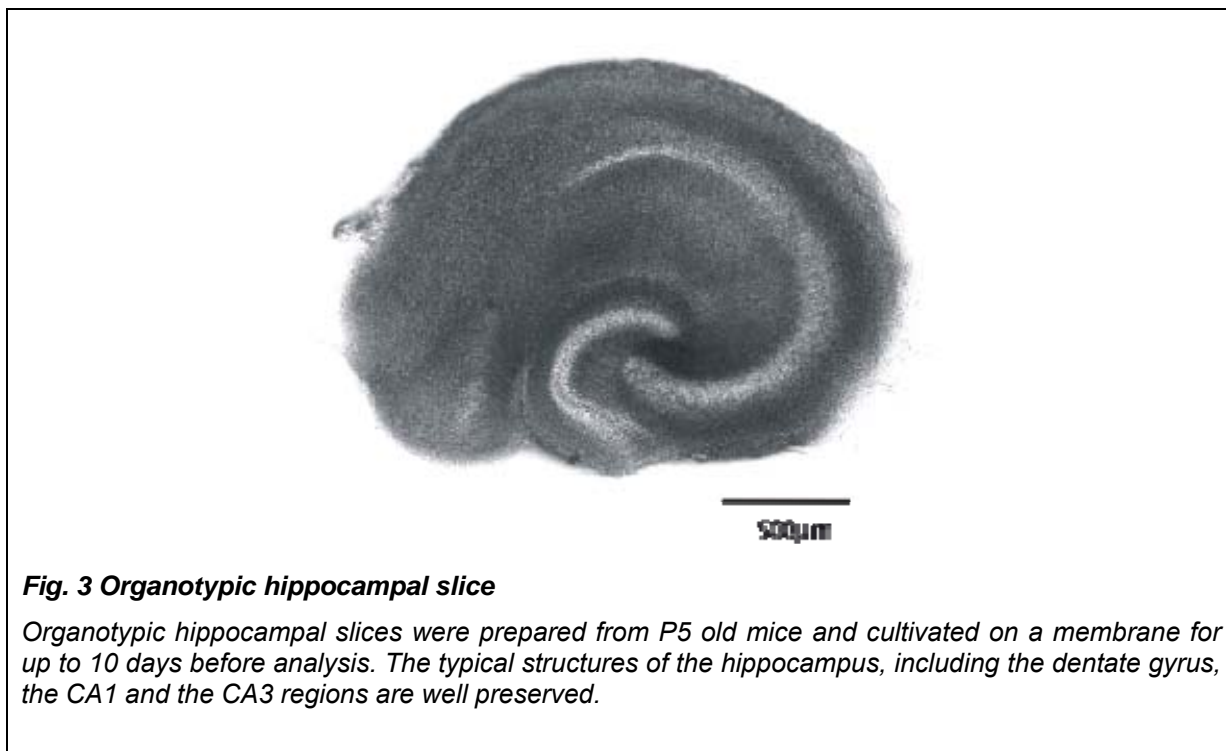
Preparation of cultures was performed according to standard procedures (Malgaroli and Tsien, 1992; Reuter, 1995) and optimized for mouse hippocampal neurons (Dityatev et al., 2000). Briefly, hippocampi of 1 - to 2 day old Naval Medical Research Institute mice were isolated, cut into small pieces in ice-cold Ca²⁺ and Mg²⁺ free Hanks balanced salt solution with supplements and then treated with trypsin (3 mg/ml) and DNase (0.75 mg/2ml) in digestion solution. After incubation in trypsin inhibitor for 10 minutes the tissue was kept in dissection medium containing horse serum for 10 minutes to allow recovery from stress. The

cells were then dissociated by pipetting up and down with three fire-polished Pasteur pipettes with sequentially smaller diameters and centrifuged at 80 x g. After counting the cells in a Neubauer counting chamber were plated on cleaned and sterilized 13 mm cover slips coated with poly-L-lysine (100 µg/ml) and laminin (40 µg/ml) at a density of 25000 – 30000 cells per cover slip.

The culturing day was defined *days in vitro 1* (DIV 1). For the next three days the cells were incubated in culture medium (MEM eagle medium containing glucose (25.2 mM), transferrin (1.3 mM), insulin (25 µg/ml), Glutamax I (2 mM), gentamicin (0.5 µl/ml), horse serum (0.1 ml/ml)) at 37° C and 5% CO₂. Thereafter, at DIV 4, and every second day half of the medium was replaced by Neurobasal-A-Medium containing L-glutamine (0.5 mM), b-FGF (125 ng/ml), B-27 supplement (20 µl/ml), penicillin/streptomycin (10 µl/ml) and cytosine arabinoside (5 µM) to feed the cells and to terminate glial mitosis. During the first week cells on the cover slip established a cellular bilayer structure with a glia monolayer on the bottom and a neuronal layer on the top. Neurons could be easily determined by their typical structure with a quite round cell body and distinct neurites and by their ability to generate action potential when recorded.

2.2.2.3 Culture of hippocampal slices (interface method)

Organotypic hippocampal slice cultures were prepared and maintained on the method for rats (Stoppini et al., 1991) but adapted for mice. In brief, 6-day-old Naval Medical Research Institute mice were decapitated. Hippocampi were removed and cut in slices (350 µm) under sterile conditions in gassed (95% O₂, 5% CO₂), ice-cold minimal essential medium (MEM) at pH 7.35. Slices were maintained on a biomembrane surface (0.4 µm, Millicell-CM, Millipore, Eschborn, Germany) between culture medium (50% MEM, 25% Hanks' balanced salt solution, 25% horse serum and 2- mM -glutamine at pH 7.3) and humidified atmosphere (5% CO₂, 36.5 °C) in an incubator (Heraeus, Hanau, Germany). Culture medium was completely replaced in the first 2 days and thereafter twice a week. Slices were used for experiments after 7–10 days in vitro.



2.2.2.4 Slice culture preparation (rollertubes)

In brief, the hippocampi were dissected from 6 day-old Naval Medical Research Institute mice pups killed by decapitation, and 350 μm -thick transverse slices were cut and attached to glass coverslips with clotted chicken plasma. The coverslip and slice were placed in individual sealed test-tubes containing semi-synthetic medium and maintained on a roller drum in an incubator at 36°C for 2-4 weeks. The culture medium consisted of 50 % Eagle's basal medium, 25 % balanced salt solution with either Hanks' or Earle's salts, 25 % heat-inactivated horse serum, 33.3 mM D-glucose and 0.1 mM glutamine.

Transfections were carried out at DIV4 (primary culture) and at DIV2 (organotypic culture) with a vector encoding for GFP using 1 μg DNA for one coverslip and Lipofectamine2000 Reagent (Invitrogen) according to the manufacturer's instruction.

All animals were housed, cared and killed in accordance with the recommendations of the European Commission.

2.2.3 Electrophysiology

2.2.3.1 Patch clamp recording

The cover slips with the plated neurons were placed in the experimental chamber which was perfused at a rate of 3.4 ml/min with room tempered extracellular solution using a perfusion pump 505 S (Watson Marlow, Falmouth, UK). The extracellular solution was pH adjusted to 7.4 using NaOH and the osmolarity was calibrated to the actual values of the culture medium of the neurons intended to use. The osmolarity of the culture medium ranged between 265 and 280 mOsm.

Neurons were patch clamped at the soma with a patch clamp amplifier EPC-9 using *Pulse* software (HEKA, Lambrecht, Germany) in the whole cell configuration. Patch electrodes with an electrode resistance of 8-10 MOhm were pulled from borosilicate capillaries (Hilgenberg, Malsfeld, Germany) using a P-97 Puller (Sutter, Novato, USA) and filled with intracellular solution, the osmolarity was calibrated to a value 15 mOsm less than the extracellular solution. The recordings were filtered at 10 kHz (four pole Bessel filter) and collected at 10 kHz.

From DIV 9 on the neurons establish functional synapses that correlate with spontaneous synaptic activity, sufficient to induce postsynaptic action potentials (Bartrup et al., 1997). In following days the frequency of EPSPs and IPSPs increased, became associated and established a burst-like activity. Neurons were recorded at DIV 11, just in the rising phase of the increase of the synaptic activity to observe the clearest effects. 4-6 neurons per drug incubation per experiment were chosen randomly and recorded in the current clamp mode at least for 5 minutes. The membrane potential was held at rest or slightly hyperpolarized to -60 mV to establish comparable conditions. The frequency of single EPSPs and action potential was obtained by counting them each second. The number of EPSPs during burst-like activity could not be counted and were excluded from analysis as well as the IPSPs.

All data recordings were transferred to a PC-readable format and analysed by Clampfit 8 (Axon Instruments, USA) and PlotIT (Scientific Programming Enterprises, Haslett, USA). Values are presented as *mean* \pm *SEM*, *N* giving the number of experiments and *n* the number of recorded neurons. Significance of effects was determined by unpaired t-tests

2.2.3.2 Miniature PSCs

Whole cell patch clamp recordings were performed in CA3 hippocampal neurons from organotypic slices from mice. The extracellular solution in all experiments was aerated with 95% O₂ and 5% CO₂ and kept at 32°C. Miniature PSCs (mPSCs) were recorded in the presence of 0.5 μM tetrodotoxin (TTX). Signals with amplitudes of at least 2 times above the background noise were selected. In all tested animals, there were no significant differences in the noise levels between different genotypes. Patches with a serial resistance of >20 MΩ, a membrane resistance of < 0.2 GΩ, or leak currents of > 300 pA were excluded. The membrane currents were filtered by a four-pole Bessel filter at a corner frequency of 2 kHz, and digitized at a sampling rate of 5 kHz using the DigiData 1322A interface (Molecular Devices, Sunnyvale, CA). All data are expressed as mean ± standard error of the mean. *P*-values represent the results of two-tailed unpaired Student's *t* tests, with or without Welch's correction, depending on the distribution of the data (tested with a Kolmogorov-Smirnov test). Data acquisition and analysis was done using commercially available software: pClamp 9.2 and AxoGraph 4.6 (Molecular Devices, Sunnyvale, CA), MiniAnalysis (SynaptoSoft, Decatur, GA) and Prism 4 (GraphPad Software, San Diego, CA)

2.2.3.3 Long Term Potentiation measurements

Animals were treated for 3 weeks twice daily with 5-HT7 antagonist SB 656104-A. Hippocampal tissue slices were placed in an interface recording chamber of the Oslo style, containing artificial cerebrospinal fluid (ACSF) and left undisturbed for at least 90 min. The chamber was kept at 35-36 C°, aerated with 95% O₂ - 5% CO₂ (400 ml/min), and perfused with oxygenated ACSF (3-4 ml/min).

The single barreled glass microelectrodes for extracellular recordings were pulled from thin-walled borosilicate glass (GC150TF-10, Harvard Apparatus) using a horizontal puller (P-97, Sutter Instruments).

Extracellular recordings of hippocampal slices were conducted in the following manner. Evoked responses were elicited by 0.1 ms unipolar stimuli (Grass S88 stimulator with PSIU6 photoelectric stimulus isolation units, Grass Instruments) delivered via microwire electrodes

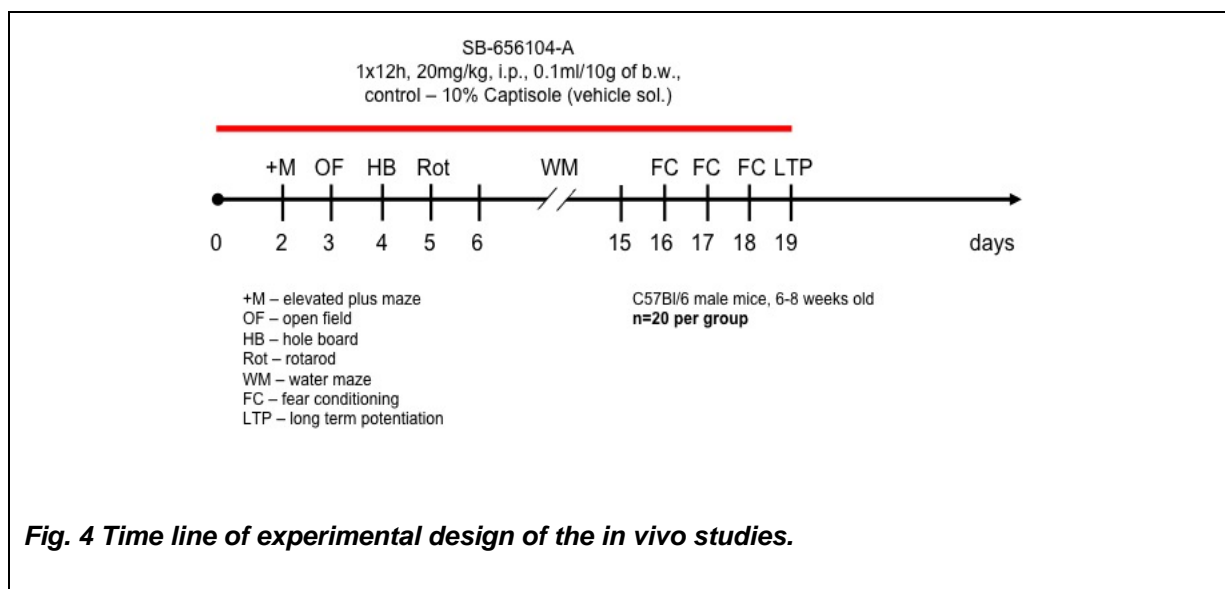
made from bare stainless steel wire (50 μm diameter, AM-Systems) and recorded as described earlier (Müller and Somjen, 1998). Orthodromic responses were elicited by stimulation of Schaffer collaterals and recorded in st. radiatum of the CA1 region, using a locally constructed extracellular DC potential amplifier. Data were digitized by a DigiData 1322A (Molecular Devices, Sunnyvale, CA, USA). Data analysis was performed in Clampfit 9.0 (Molecular Devices, Sunnyvale, CA, USA). We evoked excitatory postsynaptic potentials (fEPSPs) by placing the stimulation electrode in the stratum radiatum at CA3/CA1 junction for the activation of Schaffer collaterals. In turn the recording electrode was placed in the stratum radiatum of the CA1 region. We measured the magnitude of fEPSPs as amplitude (baseline to peak) and slope (20-80% level of the falling phase). For input-output relationship, fEPSPs were evoked with 0.1ms stimuli at 0.25Hz and an average of 4 consecutive responses was taken. fEPSP amplitudes and slopes were plotted against the stimulus intensity (10 to 150 μA). For paired-pulse facilitation (PPF) different inter-stimulus intervals (25, 50, 75, 100, 125, 150, 175 and 200ms) were measured as the ratio of the second fEPSP to the first fEPSP. The paired stimuli were set at 0.25Hz and an average of 4 consecutive responses was obtained. For long-term potentiation (LTP), baseline responses were evoked every 20s for 5 min and LTP was induced by 1 train consisting of 100Hz stimulation for 1s. The post-train responses were then measured every 20s for 60min and an average of 4 consecutive responses was taken.

2.2.4 Behavioral tests

Animals: All experiments were permitted by the local Animal Care and Use Committee. Behavioral tests were performed on C57BL/6NCrl (Charles River Laboratories, Sulzfeld, Germany) mouse strain and employed 39 age-matched males. Mice were housed at 4–5 per cage in a room with 12h light-dark cycle (lights on at 08:00h) and *ad libitum* access to food/water. The order of testing was as follows: Elevated plus maze, open field, rotarod, hole board, Morris water maze, cued and contextual fear conditioning. All mice were used for all behavioral tests. The order of testing was designed according to increasing invasiveness to minimize a possible influence of experimental history (McIlwain et al., 2001). Age of mice at

the beginning of testing was 11 weeks. Inter-test interval was at least 1-2 days. Behavioral tests were performed in a blind fashion during the light phase of the day from 10:00 until 17:00h.

Injections: SB656104-A was dissolved in captisol and administrated intraperitoneally (IP) at the dose 20 mg/kg twice a day (8:00 and 20:00h) during 3 weeks (number of animals, n=20). Freshly made solution was used each day. The volume of injection was 0.01 ml/g of mouse body weight. Control animals (n=19) were identically treated with the corresponding volume of captisol vehicle solution. SB656104-A behavioral experiments were started next day after the last injection.



2.2.4.1 Behavior: experimental setup

Elevated plus maze: In this test of anxiety, mice were placed in the central platform, facing an open arm of the plus-maze (made of grey plastic with a 5x5cm central platform, 30 x 5cm open arms and 30 x 5 x 15cm closed arms; illumination 120 lx). The behavior was recorded for 5 min by an overhead video camera and a PC equipped with “Viewer 2” software (Biobserve GmbH, Bonn, Germany) to calculate the time spent in center, open and closed arms, number of arm visits, and velocity. The time spent in open arms was used to estimate open arm aversion (fear equivalent).

Open field: Spontaneous activity in the open field was tested in a grey Perspex arena (120 cm in diameter, 25 cm high; illumination 120 lx). Mice were placed in the center and allowed to explore the open field for 7 min. The behavior was recorded by a PC-linked overhead video camera. "Viewer 2" software was used to calculate velocity, time spent in central or peripheral zones, and the number of the central zone visits in the open field.

Rotarod: The rotarod test examines motor function, balance, and coordination. It comprised a rotating drum (Ugo Basile, Comerio, Varese, Italy), which was accelerated from 4 to 40rpm over 5min. Mice were placed individually on the drum and the latency of falling off the drum was recorded using a stop-watch. To assess motor learning, the rotarod test was repeated 24h later.

Hole board: The hole board test for exploratory activity was performed in a 21 x 21 x 36 cm transparent Perspex chamber with a non-transparent floor raised 5 cm above the bottom of the chamber, with 12 equally spaced holes, 2 cm in diameter. Mice were allowed to explore the chamber for 3 min and the number of explored holes (head dips) was scored by a trained experimenter.

Spatial learning and memory was assessed in a water maze (Morris, 1984). A large circular tank (diameter 1.2 m, depth 0.4 m) was filled with opaque water ($25\pm 1^\circ\text{C}$, depth 0.3 m) and the escape platform (10x10 cm) was submerged 1 cm below the surface. The swimming patterns were monitored by a computer and the video-tracking system "Viewer 2". The escape latency, swim speed, path length, and trajectory of swimming were recorded for each mouse. During the first 2 days, mice were trained to swim to a clearly visible platform (visible platform task) that was marked with a 15 cm high black flag and placed pseudo-randomly in different locations across trials (non-spatial training). The extra-maze cues were hidden during these trials. After 2 days of visible platform training, hidden platform training (spatial training) was performed. For 8 days, mice were trained to find a hidden platform (i.e. the flag was removed) that was located at the center of one of the 4 quadrants of the pool. The location of the platform was fixed throughout testing. Mice had to navigate using extra-maze cues that were placed on the walls of the testing room. Every day, mice went through 4 trials with an inter-trial interval of 5 min. The mice were placed into the pool facing the side

wall randomly at 1 of 4 start locations and allowed to swim until they found the platform, or for a maximum of 90 s. Any mouse that failed to find the platform within 90 s was guided to the platform. The animal then remained on the platform for 20 s before being removed from the pool. The next day after completion of the hidden platform training, a probe trial was conducted in order to determine whether mice used a spatial strategy to find the platform or not. The platform was removed from the pool and the mice were allowed to swim freely for 90 s. The percentage of time spent in each quadrant of the pool as well as the number of times the mice crossed the former position of the hidden platform were recorded.

Cued and contextual fear conditioning: The fear conditioning test was performed as described by Radyushkin et al. (Radyushkin et al., 2005). Mice were trained within the same session for both contextual and cued fear conditioning. Training consisted of exposing mice for 120 s to the context to assess the baseline level of activity. This period was followed by a 10 s, 5 kHz, 85 dB tone (conditioned stimulus, CS). Immediately after the tone, a 2 s, 0.4 mA foot shock (unconditioned stimulus, US) was applied. This CS-US pairing was repeated 13 s later. All mice remained in the conditioning chambers for an additional 23 s following the second CS-US pairing. The contextual memory test was performed 24 h after this training. Mice were monitored over 2 min for freezing in the same context as used for training. The cued memory test was performed 27 h after training in a new chamber. First, mice were monitored for freezing over a 2 min pre-cue period with no tone to assess freezing in the new context. Next, a 2 min cue period followed in which the tone was presented. Duration of freezing behavior, defined as the absolute lack of movement (excluding respiratory movements), was recorded by a video camera and a PC equipped with 'Video freeze' software (MED Associates, St. Albans, Vermont, USA).

Statistical analysis: Unless stated otherwise, the data given in figures and text are expressed as mean \pm SEM. Data were compared by either 2-way ANOVA for repeated measures or by non-parametric Mann-Whitney U-test where appropriate. For analysis, SPSS v.14 software (SPSS Inc., Chicago, IL, USA) was used. A p-value below 0.05 was considered to be significant.

2.2.5 Confocal imaging and FRET analysis

2.2.5.1 Immunocytochemistry and Dendrite Morphology Analysis

For immunostaining neurons were fixed by using 4% paraformaldehyde in PBS at 4 °C for 20 min followed by quenching of free formaldehyde with 50 mM glycine for 15 min. Cell permeabilization was achieved with 0.2% Triton X-100 in PBS for 10 min. After incubation in blocking solution (10% BSA in PBS), primary antibodies against Synaptophysin (1:200, Sigma) and PSD-95 (1:200, Santa Cruz) were applied overnight followed by rinses in PBS and staining with secondary antibodies Alexa Fluor 488 (1:500, Invitrogen) and Cy3 (1:1000, Jackson ImmunoResearch) at room temperature. Coverslips were mounted in fluorescent mounting medium (Dako) and for dendritic morphology analysis.

Images were acquired on a Zeiss LSM 510 laser-scanning confocal microscope with a 40x oil-immersion Plan-Neofluor objective. Short protrusions were defined by a length $> 3 \mu\text{m}$ and long protrusions were identified by a length of 10-30 μm , synaptic clusters were identified by synaptophysin puncta. 30 randomly collected images were used and counting was performed manually on 50 μm long dendrites.

Three dimensional analysis of dendritic spines was performed using a 3D reconstruction software developed by *Herzog et al.* (Herzog et al., 2006) which allowed to measure the geometric parameters of dendritic spines from confocal microscopic image stacks. Data are presented as mean \pm SEM. Statistical comparisons were assessed with paired t-test; $p < 0.05$ was taken as significant.

2.2.5.2 Confocal imaging and single-cell acceptor photobleaching FRET analysis

“Images of N1E-115 cells expressing 5-HT1A-CFP and 5-HT1A-YFP fusion proteins were acquired with an LSM510-Meta confocal microscope (Carl Zeiss Jena) equipped with a 40x/1.3 NA oil-immersion objective at 512 x 512 pixels. The 458 nm line of a 40 mW argon laser was used at 15% power. Fluorescence emission was acquired from individual cells

over fourteen lambda channels, at 10.7 nm steps, ranging from 475 to 625 nm. For each measurement a series of 8 images was acquired over a duration of 124 seconds. After the 4th image acquisition, bleaching of the acceptor (YFP) was performed in a selected 20 x 20 pixel region of interest in the plasma membrane. For that the 514 nm line of the Argon laser set at 50% power and 100% transmission for 300 scanning interactions using a 458nm/514nm dual dichroic mirror was used. Linear unmixing was performed by the Zeiss AIM software package using CFP and YFP reference spectra obtained from images of cells expressing only 5-HT1A-CFP or 5-HT1A-YFP acquired with acquisition settings mentioned above. Apparent FRET efficiency was calculated offline using the equation,

1)

$$f_D = 1 - \left(\frac{F_{DA}}{F_D} \right)$$

where f_D is the fraction of donor participating in the FRET complex (i.e. ratio of FRET complexes over a total donor concentration, $[DA]/[D^t]$, F_{DA} and F_D are the background subtracted and acquisition bleaching corrected pre- and post-bleach CFP fluorescence intensities, respectively. The acquisition bleaching corrected post-bleach CFP intensities were calculated as

2)

$$F_D^{post} = F_D^{pre} + \left(\frac{F_D^{pre} - F_D^{bleach}}{F_D^{pre} - F_D^{ref}} \right) F_D^{ref}$$

where F_D^B and F_D^R refer to CFP intensities of the bleach and reference region of interest, and *pre* and *post* refer to pre-bleach and post-bleach measurements.

2.2.5.3 Spectral FRET analysis in living cells

Mouse N1E-115 neuroblastoma cells were co-transfected with plasmid DNAs encoding for wild-type and/or acylation-deficient 5-HT1A receptors fused with CFP and YFP. Sixteen hours after transfection, cells were resuspended in PBS. All measurements were performed

in 5 mm pathway quartz cuvettes using a spectrofluorometer (Fluorolog, Horiba JobinYvon) equipped with xenon lamp (450 W, 950V). The cell suspension was stirred with a magnetic stirrer while the temperature was maintained at 37°C during the experiment.

For calibration measurements, cells were co-transfected with plasmid encoding a single fluorophore-tagged 5-HT1A receptor together with an equal amount of plasmid encoding HA-tagged 5-HT1A receptor. During the time-course experiments, two emission spectra were obtained for each time point by exciting at 458 nm and 488 nm with 5 nm spectral resolution for excitation and emission and 0.5 second integration time. The spectral contributions due to light scattering and non-specific fluorescence of the cells were taken into account by subtracting the emission spectra of non-transfected cells (background) from each measured spectra. Before each measurement, the spectrofluorometer was calibrated for the xenon-lamp spectrum and Raman scattering peak position.

Stimulation of 5-HT1A receptors was carried out using serotonin (Sigma) at a final concentration of 10 μ M. For antagonist treatment, WAY 100135 (Tocris) at a final concentration of 1 μ M was used. Cholesterol depletion was carried out by treating cells with 2% methyl- β -cyclodextrin (M β CD) in serum-free DMEM for 45 min at 37°C.

2.2.5.4 Apparent FRET efficiency calculations

To determine changes in apparent FRET efficiency due to 5-HT1A receptor activation by serotonin we used a recently developed method described in detail by *Wlodarczyk et al.* (Wlodarczyk et al., 2008). Calibration measurements were carried out with cells expressing only donor $[D^{ref}]$ (5-HT1A-CFP) or acceptor $[A^{ref}]$ (5-HT1A-YFP) using two excitation wavelengths λ^i ($i=1,2$) as described in the previous section. Calibration measurements allowed us to obtain the concentration related extinction coefficient ratio $r^i = \varepsilon_D^i [D^{ref}] / \varepsilon_A^i [A^{ref}]$. This was done by fitting the curve resulting from acceptor reference spectra multiplied by the quantum yield and emission characteristics of the donor (i.e. emission spectra normalized to unit area) to that of donor reference spectra multiplied by the quantum yield, and emission characteristics of the acceptor (Wlodarczyk et al., 2008).

We also performed reference measurements with cells co-expressing 5-HT1A-CFP and 5-HT1A-YFP receptors. Combinations of the acceptor and donor reference spectra were fitted to the measured spectra of cells co-expressing 5-HT1A-CFP and 5-HT1A-YFP and the apparent relative acceptor and donor concentrations r_A' and δ' , respectively, were obtained as the weights of those fits.

The quantities r_A', δ' obtained together with two scaling factors (r') reflecting the excitation ratios of two fluorophores at a given excitation wavelength λ' , allow for a calculation of the total concentration ratio $[A']/[D']$ of donor and acceptor as well as the apparent FRET efficiencies Ef_A and Ef_D , where f_A and f_D are the fractions of acceptors and donors in complexes.

3)

$$E_{D'} = E \frac{[DA]}{D'} = \frac{r'^{-1} + R'}{r'^{-1} + \alpha' \cdot \delta'}$$

and

4)

$$E_{A'} = E \frac{[DA]}{[A']} = \frac{[D'']}{[A'']} \frac{\Delta\alpha}{\alpha' r'^{-1} + \alpha' r'^{-1}}$$

where R' is a concentration ratio calculated as,

5)

$$R' = \frac{[A'] [D'']}{[D'] [A'']} = \frac{\alpha' r'^{-1} + \alpha' r'^{-1}}{\Delta r \delta' - \Delta\alpha}$$

with the definitions $\Delta\alpha = \alpha' - \alpha''$ and $\Delta r = r'^{-1} - r''^{-1}$. Where $f_D = [DA]/[D']$ and $f_A = [DA]/[A']$ representing the fractions of donor and acceptor participating in complexes.

2.2.5.5 Analysis of specific vs. random receptor-receptor interactions

In order to distinguish between receptors interacting randomly from those with specific interaction, apparent FRET efficiencies were obtained for various acceptor to donor ratios by keeping the total concentration of fluorophores constant. It has been proposed that the dependency of E_{f_D} on $[A']/[D']$ for dimers differs from that of E_{f_D} resulting from random interaction (Veatch and Stryer, 1977). The apparent FRET efficiency E_{f_D} obtained from our experimental data was plotted as a function of the total acceptor to donor ratio $[A']/[D']$ and fitted by least square minimization to the following equation, as proposed previously by Veatch and Stryer (Veatch and Stryer, 1977) and later modified by James et al (James et al., 2006) to the form

6)

$$E_{f_D} = \frac{E}{(1 + [A']/[D'])^2}$$

where E is the characteristic FRET efficiency. It is also notable, that the above equation was derived for the case of high-affinity dimerization reaction (Veatch and Stryer, 1977).

2.2.5.6 Fluorescence lifetime FRET measurements

Fluorescence intensity decays were obtained by time-correlated single photon-counting measurements of fluorescence using a Fluorolog-3 spectrofluorometer (Horiba Jobin Yvon, München, Germany). Samples were placed in 10-mm pathway quartz cuvettes (10×10 mm²) and continuously stirred with a magnetic stirrer. Emission was collected in right angle geometry. Excitation was performed with a 460 nm nanoLED with a 440/40 nm transmission filter (Semrock, Tübingen, Germany). Fluorescence intensity was measured in the wavelength band from 468 nm to 482 nm to avoid acceptor fluorescence. Typical fluorescence decays were fitted with the resulting sum of one, two, or three exponentials, iteratively convolved with the instrument response function using the standard DataStation analysis software provided by Horiba Jobin Yvon and CFS LS software (available from

Center for Fluorescence Spectroscopy at <http://cfs.umbi.umd.edu/cfs/software/>). The quality of the fits was evaluated by the structure observed in the plots of residuals and by the reduced chi-square values. The mean fluorescence lifetimes were calculated as the amplitude-weighted lifetimes. In several experiments cholesterol depletion was carried out by treating cells with 2% methyl- β -cyclodextrin (M β CD) in serum-free DMEM for 45 min at 37°C before the analysis (Kobe et al, 2008).

3 RESULTS

3.1 Functional role of 5-HT7/G12 signaling

3.1.1 5-HT7 Receptor activation induces formation of dendritic filopodia and new synapses

Our recent studies demonstrated that the 5-HT7 receptor is coupled to heterotrimeric G12 proteins, and that receptor stimulation results in G12-mediated activation of Cdc42 small GTPase, which is known as a positive regulator promoting neurite extension (Kvachnina et al., 2005). To investigate the role of the 5-HT7R/G12 signaling pathway in dendritic morphogenesis, we used primary cultures of hippocampal neurons, which allowed for better visualization of morphological events as well as for functional analysis. We selected a time point (10 to 12 days *in vitro* incubation of culture, prepared at postnatal day 1) at which dendritic morphology is subject to change and well defined synapses are formed (Bartrup et al., 1997) (Figure 6). To be able to evaluate receptor-mediated morphological changes, neurons were incubated with low concentration of 5-HT7 receptor agonist 5-CT (100 nM) during the last 4 days before analysis. Neurons were also transfected with GFP, to visualize the morphology of single cells. Post-fixation, dendritic morphology of the neurons was imaged using confocal microscopy. We used single-factor ANOVA analysis to quantify this and all other data sets and to determine the statistical significance of the differences between experimental groups. Agonist treatment resulted in dramatic overall increase in the number of dendritic protrusions in comparison to non-treated control (Figure 5 D, E, number of short dendritic protrusions (SP) per 50 μm of dendritic length 4.4 ± 0.45 in control vs. 11.3 ± 1.27 after 5-CT treatment, number of long (over 10 μm) dendritic protrusions (LP) 0.4 ± 0.16 in control vs. 3.1 ± 0.5 after 5-CT treatment, $n = 30$, $p < 0,0001$). These morphogenic effects were receptor-specific because they were inhibited by an antagonist of the 5-HT7 receptor, SB-269970 (Figure 5).

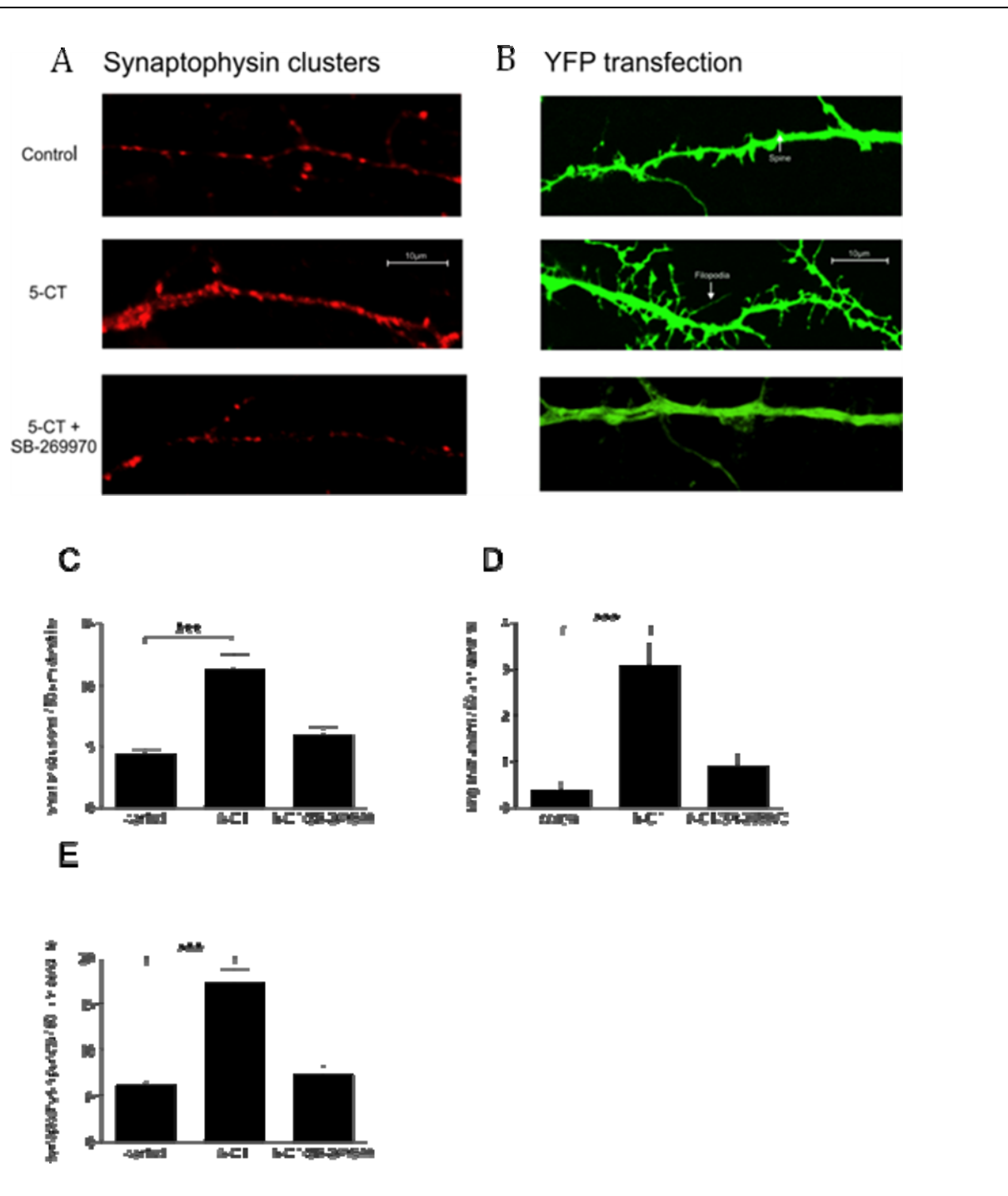
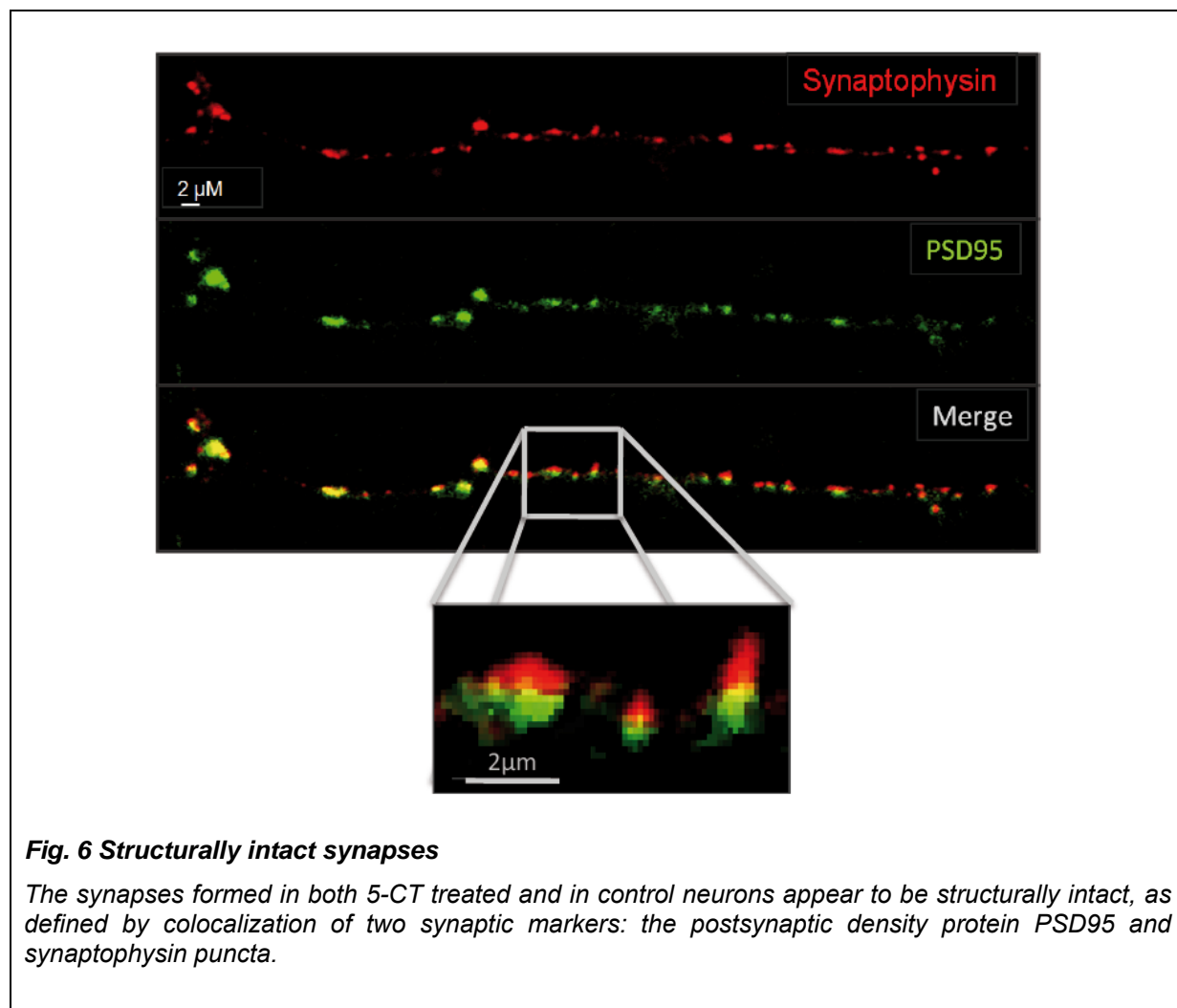


Fig. 5 Synaptic clusters and morphological changes in dendrites after stimulation of the 5-HT7 receptor

(A) Synaptophysin puncta in dendrites of control, 5-CT and 5-CT + SB-269970 treated neurons. (B) Dendrite morphology of control, 5-CT (100 nM) and 5-CT + SB-269970 (1 μM) treated neurons. The number of short (< 3 μm) (D) and long dendritic protrusions (> 10 μm) (E) were increased in 5-CT treated neurons as compared to control neurons. (C) Quantification of synaptophysin puncta in control and in 5-CT treated neurons shows an increase of puncta in the 5-CT treated neurons. Protrusions and puncta were counted on 50 μm long dendrites. $n = 30$, Values represent means \pm SE, $p < 0.0001$.

To address the question whether the 5-HT₇R-mediated signaling affects synaptic density, we quantified the number of synapses by labeling of GFP transfected neurons with the presynaptic structural synaptic marker synaptophysin (De Paola et al., 2003). Prolonged treatment of neurons with 5-CT increased the density of synaptophysin puncta from 6.2 ± 0.49 ($n = 30$) to 17.4 ± 1.46 ($n = 30$) per 50 μm of dendrite (Figure 5C). The synapses formed in both 5-CT treated and in control neurons appear to be structurally intact, as defined by colocalization of postsynaptic density protein PSD95 and synaptophysin puncta with respect to each other (Figure 6). Similarly to the effects on formation of dendritic protrusions, the synaptogenic effects of 5-CT were abolished upon treatment with 5-HT₇ receptor antagonist (Figure 5).



3.1.2 Morpho- and synaptogenic effects of the 5-HT7 receptor are mediated by the G α 12 Protein

In addition to coupling to the heterotrimeric G α 12 protein, the 5-HT7 receptor can stimulate cAMP formation by activating adenylyl cyclases via a stimulatory G α_s -protein. The G α_s -mediated signaling is also known to regulate the cellular morphology either by modulating cAMP concentration (Corset et al., 2000) or by direct binding of G α_s to the cytoskeleton (Yu et al., 2009). To investigate whether the morphogenic effects of 5-HT7 receptor include the G α_s -mediated component, we analyzed the primary hippocampal neurons prepared from G α 12 deficient mice. Initial studies of the G α 12-knockout mice have demonstrated that these animals are alive and show no apparent phenotype (Gu et al., 2002). Analysis of dendritic morphology revealed that even without any treatment the number of dendritic protrusions in G α 12-knockout neurons was significantly reduced in comparison to the neurons from the wild type mice (SP to $72.5 \pm 3.7\%$, LP to $68.2 \pm 11.8\%$, $n=30$, $p<0.001$ Figure 7 D, E). Additionally the density of synapses assessed by the analysis of synaptophysin puncta was diminished to $88.5 \pm 3.2\%$ (Figure 7C), suggesting that basal G12-mediated activity may be involved in neuronal morpho- and synaptogenesis. Prolonged treatment of G α 12 deficient neurons with 5-HT7 receptor agonist 5-CT had no effect on neuronal morphology. (Figure 7). Statistical analysis revealed that both the number of dendritic protrusions as well as the density of synaptophysin puncta in treated and non-treated neurons isolated from G α 12 - knockout were similar and statistically indistinguishable (5-CT, SP, $81 \pm 5.9\%$, LP, $65.9 \pm 10.6\%$, synaptic cluster density, $86.9 \pm 2.9\%$, Figure 7). In contrast, these parameters were significantly increased after agonist treatment of neurons prepared from the wild-type animals (5-CT, SP, $169.3 \pm 10.4\%$, LP, $245.5 \pm 28.8.6\%$, synaptic cluster density, $179.2 \pm 2.9\%$, Figure 7), demonstrating that receptor-mediated activation of G α 12 protein is necessary for the morpho- and synaptogenic effects obtained upon stimulation of the 5-HT7 receptor.

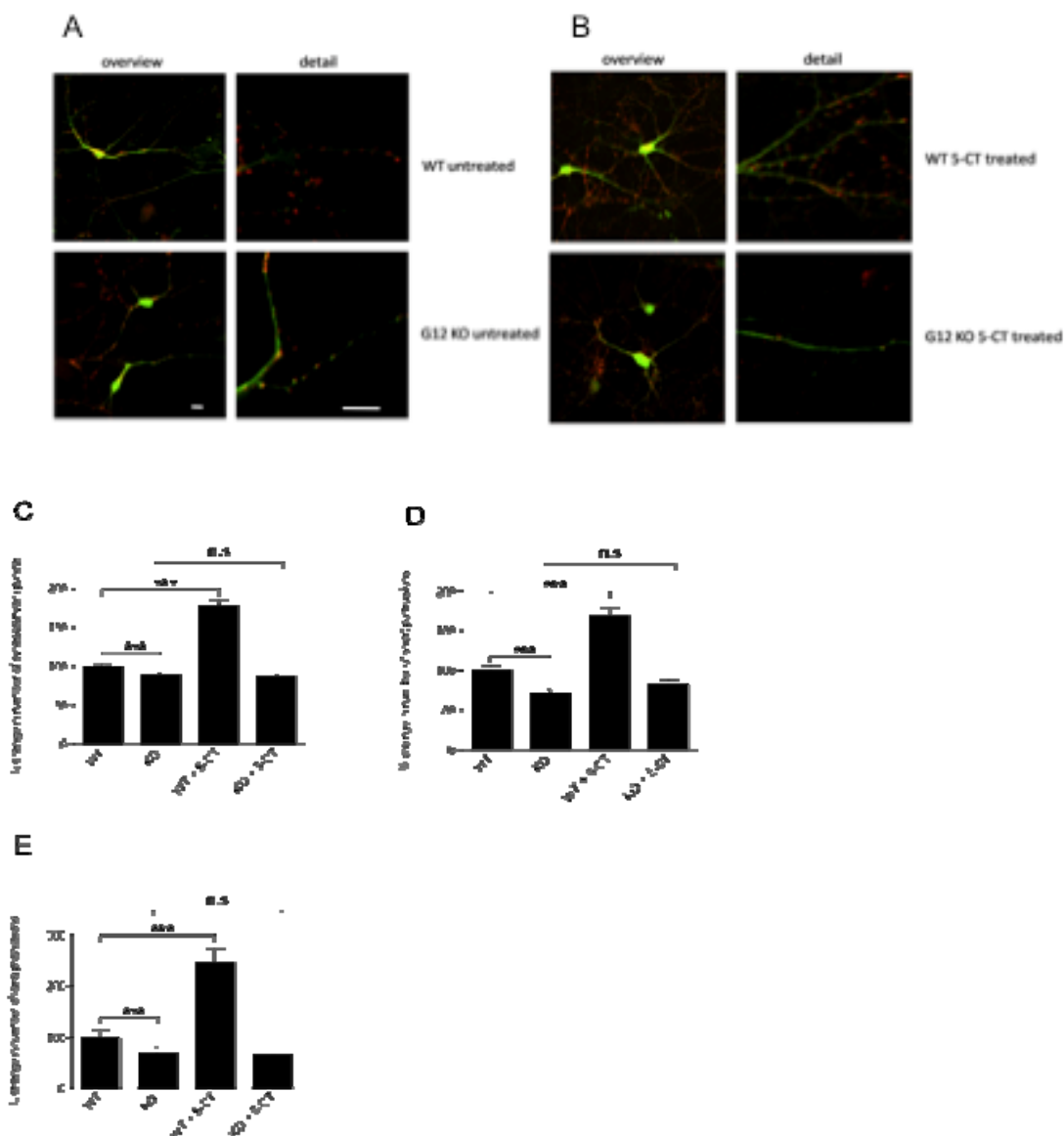
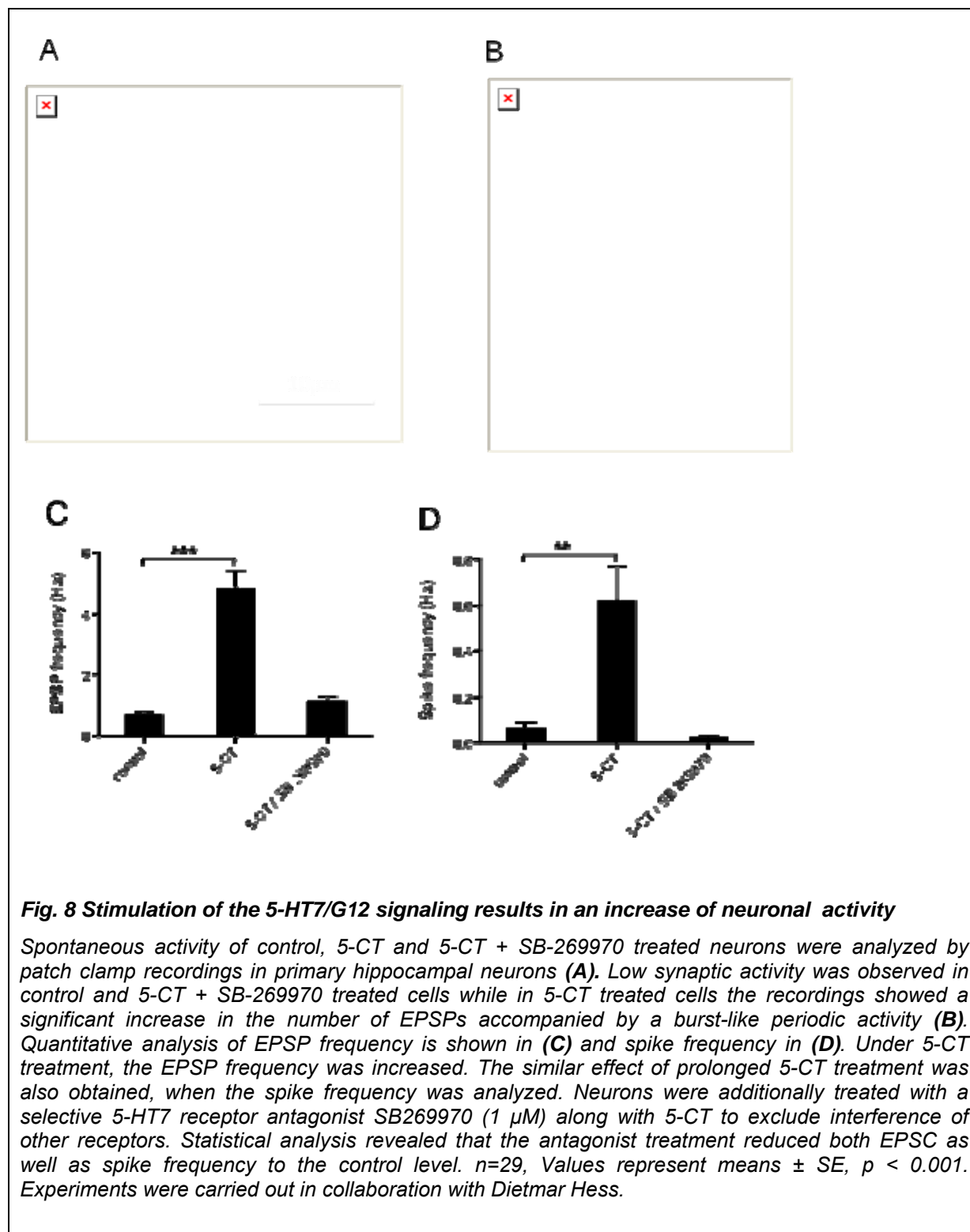


Fig. 7 Synaptogenesis and morphological changes in dendrites are mediated by the G12 protein

Synaptophysin puncta, short and long protrusions in dendrites of wild-type and G12 knockout mice after treatment with vehicle, 5-CT and 5-CT + SB-269970. Cells were treated with 100 nM 5-CT and 1 μM SB-269970 up to 4 days. **(A)** shows changes in morphology of dendrites in G12 knockout mice compared to wild-type mice whereas **(B)** represents changes in morphology after 5-CT treatment. (scale bars: 10 μm) **(C)** shows a significant decrease (in %) in the number of synapses of dendrites of G12 knockout mice compared to wild-type; after treatment with 5-CT the number of synapses become significantly increased in wild-type mice but remain almost unchanged in G12 knockout mice. **(D)** demonstrates a significant decrease (%) in the number of short protrusions in neurons of G12 knockout mice compared to wild-type mice, again after treatment with 5-CT a significant increase in the number of short protrusions in wild-type neurons can be observed while the number of short protrusions in G12 knockout mice are not significantly changed. **(E)** indicates that there is also a significant decrease in the number of long protrusions between in neurons of G12 knockout mice compared to wild-type mice, and similarly treatment with 5-CT leads only in neuron of wild-type mice to an increase of long protrusions. All experiments were carried out on 50 μm long dendrites. n = 30, Values represent means ± SE, p < 0.0001.

3.1.3 Effect of 5-HT7/G12 signaling on EPSCs and spike frequency

Having demonstrated that 5-HT7 receptor-mediated activation of the $G_{\alpha 12}$ increases dendritic arborisation and stimulates formation of new synapses, we tested whether the synaptic properties of these neurons become changed. Spontaneous excitatory postsynaptic currents (EPSCs) as well as spontaneous firing activity were monitored by whole-cell recording from neurons cultured from P2 mouse hippocampus after 10 days in culture (DIV10, Figure 8A). At this time point neurons form synaptic connections and both spontaneous EPSCs and spikes are measurable. Under control conditions, the EPSP frequency ranged from 0.03 to 2.4 Hz with a mean of 0.69 ± 0.11 Hz (Figure 8 B, C, D; $n=29$; mean \pm SEM). The values were similar between different preparation, indicating comparable culturing and developmental conditions. In neurons incubated with 5-CT (100 nM) during the last 4 days before recording, the EPSP frequency was significantly increased (Figure 8, D, E, mean of 4.85 ± 0.53 Hz, $n=29$; $P<0.0000001$). The similar effect of prolonged 5-CT treatment was also obtained, when the spike frequency was statistically evaluated (0.06 ± 0.03 Hz in control vs. 0.62 ± 0.15 Hz in 5-CT treated neurons, $n=29$; $P<0.001$). It is known that 5-CT is a partial agonist for other serotonin receptors, including 5-HT1 and 5-HT5 (Beer et al., 1992; Wood et al., 2000). To prove that synaptic effects obtained after prolonged 5-CT treatment were mediated only by the 5-HT7 receptor, neurons were treated with the selective 5-HT7 receptor antagonist SB269970 (1 μ M) along with 5-CT. Statistical analysis revealed that the antagonist treatment reduced both EPSC as well as spike frequency to the control level (EPSC, 1.14 ± 0.17 , $N=3$, $n=16$; spike frequency, 0.02 ± 0.01 Hz, $N=2$, $n=11$). These results demonstrate that prolonged activation of the 5-HT7/G12 signaling pathway may result not only in structural, but also in functional changes of neuronal properties. Experiments were carried out in collaboration with Dietmar Hess.



3.1.4 Effects of 5-HT7R/G12 signaling on neuronal morphology in organotypic cultures

The critical question for any results obtained in dissociated neuronal cultures is whether they can be reproduced *in vivo*. To analyze the role of 5-HT7R/G12 signaling under *in vivo*-like conditions, we established organotypic slice cultures from the hippocampus of the mouse. In such preparations the main characteristic morphological organization of the hippocampus is well-preserved (Figure 3), and the maturation of different cell types, synaptic contacts, and receptor expression resembles that seen *in vivo* (Gähwiler et al., 1997; Gogolla et al., 2006). Organotypic slices were prepared from P5 mice and maintained for 5 to 6 days *in vitro* before analysis. The day after preparation, slices were transfected with GFP to visualize the morphology of single neurons. During the last 4 days, 5-HT7 receptor agonist 5-CT (either alone or in combination with the antagonist SB269970) was added to the cell culture medium. Post-fixation, dendritic morphology of GFP-positive neurons was imaged by confocal microscopy and 3D reconstructed (Figure 9 A,) (Herzog et al., 2006). We observed that 5-CT treatment resulted in dramatic spine morphogenesis. This structural plasticity appeared as an increase in the number of spines, while the spine morphology was not affected. Morphological effects were mediated by the 5-HT7 receptor, because they were reduced by the selective receptor antagonist SB269970 (Figure 9B). In treated neurons the spine density (2.06 ± 0.11 spines/10 μm versus 5.92 ± 0.09 spines/10 μm , $p, < 0,0001$, agonist + antagonist, 3.45 ± 0.16 spines/10 μm) was markedly increased as compared to control preparations (Figure 8B). In contrast the surface area ($0.67 \pm 0,11 \mu\text{m}^2$ versus $0.83 \pm 0,04 \mu\text{m}^2$), length ($2.85 \pm 0,17 \mu\text{m}$ versus $2.75 \pm 0.09 \mu\text{m}$), diameter ($0.20 \pm 0.02 \mu\text{m}$ versus $0.20 \pm 0.01 \mu\text{m}$) and volume ($0.039 \pm 0.04 \mu\text{m}^3$ versus $0.042 \pm 0.004 \mu\text{m}^3$) of spines in neurons from treated preparations were similar to the control values (Figure 8B), suggesting a critical role of the 5-HT7/G12 signaling in formation of the new spines. 3D reconstructions were carried out in collaboration with Sören Westerholz.

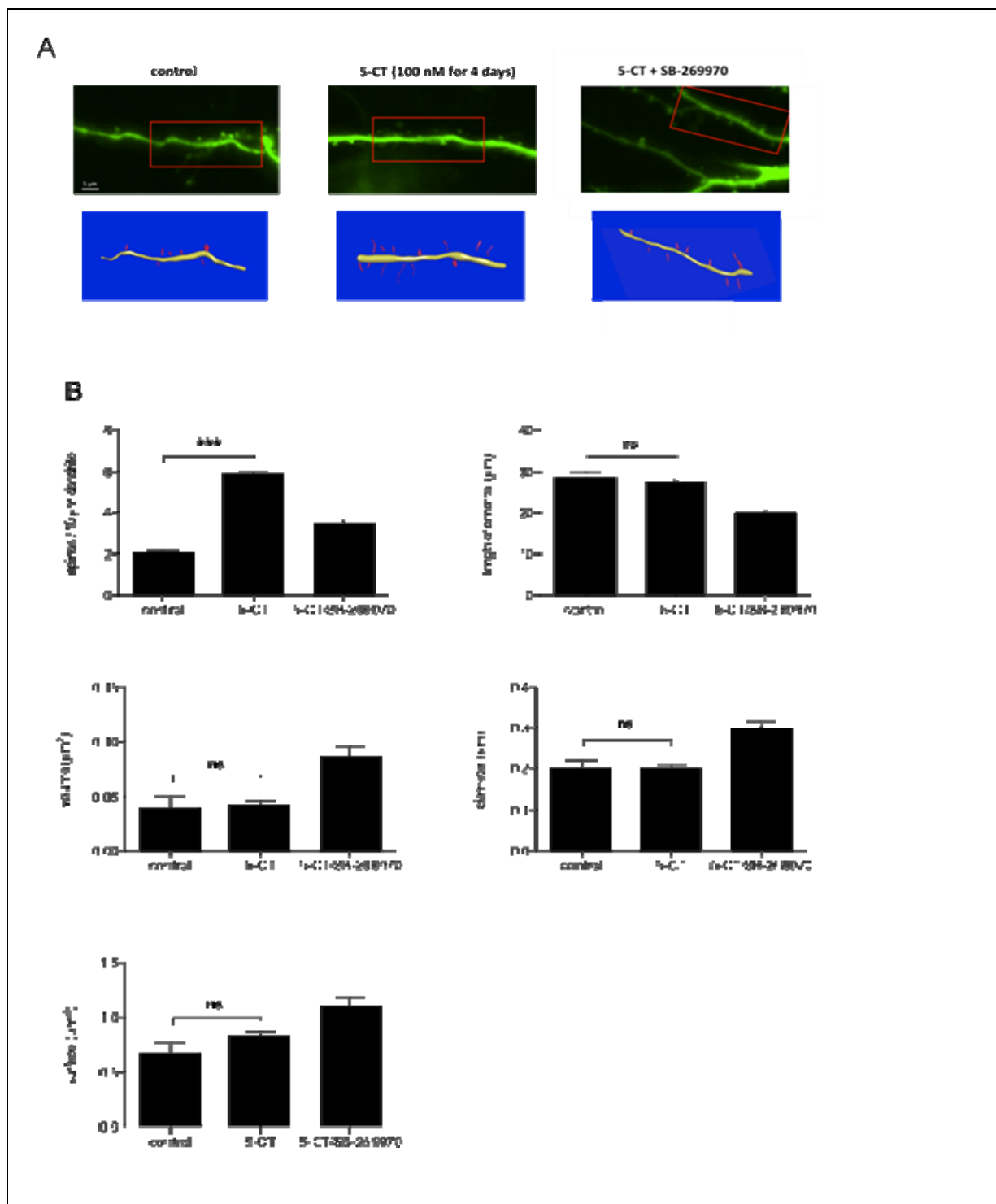


Fig. 9 Confocal images and 3D reconstructions of neurons in hippocampal slices

(A) Organotypic hippocampal slices were prepared as described in Material and Methods, Z-stacks of confocal images of dendrites were taken of control, 5-CT and 5-CT + SB-269970 treated preparations. From these data 3D images were reconstructed and analyzed according to the method described in Material and Methods. (B) Quantitative morphological analysis of reconstructed 3D images of dendrites in hippocampal slices. In treated neurons the spine density was markedly increased as compared to control preparations, $p < 0.001$. In contrast the surface area, diameter and volume of spines in neurons from treated preparations were similar to the control values. $n=30$, values represent means \pm SE. Experiments were carried out in collaboration with Sören Westerholz.

3.1.5 5-HT7R/G12 signaling leads to changes in miniature postsynaptic currents (mPSCs) in organotypic hippocampal slices

To investigate whether the elevated spinogenesis obtained upon stimulation of 5-HT7/G12 signaling pathway can modulate synaptic strength, we measured the basal synaptic properties of the CA3 neurons from organotypic hippocampal slices by recording miniature postsynaptic currents (mPSCs) using whole-cell patch-clamp recordings in the presence of TTX (0.5 μ M) (Figure 10A). The treatment of organotypic slices for 4 days with 5-CT (100 nM) increased amplitudes (52.19 ± 0.3 pA in treated neurons, $n = 9$; 43.37 ± 0.22 pA in control neurons, $n = 9$; $p < 0.01$) (Figure 10B), without significantly affecting mPSCs frequency (Figure 10C).

These results suggest that in addition to morphological effects (formation of new spines), activation of 5-HT7/G12 signaling results in an increase of total synaptic strength. To analyze, whether the changes in mean mPSCs amplitude take place in proportional manner and therefore reflect a synaptic scaling (Turrigiano and Nelson, 2004), we plotted mPSC amplitude as a cumulative probability histogram (Figure 10D). As expected from the changes in mPSC amplitudes, the graph from neurons chronically treated with 5-CT was shifted to the right, when compared to the control cultures. Transforming of experimental graphs by multiplying each value by the same factor derived from the best-fit equation (Turrigiano et al., 1998) results in the left shifting and essential overlay of the graphs with the control distribution. These results suggest that by changing the number of functional synapses, the activation of 5-HT7/G12 signaling pathway can trigger the synaptic scaling. Measurements were carried out in collaboration with Lucian Medrihan.

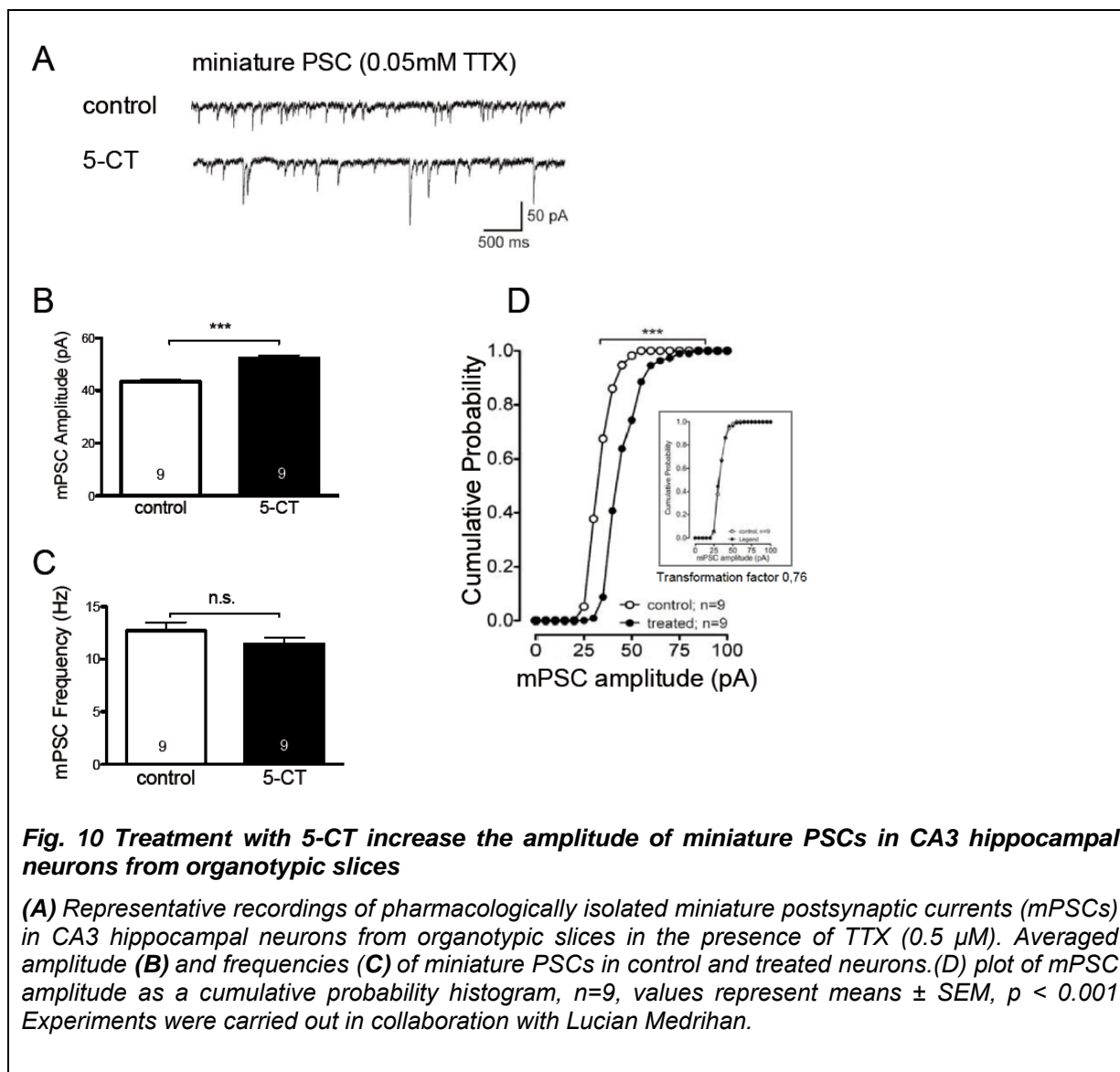


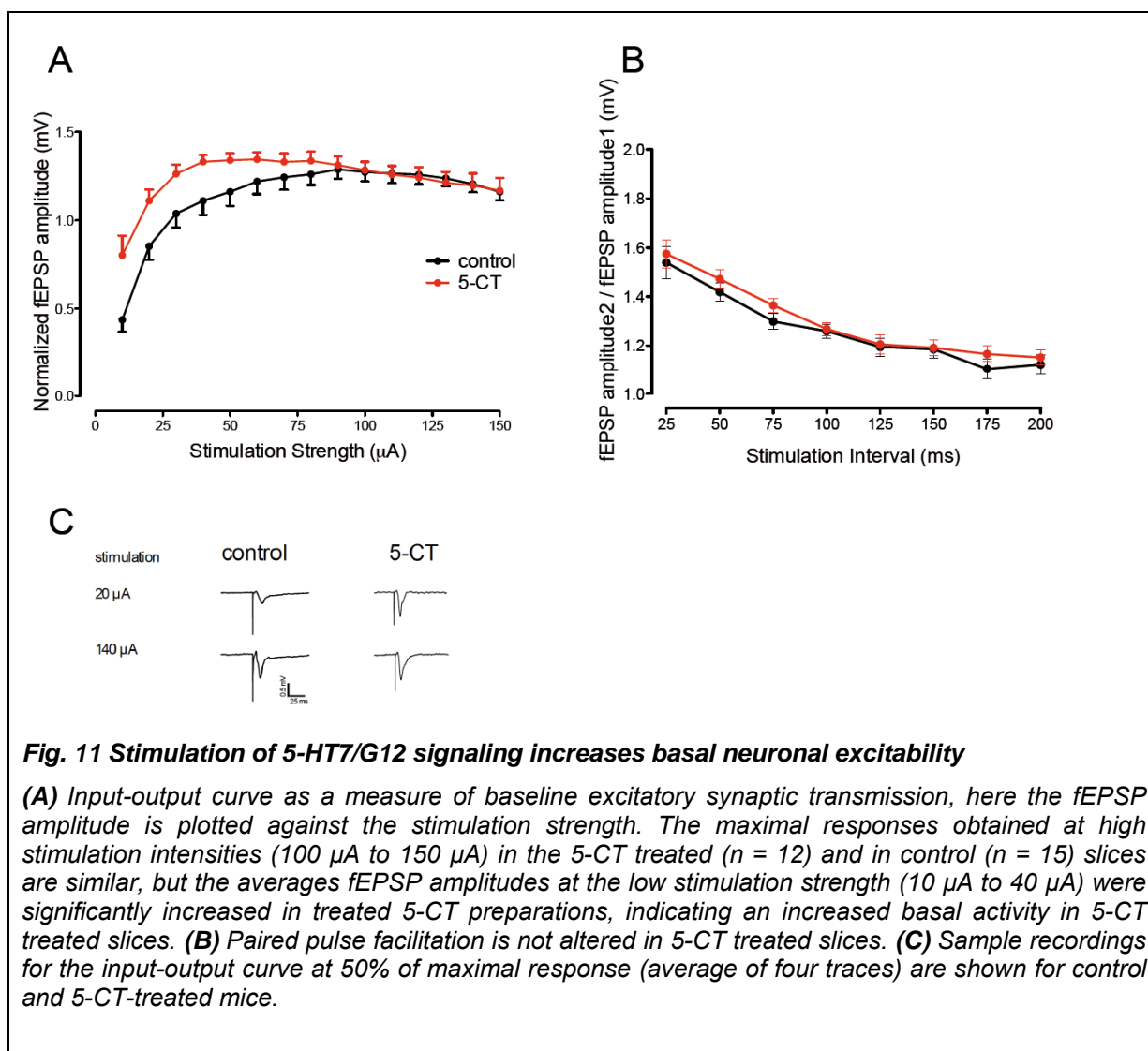
Fig. 10 Treatment with 5-CT increase the amplitude of miniature PSCs in CA3 hippocampal neurons from organotypic slices

(A) Representative recordings of pharmacologically isolated miniature postsynaptic currents (mPSCs) in CA3 hippocampal neurons from organotypic slices in the presence of TTX (0.5 μ M). Averaged amplitude (B) and frequencies (C) of miniature PSCs in control and treated neurons. (D) plot of mPSC amplitude as a cumulative probability histogram, $n=9$, values represent means \pm SEM, $p < 0.001$ Experiments were carried out in collaboration with Lucian Medrihan.

3.1.6 5-HT7R/G12 Signaling modulates neuronal excitability and LTP in organotypic cultures

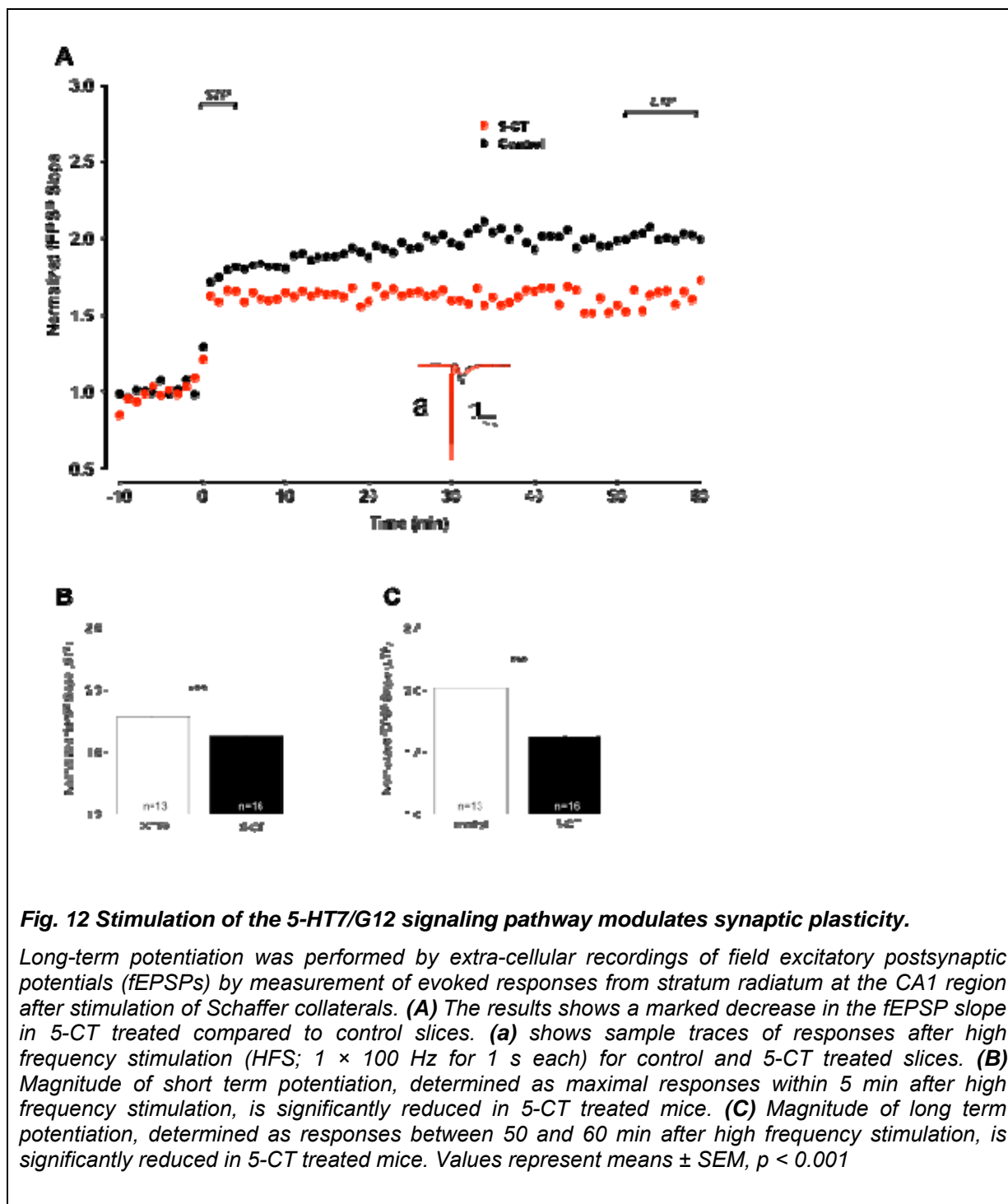
Having demonstrated that stimulation of the 5-HT7 receptor results in pronounced structural change of hippocampal neurons, we asked whether it can influence the functional properties of neurons and thus modulate hippocampal networks. For that, we performed electrophysiological recordings in organotypic slices prepared from P5 mice at DIV7, after 4 days *in vitro* incubation with low concentration of 5-HT7 agonist 5-CT (100 nM). To investigate the effect of 5-HT7/G12 signaling on synaptic transmission, we performed extracellular recordings of field excitatory postsynaptic potentials (fEPSPs) by measurement of

evoked responses from the stratum radiatum at the CA1 region after stimulation of Schaffer collaterals. First, input-output curves were generated by plotting the stimulation intensity versus the amplitude of fEPSP (Figure 11A). While the maximal responses obtained at the higher stimulation intensity (100 μ A to 150 μ A) in the 5-CT treated ($n = 12$) and in control ($n = 15$) slices were quite similar, the average fEPSP amplitudes at the low stimulation strength (10 μ A to 40 μ A) were significantly increased in treated preparations (Figure 11A,C). The shift of the input-output curve to the left means that in the 5-CT treated slices the same presynaptic stimulus elicited a larger postsynaptic response, indicating an increase in basal excitability, which results in a decrease in threshold for the generation of evoked population spikes.



This finding raises the question whether the 5-HT mediated enhancement of the fEPSP amplitudes occurs pre- or post-synaptically. To test this we investigated the differences in paired-pulse facilitation (PPF), which is measure of use-dependent changes in synaptic efficacy and is considered to be a pre-synaptic form of short-term plasticity (Turrigiano et al., 1998; Thompson, 2000; Zucker and Regehr, 2002). Analysis of the ratio of PPF evoked using inter-stimulus intervals between 25 and 200 ms does not reveal any significant differences between control and 5-HT treated slices (Figure 6), suggesting a postsynaptic mechanisms of the 5-HT7 receptor-mediated enhancement of neuronal excitability.

The reduction of threshold for generation of evoked population spikes in 5-HT treated slices prompted us to investigate whether the induction of activity-dependent synaptic plasticity is also affected upon stimulation of 5-HT7R/G12 signaling. Long-term potentiation (LTP) was induced by theta-burst stimulation (TBS) of Schaffer collaterals at 100 Hz. In these experiments we reproducibly found that 5-HT treatment markedly changed induction of LTP in organotypic cultures (Figure 7). Already the initial increase in the fEPSP slope (0 - 5 min) was significantly lower in 5-HT treated ($1,624 \pm 0,01591$ SEM $n=13$) than in control cultures ($1,773 \pm 0,01853$ SEM, $n=16$, $p<0.001$, Figure7). One hour after the LTP-inducing, the potentiation remained significantly decreased in 5-HT treated cultures (50–60 min: $1,622 \pm 0,02009$ SEM, $n=16$) as compared to control preparation ($2,016 \pm 0,008221$ SEM, $n=13$, $p<0.001$, Figure 7). In combination with results obtained by measurement of evoked fEPSPs (Figure 6) and mEPSC (Figure5) this data suggest that increased basal neuronal excitability mediated by the stimulation of 5-HT7/G12 signaling pathway may result in pre-potentiation of synaptic transmission leading to quick LTP saturation, which prevents further potentiation.



3.1.7 In vivo effects of treatment with 5-HT7 receptor antagonist

Experiments performed in organotypic slices from young (P5) mice showed apparent changes in neuronal morphology and synaptic plasticity upon 5-HT7 receptor activation. To test for the possible functional role of 5-HT7/G12 signaling upon *in vivo* conditions, behavioral and electrophysiological studies were performed by using 10 weeks old male mice chronically treated with the highly selective 5-HT7 receptor antagonist SB656104. This antagonist penetrates the blood brain barrier, and its pharmacokinetic properties are well known (Forbes et al., 2002). Animals were treated for 3 weeks twice daily by IP injection of 20mg compound per kg/bodyweight. Analysis of different behavior aspects including anxiety, general activity, motor balance / coordination and exploratory activity demonstrated no significant changes between treated and control groups, although the motor learning and exploration behavior were negatively affected by the treatment with antagonist (Figure 13). Also no effects of chronic treated with SB656104 were found on both hippocampus dependent and independent learning and memory, which were analyzed by Morris water maze and fear conditioning tasks, respectively (Figure 14). Behavioral studies were performed in collaboration with Konstantin Radyushkin and Ahmed El-Khordi. Analysis of the basal neuronal excitability and synaptic plasticity in acute slices obtained from antagonist-treated mice revealed the opposite to 5-CT effects (decrease of basal excitability (Figure 15) and increase of LTP Figure 15)), although the extent of changes were moderate. The fEPSP slope (0 - 5 min) was almost unchanged in SB656104 treated ($1,566 \pm 0,009372$ SEM, $n=8$) compared to control cultures ($1,573 \pm 0,01243$ SEM, $n=7$, n.s., (Figure 15 B). One hour after the induction of LTP a slight but significant potentiation was observed in SB656104 treated cultures (50–60 min: $1,302 \pm 0,002023$ SEM $n=8$) as compared to the control preparation ($1,231 \pm 0,004910$ SEM $n=7$, $p<0.001$, Figure 15 C).

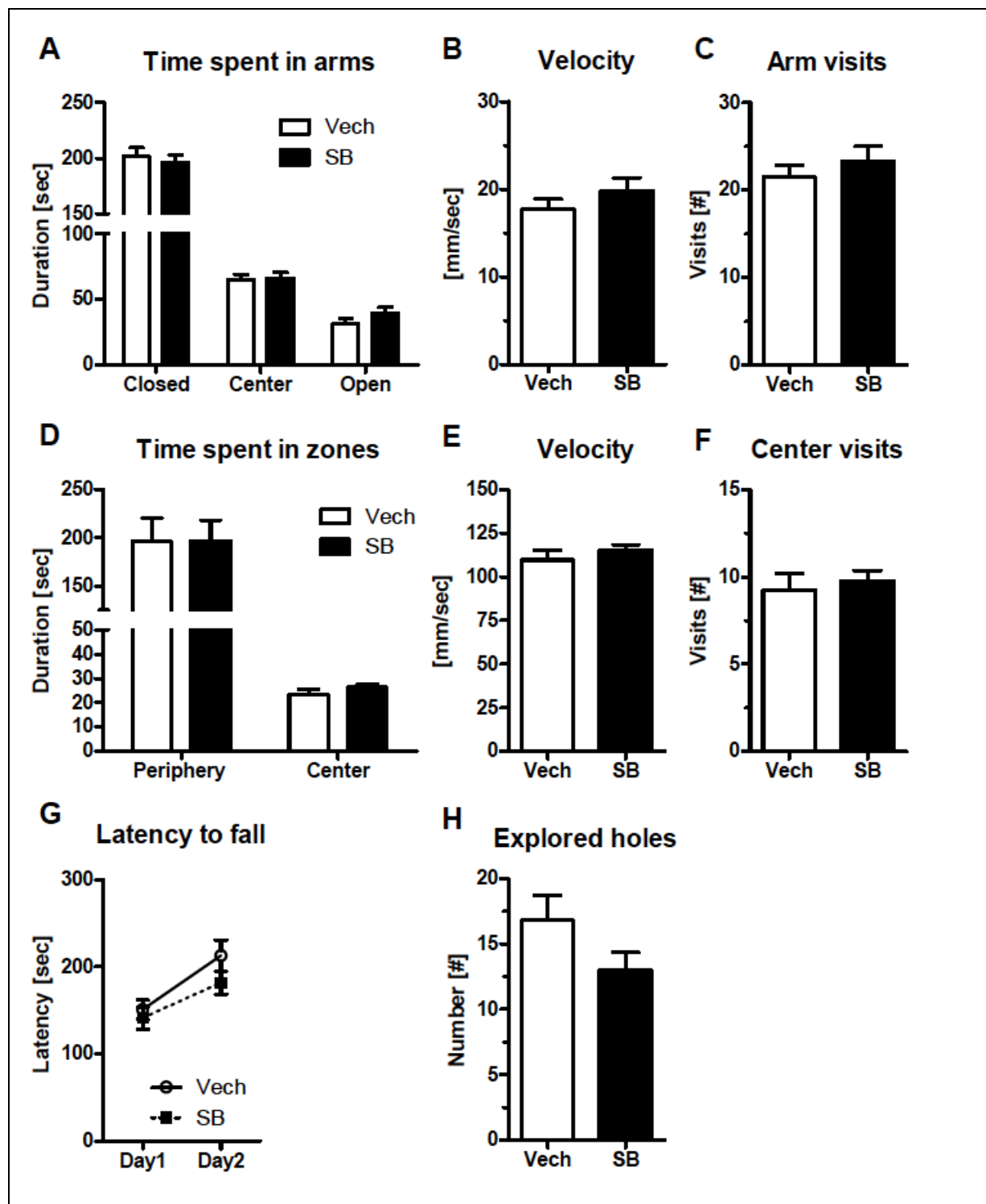


Fig. 13 Treatment of adult mice with SB656104-A does not change basic behavior

A-C. Elevated plus maze. **D-E.** Open field test. **G.** Rotarod. **H.** Hole board test. Abbreviations: Veh - vehicle treated group; SB - SB656104-A treated group. No statistically significant differences were detected. Experiments were carried out in collaboration with Konstantin Radyushkin and Ahmed El-Khordi.

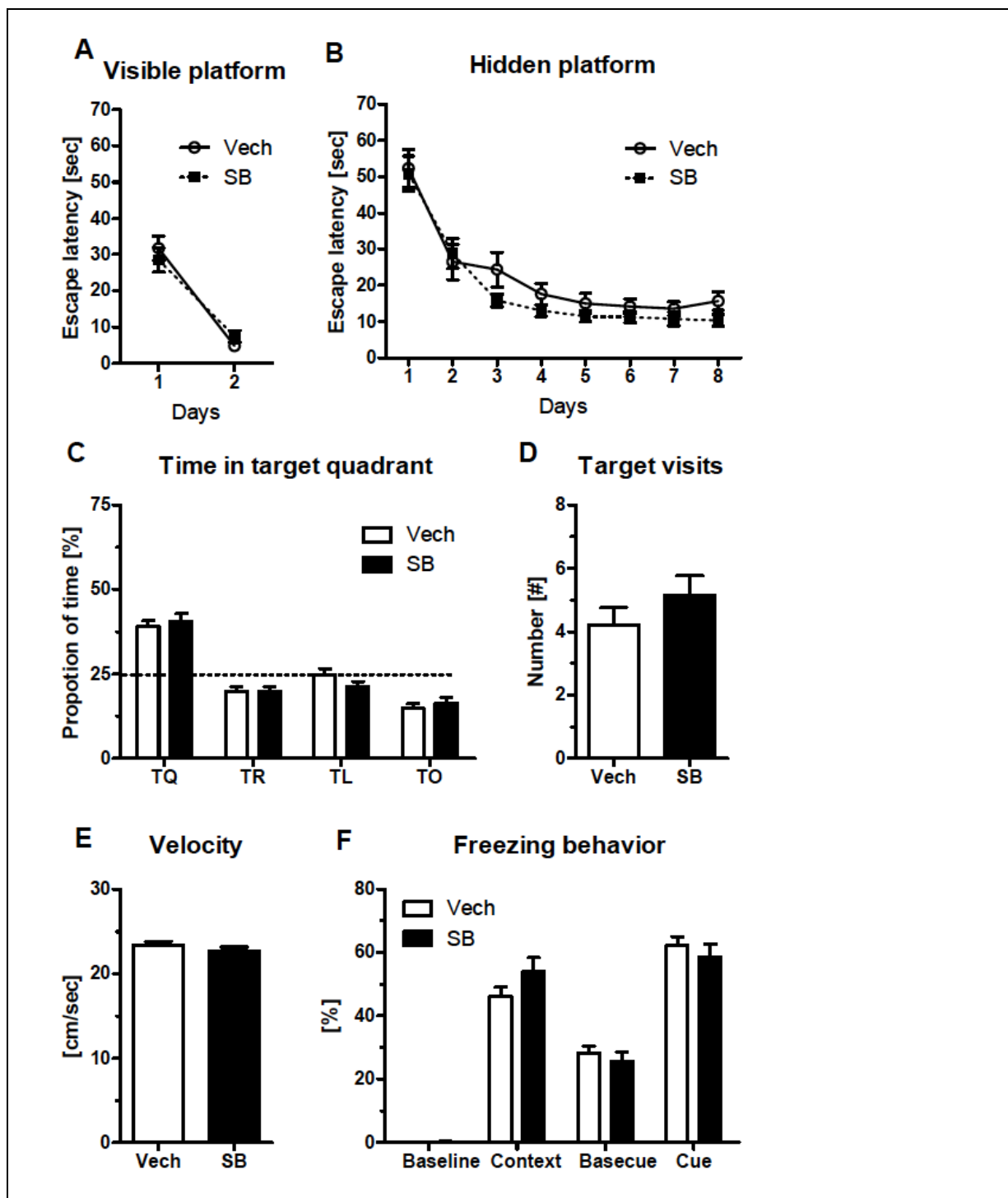


Fig. 14. Chronic treatment of adult mice with SB656104-A does not change learning and memory in Morris water maze and fear conditioning

Water maze: **A** – visible platform task; **B** – hidden platform task; **C** – time spent in quadrants during probe trial; **D** – visits of the former target location during probe trial; **E** – probe trial swimming velocity. **F** – cued and contextual fear conditioning. Abbreviations: Veh – vehicle treated group; SB – SB656104-A treated group. No statistically significant differences detected. Experiments were carried out in collaboration with Konstantin Radyushkin and Ahmed El-Khordi.

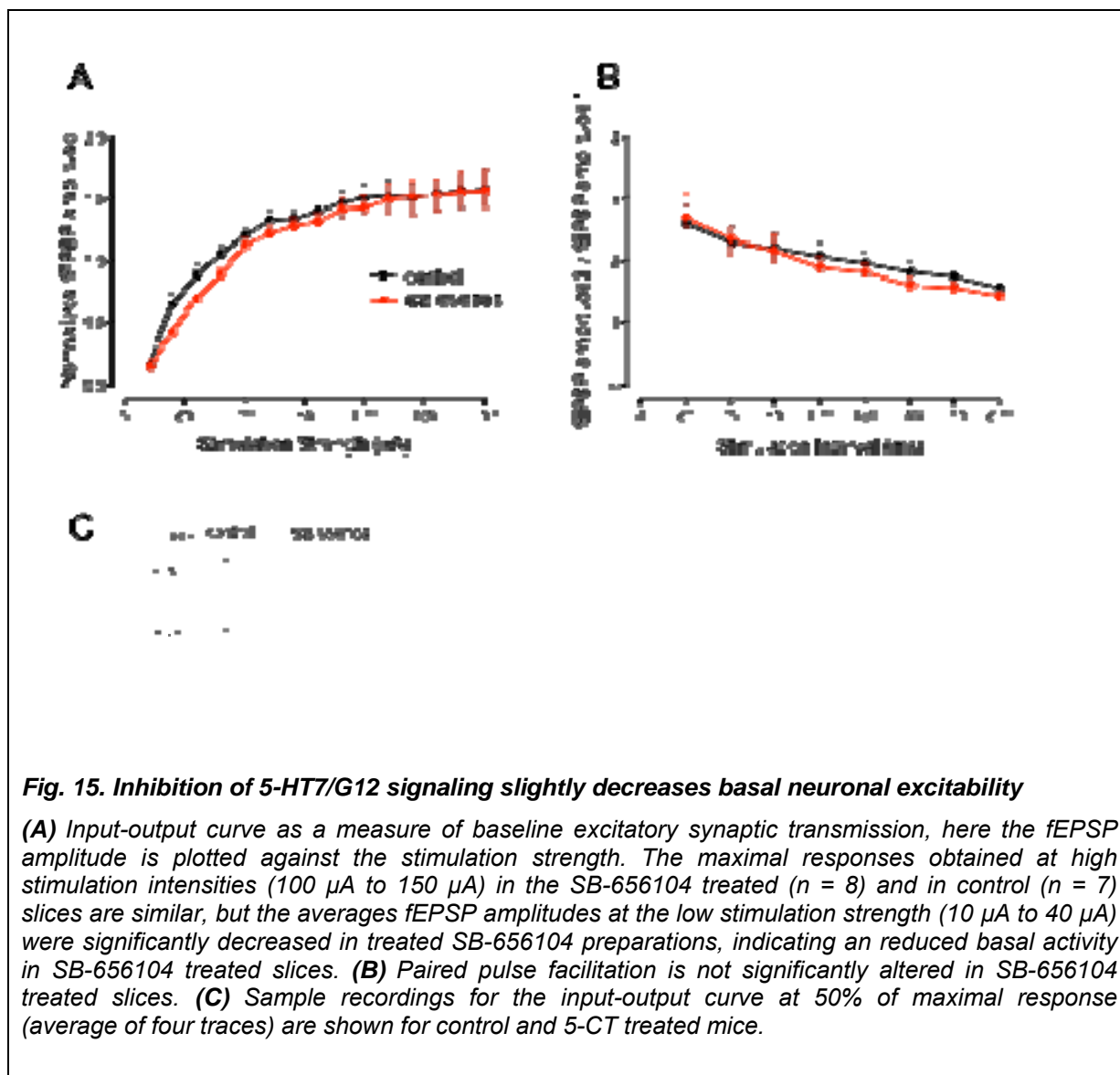
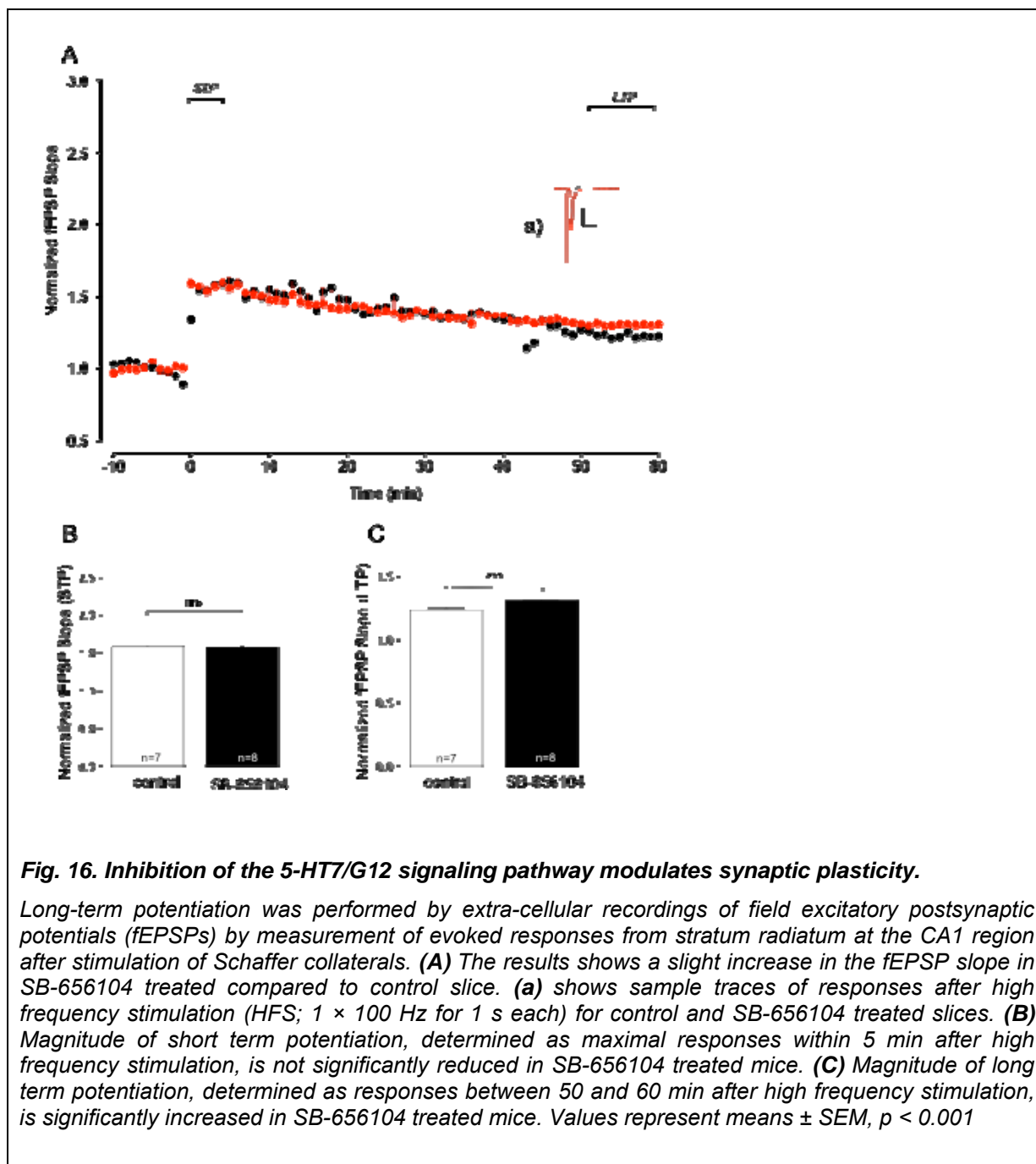


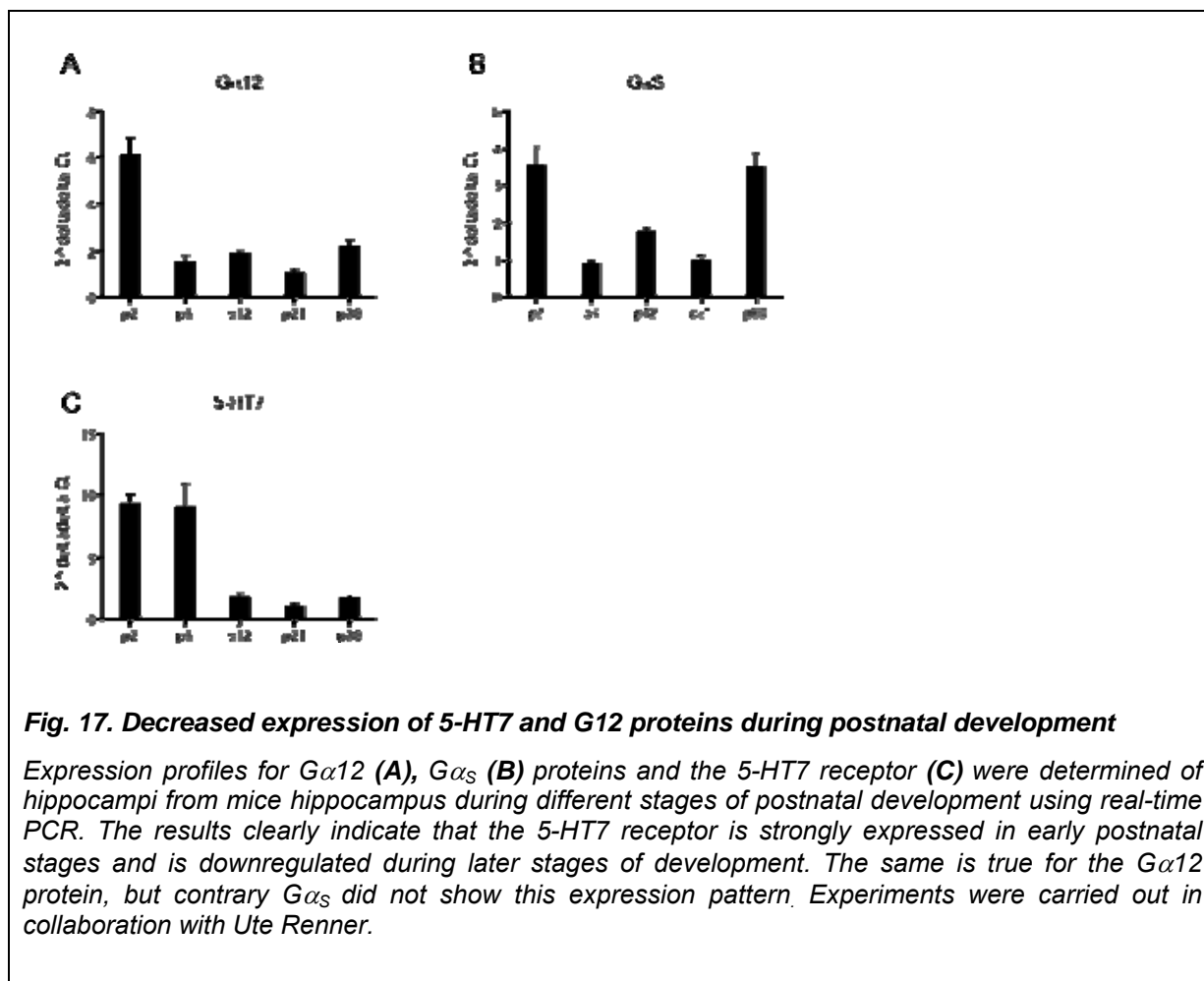
Fig. 15. Inhibition of 5-HT7/G12 signaling slightly decreases basal neuronal excitability

(A) Input-output curve as a measure of baseline excitatory synaptic transmission, here the fEPSP amplitude is plotted against the stimulation strength. The maximal responses obtained at high stimulation intensities (100 μ A to 150 μ A) in the SB-656104 treated ($n = 8$) and in control ($n = 7$) slices are similar, but the averages fEPSP amplitudes at the low stimulation strength (10 μ A to 40 μ A) were significantly decreased in treated SB-656104 preparations, indicating an reduced basal activity in SB-656104 treated slices. (B) Paired pulse facilitation is not significantly altered in SB-656104 treated slices. (C) Sample recordings for the input-output curve at 50% of maximal response (average of four traces) are shown for control and 5-CT treated mice.



3.1.8 Expression of 5-HT7 and G12 proteins is decreased during postnatal development

While the experiments performed in dissociated and organotypic hippocampal preparations clearly demonstrated the importance of 5-HT7/G12 signaling for modulation of neuronal morphology and functions, only moderate behavioral and electrophysiological effects were obtained *in vivo*. One possible explanation for such discrepancies may be developmental changes in the expression level of protein(s) involved in the 5-HT7/G12 signaling pathway. Therefore, we determined the expression profile for both 5-HT7 receptor and G α 12 protein in the mice hippocampus during different stages of postnatal development using real-time PCR. The 5-HT7 receptor transcripts were strongly expressed at early postnatal stages (P2 and P6) and down-regulated (up to 9 fold) during later development (Fig. 9). Similar expression profiles were obtained for the G α 12 protein. Contrary to that, expression level of the G α s protein, which can also be activated by the 5-HT7 receptor, was not significantly modulated during development (Fig. 9). Furthermore, expression analysis of other Gs- and G12/13-coupled serotonin receptor, 5-HT4, (Ponimaskin et al., 2002b) revealed that the amount of receptor mRNA does not undergo strong variation during development. Thus 5-HT7 and G12 proteins display dynamic expression patterns characterized by the strong and transient expression during early postnatal stages of the hippocampal development. Such changes in the expression level may also explain the diminished functional effects obtained upon modulation of 5-HT7/G12 signaling pathway in adult mice.



3.2 Oligomerization of the 5-HT1A receptor

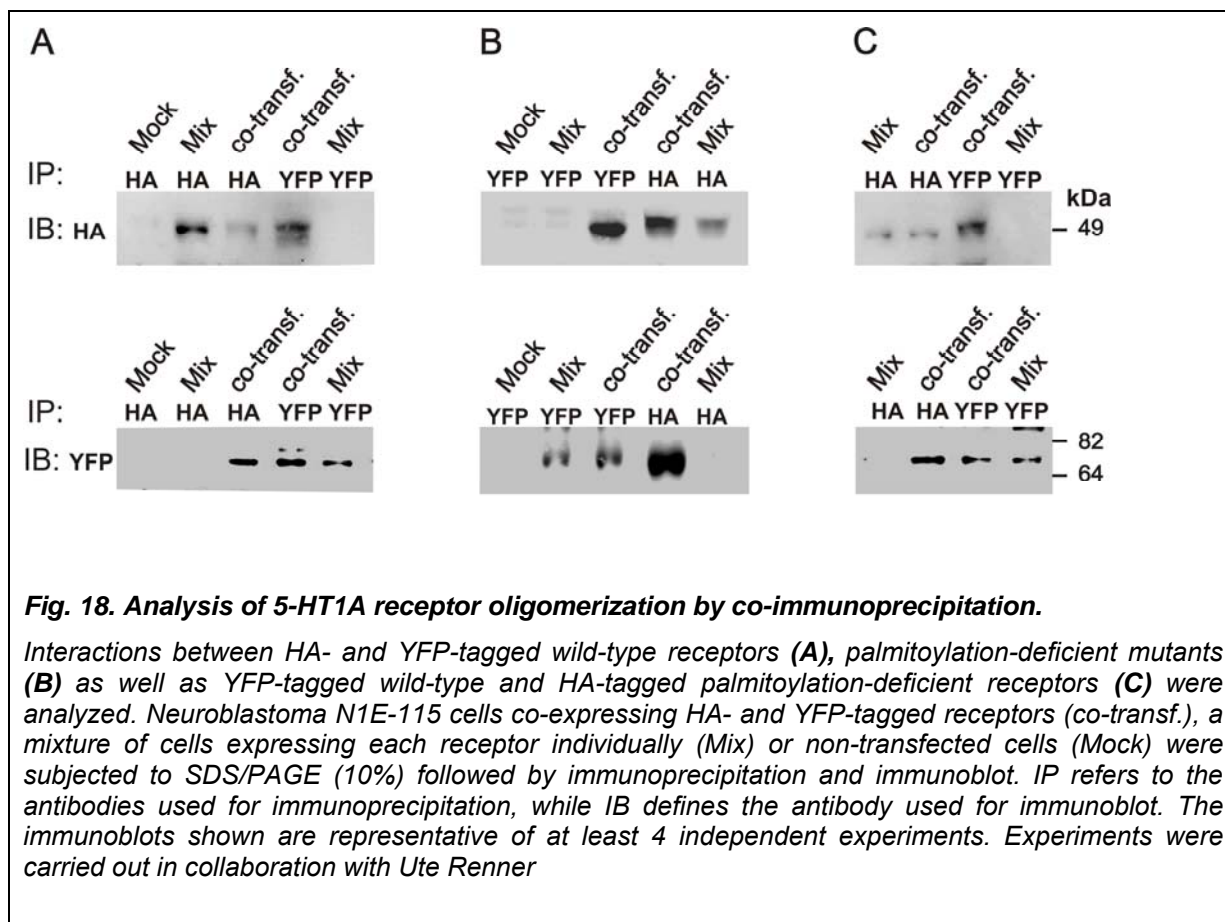
3.2.1 Biochemical analysis of 5-HT1A receptor oligomerization.

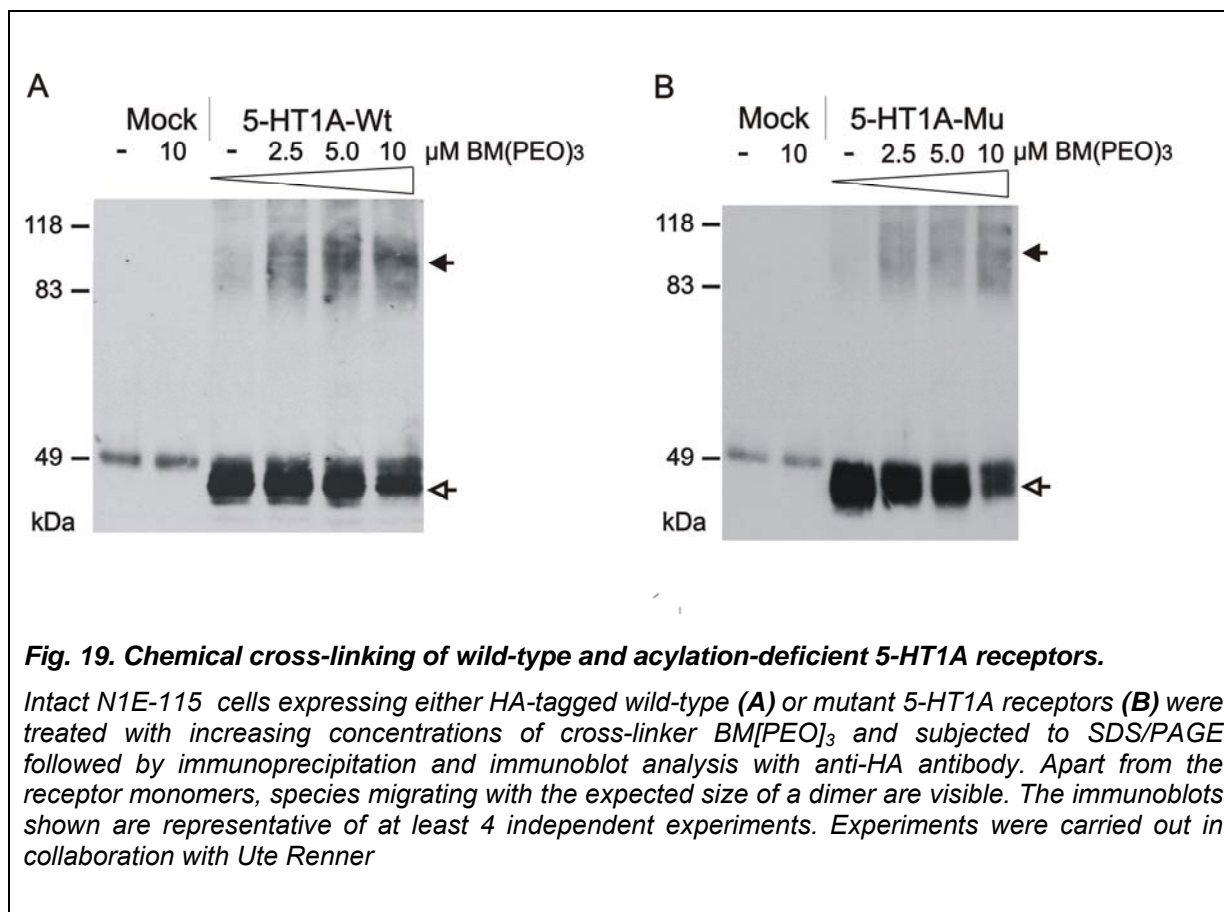
“In order to determine whether the 5-HT1A receptor undergoes oligomerization, we applied a co-immunoprecipitation assay to N1E-115 mouse neuroblastoma cells co-expressing HA- and YFP-tagged receptors. The HA-tagged 5-HT1A receptor has a molecular weight of approximately 48 kDa (Fig. 18, *upper panel*), while the molecular weight of YFP-tagged receptors is shifted to 74 kDa (Fig. 18, *lower panel*). Figure 1A also shows that after immunoprecipitation with an antibody against HA-tag, YFP-immunoreactive receptor bands were identified only in samples derived from cells co-expressing both HA- and YFP-tagged receptors. Equal results were obtained after initial immunoprecipitation of cell lysates with an anti-YFP antibody followed by immunoblotting with an anti-HA-tag antibody (Fig. 18A). To exclude the possibility that the identified bands represent artificial protein aggregates, cells expressing only one type of receptor (HA- or YFP-tagged) were mixed prior to lysis and analyzed in parallel as a control. As shown in Figure 18, individual receptors can be precipitated and detected by the same antibody, whereas co-immunoprecipitation did not occur, supporting specificity of 5-HT1A receptor oligomerization.

We have recently shown that the 5-HT1A receptor is modified by covalently attached palmitate (Papoucheva et al., 2004). Therefore, we analyzed the impact of palmitoylation on receptor oligomerization. Figure 18B und 18C demonstrate that differently tagged 5-HT1A receptors were efficiently co-immunoprecipitated independently of their acylation state.

To investigate 5-HT1A receptor oligomerization in a physiological environment, N1E-115 cells expressing either wild-type or acylation-deficient HA-tagged receptors were treated with chemical cross-linker BM[PEO]₃. This homobifunctional cross-linker interacts with sulfhydryl groups on polypeptides to form stable thioether linkages that induces an irreversible cross-linking of proteins located within close proximity (app. 15 Å) of each other. It is notable that the plasma membrane is impermeable for BM[PEO]₃, allowing oligomerization analysis of the receptors localized on the cell surface of intact cells. Immunoblotting analysis of N1E-115 cells expressing the wild-type or the palmitoylation-deficient receptors revealed that, in the

absence of cross-linker, the majority of 5-HT_{1A} receptors is detectable as monomers, while only a minor fraction migrating as a band with molecular weight of app. 95 kDa, which is the molecular weight predicted for a dimer (Fig. 19A). Treatment of intact cells with increasing concentrations of cross-linker leads to a decline of the amount of monomers that is accompanied by an increase in the dimer population. Similar results were also obtained for the acylation-deficient mutant (Fig. 19B).



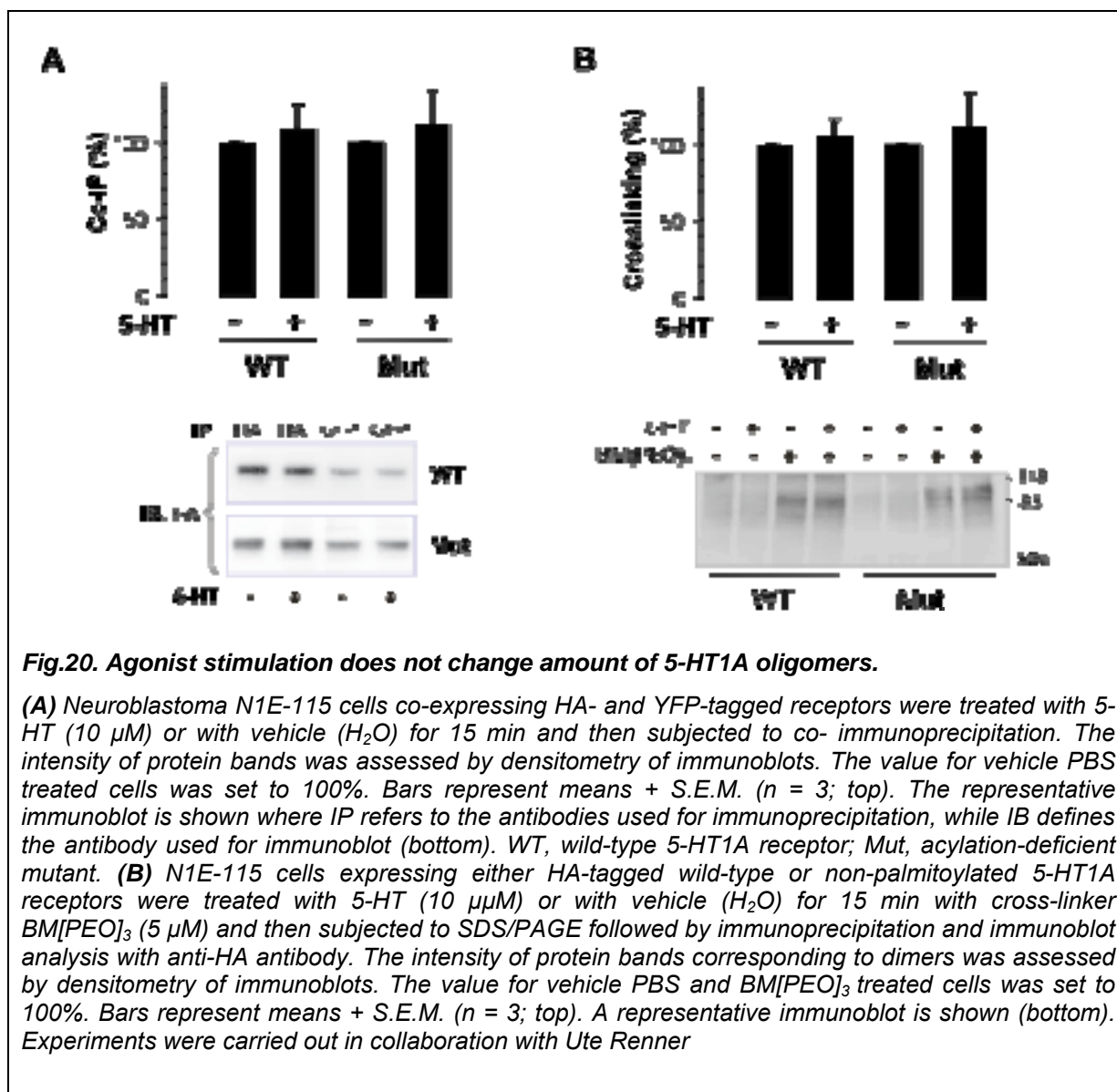


To analyze effect of agonist stimulation on receptor oligomerization, N1E-115 cells expressing wild-type or acylation-deficient 5-HT1A receptors were treated with 5-HT at 10 μM concentration followed by co-immunoprecipitation or cross-linking analysis. Figure 3A demonstrates that stimulation of either wild type or non-palmitoylated receptors with agonist does not change amount of co-immunoprecipitated receptors. Similar results were also obtained after application of cross-linker BM[PEO]₃ to the simulated and non-stimulated cells (Fig. 20B), demonstrating that the oligomerization state of 5-HT1A receptor is not modulated upon agonist stimulation. Experiments were carried out in collaboration with Ute Renner.

3.2.2 Acceptor photobleaching analysis of 5-HT1A receptor oligomerization.

Förster Resonance Energy Transfer (FRET) is a powerful biophysical approach for the quantitative analysis of protein-protein interactions (Lakowicz, 2006). To determine whether FRET could be measured in the plasma membrane of living cells co-expressing 5-HT1A-CFP and 5-HT1A-YFP fusion proteins, a confocal microscopy-based acceptor photobleaching

method was applied to transfected N1E-115 cells. To avoid artefacts resulting from overexpression, we adjusted the total expression level for the CFP- and YFP-tagged receptor to 1.000 - 1.200 fmol/mg proteins in all following FRET experiments, which allows for



quantitative analysis of results obtained in different experiments. Moreover, similar amounts of endogenous 5-HT1A receptors has been obtained in hippocampus under physiological conditions (Pazos and Palacios, 1985; Hoyer et al., 1986).

CFP and YFP were excited simultaneously with a 458 nm laser line. Fluorescence emission was acquired at multiple wavelengths using the LSM510-Meta detector allowing for the linear

unmixing of the CFP and YFP emission spectra. Confocal microscopy performed after the transfection of N1E-115 cells revealed that the majority of YFP and CFP tagged 5-HT1A receptors were localized in the plasma membranes with only a minor fraction existing in the intracellular compartments (Fig. 21A).

To perform acceptor photobleaching, a defined region of plasma membrane was selectively illuminated using a 514 nm laser line. A 458/514 nm dual dichroic mirror was used to allow rapid image acquisition before and immediately after photobleaching. Figure 21A shows the bleached region of interest with a loss of YFP intensity as well as a reference region of interest from which the acquisition bleaching rate was determined for correct FRET calculation. Figure 21B illustrates the changes in emission intensities of donor and acceptor fluorescence in the bleached region of interest demonstrating that with the loss of acceptor fluorescence there is a corresponding increase of donor emission intensity that is characteristic of FRET. In contrast, intensities of both CFP and YFP fluorescence of non-bleached regions undergo only minor decrease, reflecting acquisition bleaching (Fig. 21C).

Finally, apparent FRET efficiency Ef_D was calculated according to Eq.1, where F_{DA} is the pre-bleach and F_D is the corrected post-bleach donor fluorescence according to Eq. 2. Data were background subtracted and corrected for acquisition bleaching using the measurements from the reference region of the plasma membrane (Fig. 21D). The wild-type receptor fusion proteins from cells with similar donor to acceptor ratios were found to have a mean apparent FRET efficiency of $16.4 \% \pm 0.7 \%$. For the negative controls obtained after co-transfection of receptor-YFP and cytosolic CFP an apparent FRET efficiency was $5.5 \% \pm 3.8\%$. To examine whether oligomerization may depend on palmitoylation state of the receptor, we made acceptor photobleaching trials in cells expressing non-palmitoylated mutants. The palmitoylation-deficient 5-HT1A receptors exhibited apparent FRET efficiency with a mean Ef_D of $23.6 \% \pm 2.9 \%$. In addition, we analyzed the interaction between wild-type receptors coupled to YFP and mutant receptors coupled to CFP. In this case a mean Ef_D value of $29.8 \% \pm 5.6 \%$ was estimated. These results indicate that 5-HT1A forms oligomers and that the extent of oligomerization depends on the palmitoylation status of the complex-forming units. Experiments were carried out in collaboration with Andrew Woehler.

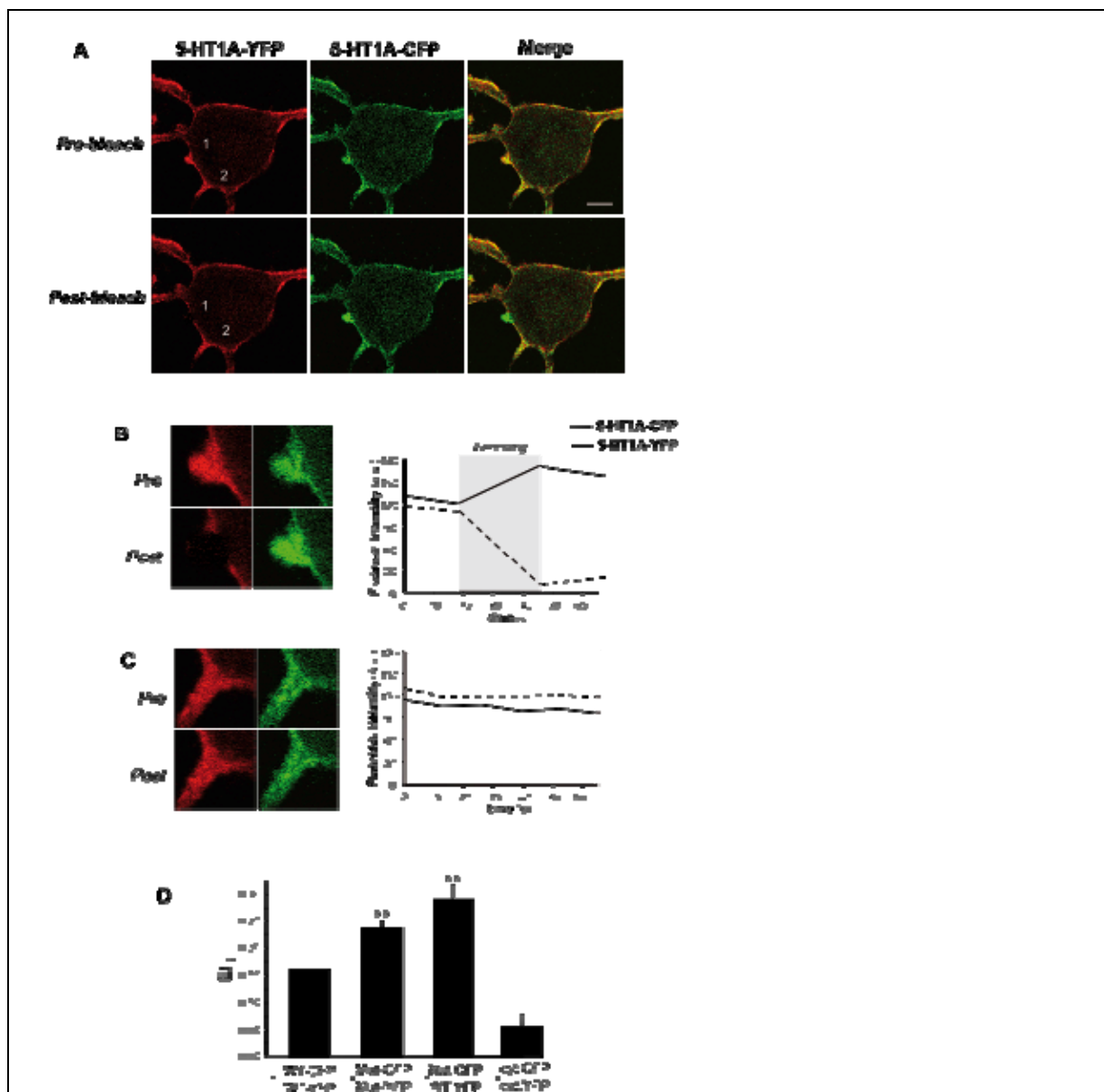


Fig. 21. Acceptor photobleaching FRET analysis of 5-HT1A oligomerization.

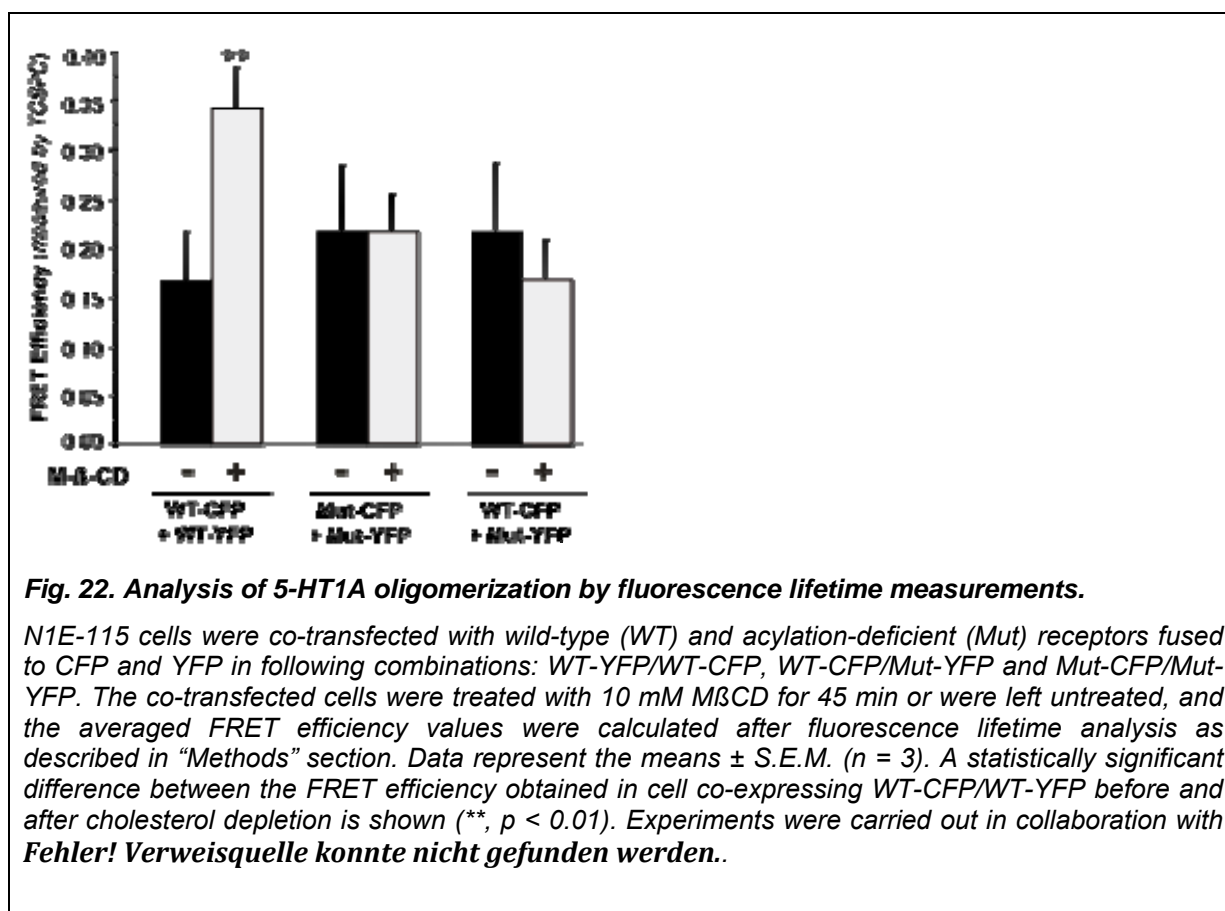
(A) Confocal microscopy was used to visualize 5-HT1A-CFP and 5-HT1A-YFP coexpressed in the plasma membrane of N1E-115 cells. Fluorescence spectra were collected from a 2 μ m optical slice and unmixed to CFP and YFP components using the Zeiss LSM510-Meta detector. The fluorescence image of the CFP channel (green), the YFP channel (red) and composite channel before and after bleaching are shown. The box 1 corresponds to the bleached regions of interest, while the box 2 corresponds to the non-bleached region of interest. Scale bar, 10 μ m. (B) Enlargement of the box 1 is shown on the left. The 12-bit grayscale intensities of YFP and CFP during the whole trial are plotted for the bleached region of interest (right). (C) Enlargement of the box 2 is shown on the left. The 12-bit grayscale intensities of YFP and CFP during the whole trial are plotted for the non-bleached region of interest (right). (D) Apparent FRET efficiency E_f^D was calculated according to Eq. 1 and 2. Data represent the means \pm S.E.M. from at least five independent experiments. Cells co-expressing cytosolic CFP and YFP were used as a negative control. A statistically significant difference between the FRET values obtained in cell co-expressing WT-CFP/WT-YFP and Mut-CFP/Mut-YFP or Mut-CFP/WT-YFP are indicated (**, $p < 0.01$). Mut, acylation-deficient 5-HT1A mutant. Experiments were carried out in collaboration with Andrew Woehler.

3.2.3 Analysis of receptor oligomerization by fluorescence lifetime FRET measurements.

In addition to acceptor photobleaching, we quantified the FRET efficiency (E) in living cells by measuring fluorescence lifetime of tagged 5-HT1A receptors. N1E-115 cells were transfected either with 5-HT1A receptor fused to CFP or co-transfected with wild-type (WT) and acylation-deficient (Mut) receptors fused to CFP and YFP to create appropriate donor/acceptor pair at the ratio 1:1 in following combinations: WT-YFP/WT-CFP, Mut-CFP/Mut-YFP and WT-CFP/Mut-YFP. The fluorescence decays of donor fusion proteins were measured by time-correlated single photon counting as described in Experimental Procedures. Experimental decay curves were analyzed and mean value of fluorescence lifetime was calculated. The averaged fluorescence lifetime value calculated for CFP fused with receptor was found to be $\tau_D = 2.01 \pm 0.05$ ns. The decay kinetic of CFP in the cells expressing different receptor combinations was strongly affected by the presence of acceptor (YFP) leading to a shortening of the lifetime. Fluorescence lifetimes were found to be $\tau = 1.67 \pm 0.11$ ns, $\tau = 1.56 \pm 0.16$ ns and $\tau = 1.57 \pm 0.2$ ns for WT-CFP/WT-YFP, Mut-CFP/Mut-YFP and WT-CFP/Mut-YFP, respectively. FRET efficiency was calculated from these average lifetimes using the equation $E = 1 - (\tau_D / \tau)$, and was determined to be $E = 0.17 \pm 0.04$ for WT-CFP/WT-YFP, $E = 0.22 \pm 0.06$ for Mut-CFP/Mut-YFP, $E = 0.22 \pm 0.05$ for WT-CFP/Mut-YFP (Fig. 22). This confirms acceptor-photobleaching data and demonstrates that FRET efficiency for oligomers composed by acylation-deficient mutants as well as for mixed oligomers (i.e. combined by wild-type and mutant) is increased in comparison to the wild-type oligomers.

We have recently shown that a significant fraction of the 5-HT1A receptor resides in membrane rafts, while the yield of the palmitoylation-deficient receptor in these membrane microdomains is considerably reduced (Renner et al., 2007). To analyze the role of lipid raft localization of 5-HT1A receptor for its oligomerization we measured the fluorescence lifetime after treatment of transfected cells with methyl- β -cyclodextrin (M β CD). The cholesterol-binding reagent M β CD was previously shown to disrupt the cholesterol-enriched membrane subdomains by depletion of cholesterol from the plasma membrane (Harder et al., 1998).

Destroying of lipid rafts resulted in shortening of fluorescence lifetime only in case of WT-CFP/WT-YFP ($t = 1.33 \pm 0.05$ ns), leading to significant increase of FRET value to $E = 0.34 \pm 0.02$ (Fig. 5). In contrast, FRET efficiency calculated for Mut-CFP/Mut-YFP and WT-CFP/Mut-YFP was not affected by cholesterol depletion and was determined to be $E = 0.22 \pm 0.02$ ($t = 1.56 \pm 0.06$ ns) and $E = 0.16 \pm 0.03$ ($t = 1.68 \pm 0.1$ ns), respectively (Fig. 22). Experiments were carried out in collaboration with **Fehler! Verweisquelle konnte nicht gefunden werden.**



3.2.4 Spectrometric detection of FRET between 5-HT1A receptors in living cells.

We further examined FRET occurrence between fluorophore-labeled 5-HT1A receptors in living cells by analysis of emission spectra collected with a spectrofluorometer. Figure 23 shows the typical fluorescence emission spectra at 420 nm excitation obtained in N1E-115

cells expressing WT-CFP, WT-YFP or co-expressing WT-CFP and WT-YFP as a FRET pair. The spectral contaminations due to light scattering and nonspecific fluorescence of cells were taken into account by subtracting the emission spectra of HA-tagged receptor cells (background) from each measured spectra. When cells were transfected with only CFP-fused receptor, the typical emission spectrum of CFP with emission peaks at 475 nm and 500 nm was obtained (Fig. 23A). The emission spectrum obtained for cells expressing only YFP-fused receptor was similar to that obtained in HA-tagged receptor cells with only a very weak peak at 525 nm. In contrast, cells co-expressing WT-CFP and WT-YFP receptors demonstrated a significantly larger emission peak at 525 nm concomitant with a smaller CFP emission, which demonstrates the energy transfer from CFP to YFP (Fig. 23A). Similar results were also obtained when cells were co-transfected with acylation-deficient 5-HT1A mutant (Fig. 23B). This data confirms the oligomerization of 5-HT1A receptors in living cells.

3.2.5 Specificity of 5-HT1A receptor oligomerization.

The apparent FRET efficiency, Ef_D , measured by acceptor photobleaching is inherently dependent on f_D , the fraction of donor participating in FRET complexes. This is in turn dependent upon the ratio of intact donor concentration to intact acceptor concentration present in the sample. It has been therefore suggested that the dependence of Ef_D on $[A^t]/[D^t]$ may be useful in differentiating FRET resulting from specific vs. random interactions (Hagan et al., 2000; Herrick-Davis et al., 2004; Herrick-Davis et al., 2005; James et al., 2006). In the case of random interaction, Ef_D has been predicted to be independent of the total donor to acceptor ratio at a fixed surface density above a certain ratio. For receptor dimers, Ef_D values are expected to be dependent on the relative donor concentration at a higher $[A^t]/[D^t]$ threshold, resulting in a higher asymptotic Ef_D value.

To analyze whether the measured apparent FRET efficiency reflects specific receptor-receptor interaction or resulted from random molecular interaction, Ef_D values were measured over a range of acceptor to donor ratios, wherein the combined concentration of plasmids encoding for donor and acceptor was held constant. Figure 24A shows Ef_D values obtained for wild-type 5-HT1A receptors plotted against the $[A^t]/[D^t]$ ratio. As a negative

control we used co-transfections of non-interacting cytosolic CFP and YFP proteins. Ef_D values obtained for cytosolic CFP and YFP and the corresponding $[A^{\dagger}]/[D^{\dagger}]$ ratio were fitted according to the equation 6. Evaluation of the fit quality clearly shows that data obtained from the co-transfected cytosolic CFP/YFP ($R^2 = 0.37$) cannot be properly characterized by a model assuming specific oligomerization. This demonstrates that detected FRET resulted from non-specific, random interactions. Using this as a negative control for oligomerization, we analyzed the data collected for the cells co-transfected with 5-HT1A-CFP and 5-HT1A-YFP receptors. In this case, we found that Ef_D values were substantially higher (Fig. 24A), and Eq. 6 provides a very good fit quality of Ef_D data ($R^2 = 0.90$). Furthermore, in a proper fit to the proposed model, experimentally measured Ef_D value at a donor/acceptor ratio of 1:1 should represent half of the asymptotic value for Ef_D . In the case of receptor we found that the Ef_D values at a ratio of 1:1 was approximately 0.12, which corresponds to the obtained asymptotic value for the fit of approximately $Ef_D = 0.24$ (Fig. 24A). In contrast, the Ef_D value measured for co-transfected CFP and YFP at a ratio of 1:1 was equal to 0.025, which is a clear underestimate when compared to the fitted curve (Fig. 24A). Similar results were also obtained after analysis of Ef_A values (Fig. 25) and for cells co-transfected with Mut-CFP/WT-YFP and Mut-CFP/Mut-YFP combinations (data not shown).

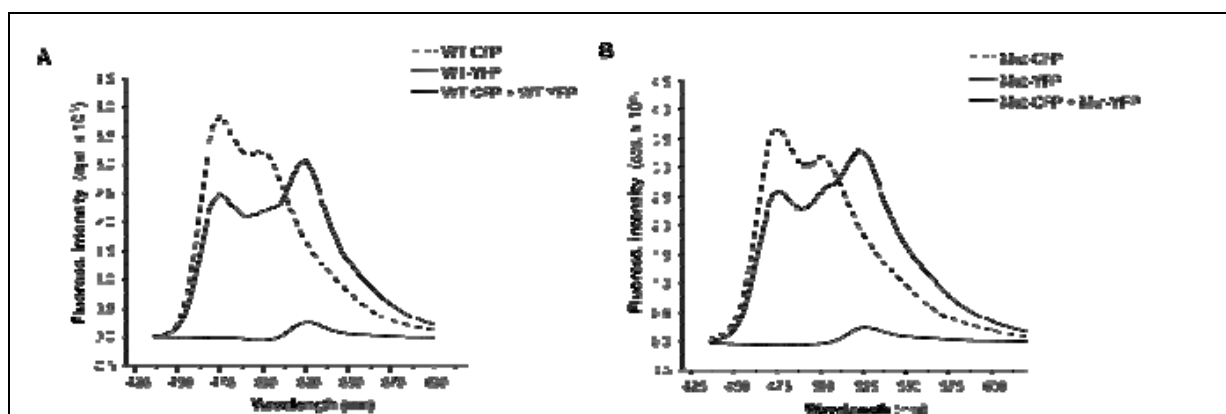


Fig. 23. Spectral analysis of living N1E-115 cells co-expressing CFP- and YFP-tagged 5-HT1A receptors.

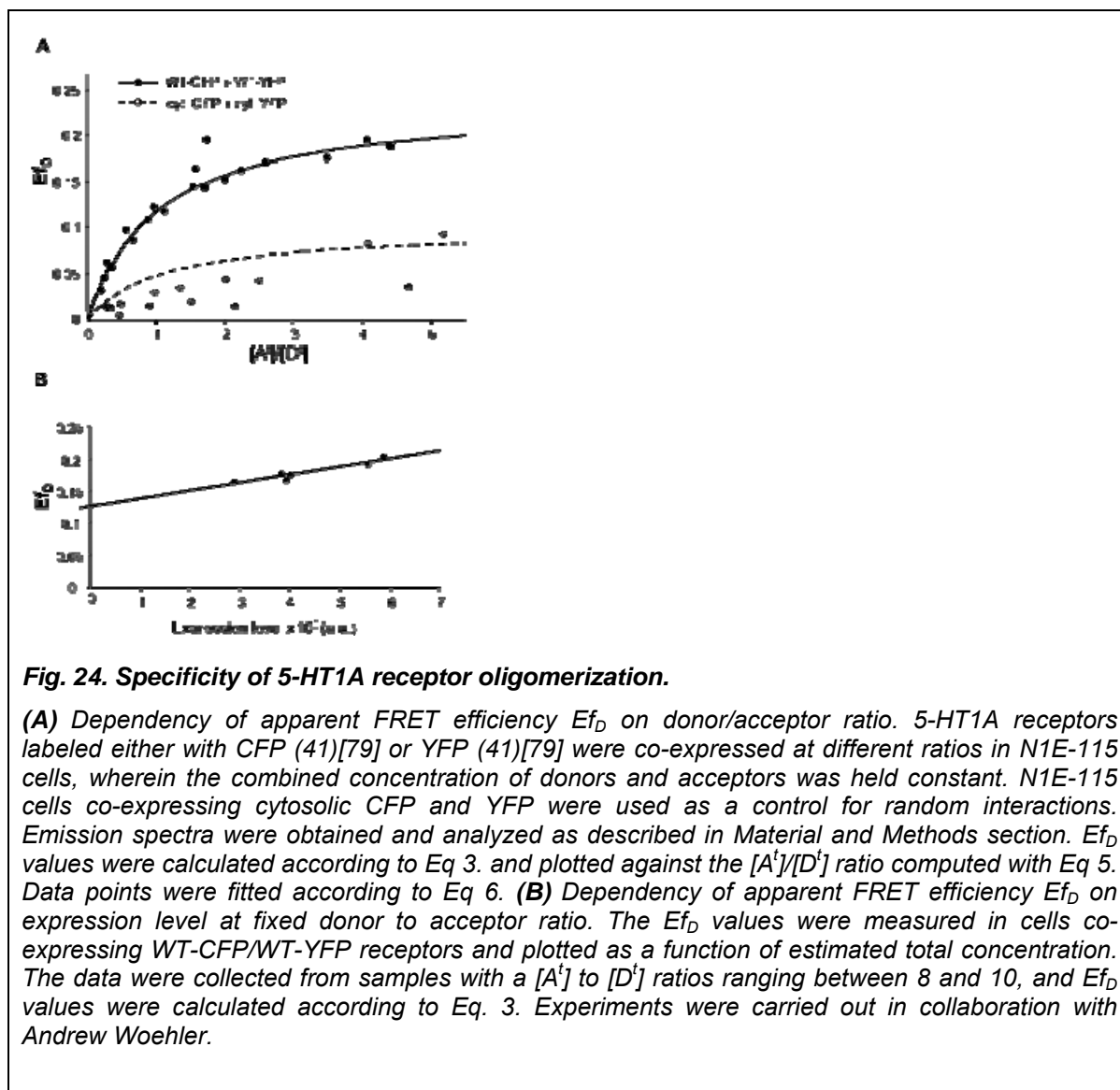
Fluorescence emission spectra of N1E-115 cells transfected with wild-type (A) or acylation-deficient (B) 5-HT1A receptors are shown. In both cases cells were transfected either with only CFP- (dashed line) or only with YFP-tagged (dotted line) receptors or were co-transfected with both YFP- and CFP-tagged receptors (solid line). Emission spectra were collected at excitation wavelength $\lambda_{exc} = 420$ nm. Spectra were normalized to that obtained in cells transfected HA-tagged 5HT1A receptor. The data shown are representative of at least 3 independent experiments

Interaction specificity may also be analyzed by plotting energy transfer efficiency as a function of expression level at fixed donor/acceptor ratio (James et al., 2006). In the case of random interaction, the energy transfer between two fluorophores is linearly dependent on expression level and will diminish to zero at very low concentration of fluorophores. In the case of completely non-random interaction, the apparent FRET efficiency should be independent on concentration with an Ef_D intercept greater than zero. Fig. 24B shows Ef_D values measured in cells co-expressing WT-CFP/WT-YFP receptors and plotted as a function of estimated total concentration. The analysis revealed that a linear fit resulted in an Ef_D intercept at 0.13, confirming non-random interactions between the receptors. The fit also shows a slightly positive slope suggesting that in addition to the specific interactions, there is some contribution of random interaction to the measured Ef_D . Finally, two different types of analysis applied here confirm the specificity of 5-HT1A receptor oligomerization.

3.2.6 Quantitative analysis of oligomerization dynamics in living cells.

To investigate the effect of receptor activation on 5-HT1A oligomerization, we applied a novel FRET approach named lux-FRET (linear unmixing of FRET spectral components) (Włodarczyk et al., 2008), which allows quantitative measurements of oligomerization during receptor stimulation with agonist. To evaluate time- and activation-correlated changes in receptor interaction, apparent FRET efficiencies measured from N1E-115 cells co-expressing 5-HT1A fusion proteins were monitored over time before and during incubation with agonist and/or antagonist. Cells were co-transfected with donor (5-HT1A-CFP) and acceptor (5-HT1A-YFP) proteins at a 1:1 ratio and emission spectra were recorded every 2 min using excitation wavelengths of 458 nm and 488 nm. For each time point, two quantities were determined, i.e. the product of characteristic FRET efficiency (E) and the fraction of donor participating in complexes (f_D) as well as the corresponding quantity describing the product of E and the fractions of acceptor participating in complexes (f_A). Both values characterize the stoichiometry of fluorescently labelled receptors and are used to verify the data obtained.

In the absence of receptor stimulation we obtained only slight fluctuations of Ef_D around the initial values in cells expressing wild-type 5-HT1A receptors. After treatment with serotonin at 10 μ M, the values of Ef_D continuously decreased reaching a plateau after 10 min (Fig. 26A). In contrast, cells treated with PBS, did not show any significant changes of Ef_D values (Fig. 26A). The treatment of co-transfected cells with the selective 5-HT1A receptor antagonist, WAY100635 at 1 μ M concentration blocked the agonist-mediated decrease of Ef_D (Fig. 26A).

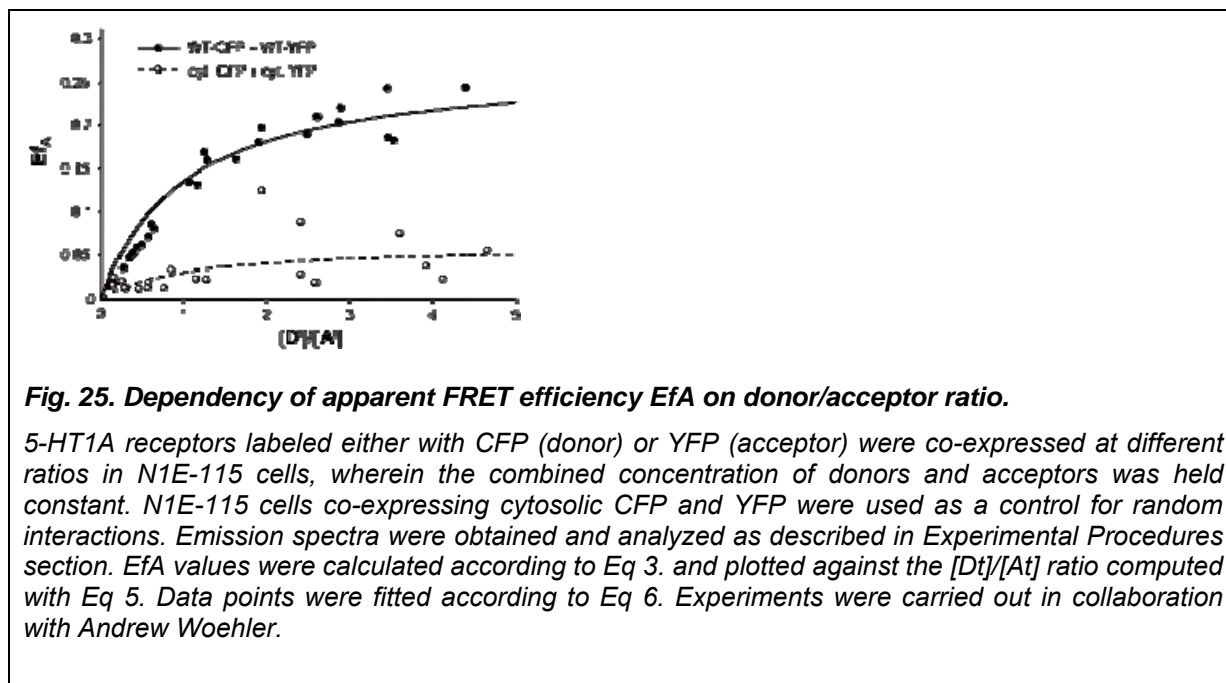


In order to quantify agonist-mediated changes of Ef_D , we chose a representative time point before adding serotonin (5 min before) and compared its value with that of a representative time point after agonist stimulation (15 min after 5-HT application) (Fig. 26B). This

comparison revealed that stimulation of the 5-HT_{1A} receptor with agonist results in a significant decrease of the Ef_D value by $12\% \pm 2.1\%$.

We also analyzed, whether the localization of receptor in lipid rafts may influence agonist-mediated decrease of Ef_D . Figure 26B demonstrates that depletion of cholesterol by treatment of cells expressing wild-type receptor with methyl- β -cyclodextrin abolished this effect, suggesting importance of lipid rafts for the agonist-mediated changes in receptor oligomerization.

Analysis of the time course of the apparent FRET efficiency in cells expressing acylation-deficient 5-HT_{1A} receptor demonstrated that non-palmitoylated receptors do not produce any significant changes of Ef_D values after agonist stimulation (Fig. 26C and D). When the wild-type receptor was co-expressed with the acylation-deficient receptor, the agonist-mediated decrease of Ef_D value was also completely abolished, demonstrating the dominant-negative effect of non-palmitoylated receptor on the dynamic changes in receptor-receptor interactions (Fig. 26E and F).



We also performed a time course analysis of Ef_A values for the wild-type and the acylation-deficient mutant. Similar to the results obtained for Ef_D , we observed a significant decrease of

Ef_A values by $15.2 \% \pm 2.9 \%$ after adding $10 \mu\text{M}$ serotonin to the cells expressing wild-type 5-HT_{1A} receptors (Fig. 27). The Ef_A values obtained for the acylation-deficient receptor mutant as well as for the combination of wild-type and non-palmitoylated mutant were not affected by the agonist treatment (Fig. 27).

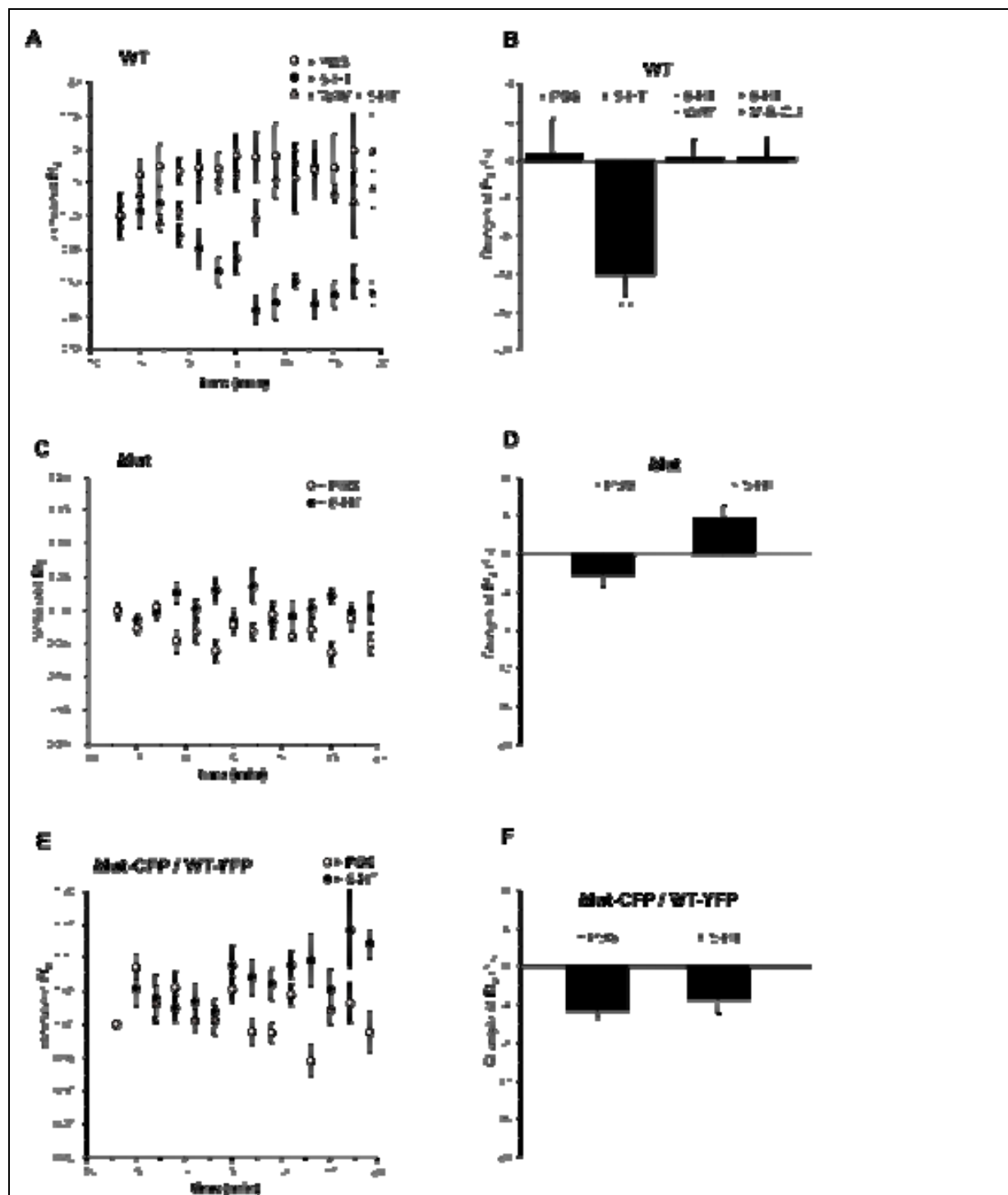


Fig. 26. Time course of FRET efficiency E_fD upon receptor stimulation.

The graphs on the left show the time course of E_fD values calculated according to Eq. (1) for N1E-115 cells co-expressing WT-CFP/WT-YFP (A), Mut-CFP/Mut/YFP (C) or Mut-CFP/WT-YFP (E) receptors as FRET pairs. The cells were treated at zero time point with serotonin (10 μ M), PBS, with serotonin together with WAY (1 μ M) or with serotonin together with MIBCD. All time-course values were normalized to unity at start for better visualization of differences. Data points represent mean \pm S.E.M. ($n = 6$). The data on the right shows percentage of changes of apparent FRET efficiency (E_fD) obtained 5 min before and 15 min after treatment for WT-CFP/WT-YFP (B), Mut-CFP/Mut-YFP (D) or Mut-CFP/WT-YFP (F). A statistically significant difference between values is noted ($\square\square$, $p < 0.01$).

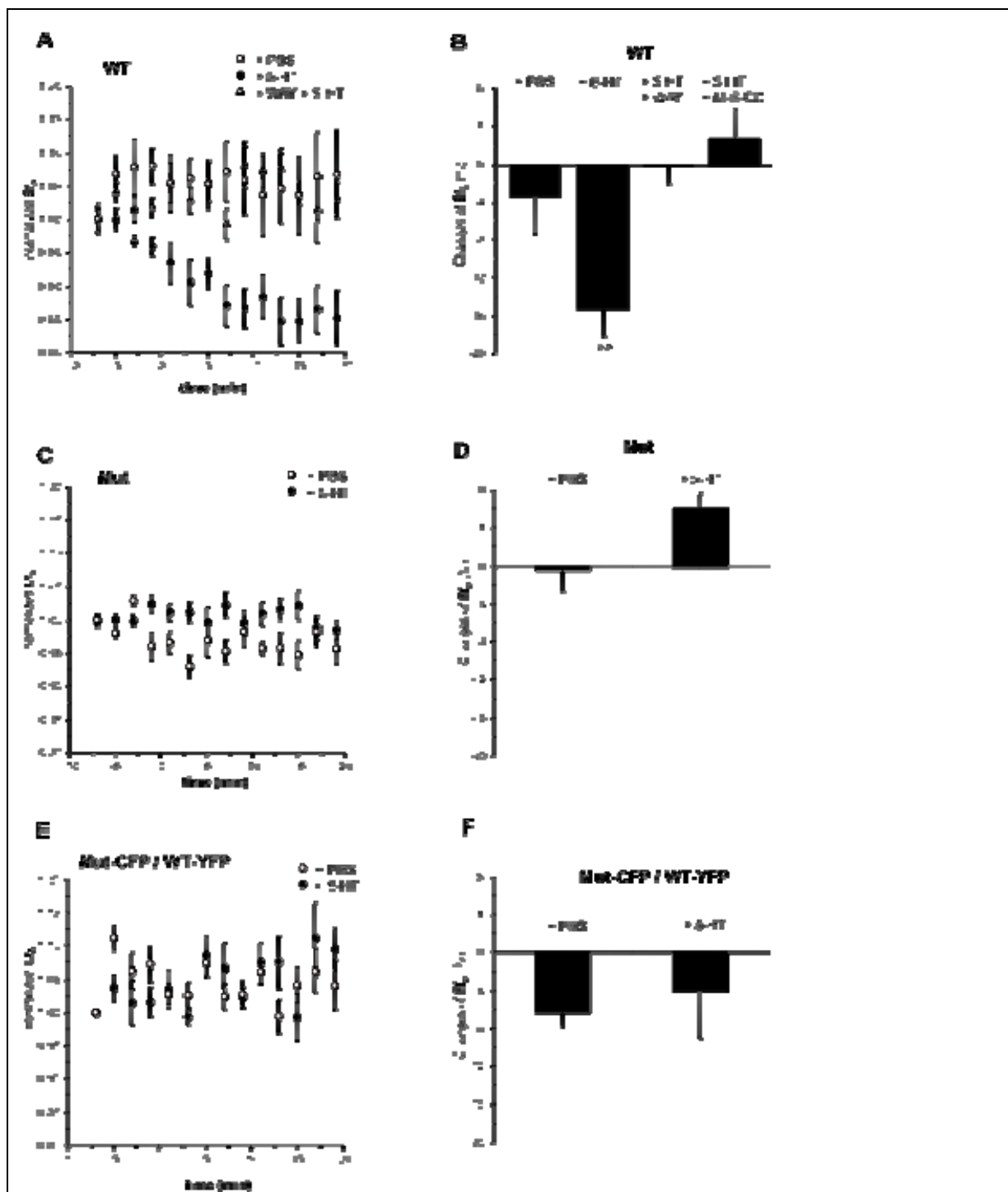
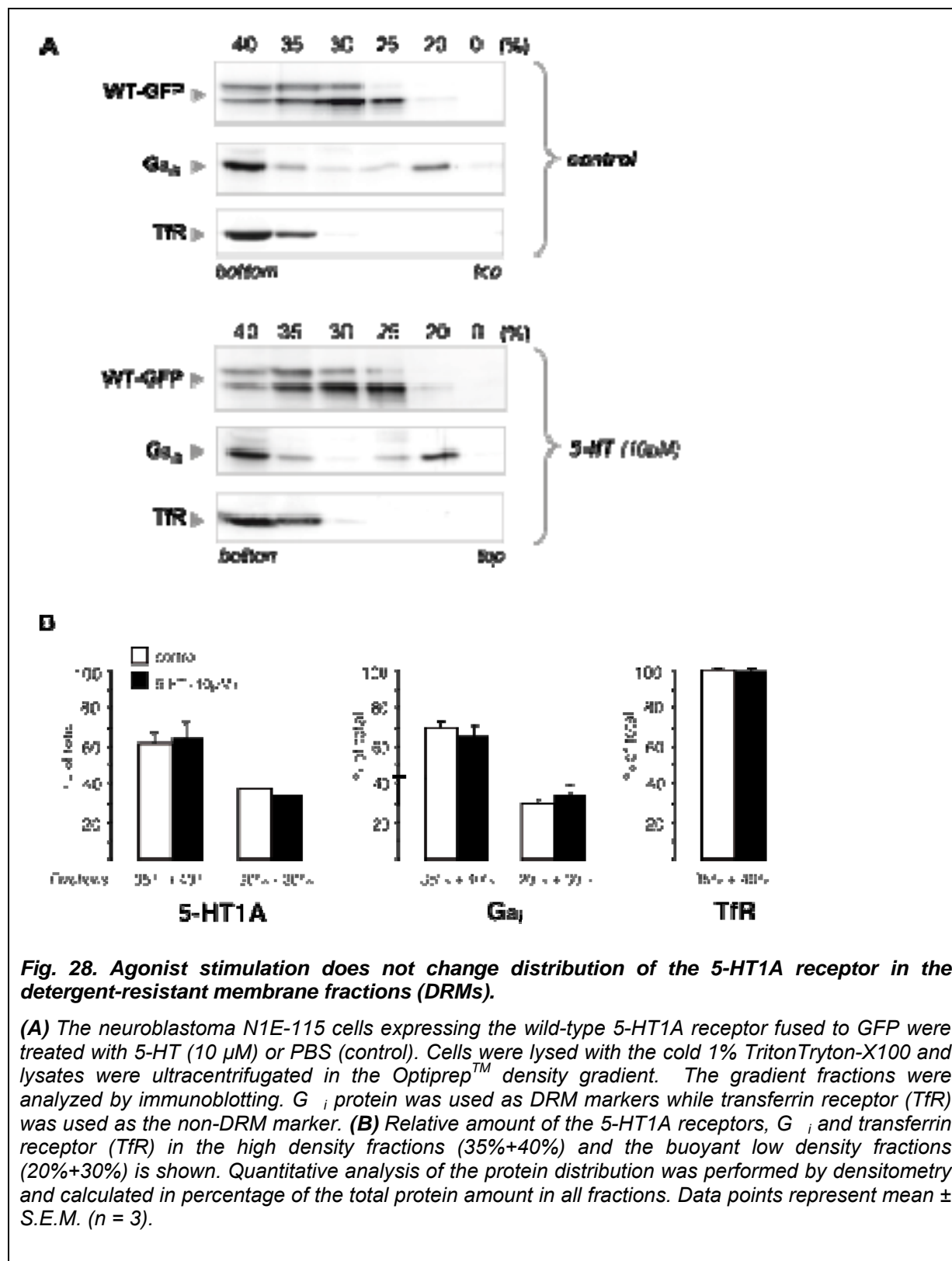


Fig. 27. Time course of FRET efficiency $E_f A$ upon receptor stimulation.

The graphs on the left show the time course of $E_f A$ values calculated according to Eq. 1 for N1E-115 cells co-expressing WT- CFP/WT-YFP (A), Mut-CFP/Mut/YFP (C) or Mut-CFP/WT-YFP (E) receptors as FRET pairs. The cells were treated at zero time point with serotonin ($10 \mu\text{M}$), PBS or with serotonin together with WAY ($1 \mu\text{M}$). All time courses values were normalized to unity at start for better visualization differences. Data points represent mean \pm S.E.M. ($n = 6$). The graph on the right shows percentage of changes of apparent FRET efficiency ($E_f A$) obtained 5 minutes before and 15 minutes after treatment for WT-CFP/WT-YFP (B), Mut-CFP/Mut/YFP (D) or Mut-CFP/WT-YFP (F). A statistically significant difference between values is noted (*, $p < 0.01$).

3.2.7 Agonist stimulation and lipid rafts localization of the 5-HT_{1A} receptor.

Results obtained in the present study suggested the importance of cholesterol-enriched membrane subdomains for receptor oligomerization (Fig. 20 and 26). Therefore, we compared the membrane distribution of the wild-type receptor before and after stimulation with agonist using density gradient centrifugation. N1E-115 cells expressing the 5-HT_{1A} receptor were solubilized in cold Triton X-100 (TX-100) and subjected to centrifugation in Optiprep™ density gradient in order to isolate detergent-insoluble membrane fractions. Immunoblot analysis of gradient fractions revealed that 38% ± 7.8% (n = 3) of the wild-type 5-HT_{1A} receptor floated with the detergent-resistant low density fractions along with the Ga_{i3}-subunit of heterotrimeric G-protein (Fig. 28). After treatment of cells with 10 μM of 5-HT, the yield of receptor in the light Triton X-100-resistant membrane fraction was not significantly changed and was found to be 34.6% ± 4.9% (n = 3; Fig. 28). Chemical cross-linking performed before the TX-100 treatment and gradient centrifugation revealed that amount of receptor oligomers in lipid rafts was not changed upon agonist stimulation (data not shown). It is also notable that distribution of the Ga_{i3} protein and the transferring receptor, which were used as rafts and non-rafts markers, respectively, did not change after agonist treatment (Fig. 28) (Kobe et al, 2008).



4 DISCUSSION

4.1 Role of 5-HT₇/G12 signaling in morpho- and synaptogenesis

4.1.1 Early structural and functional changes are modulated via the 5-HT/G12 pathway

It is widely accepted that patterns of neuronal activity play a major role in the re-organization of neuronal connection and circuits (Katz and Shatz, 1996; Maletic-Savatic et al., 1999; Jontes and Smith, 2000). However, the mechanisms driving the formation of initial (activity-independent) population of synaptic connections during early development are not entirely clear. Over the past several years it has become evident that serotonin may modulate different aspects of early neuronal differentiation, including neurite outgrowth and synaptogenesis, before it acts as a neurotransmitter (Mazer et al., 1997; Udo et al., 2005). Such morphogenic functions may be mediated by a variety of 5-HT receptor subtypes (Barnes and Sharp, 1999; Hoyer et al., 2002). We have recently demonstrated that activation of the 5-HT₇ receptor promotes neurite outgrowth in hippocampal neurons (Kvachnina et al., 2005). In the present study we demonstrated that prolonged stimulation of 5-HT₇ receptor leads to pronounced elevation in the number of dendritic protrusions. It has been proposed that dendritic filopodia participate actively in the formation of synapses, and that initial synaptogenesis may be the result of contact between dendritic protrusions and axons (Mattila and Lappalainen, 2008). Supporting this view, we found that the number of structurally intact synapses was significantly increased upon stimulation of 5-HT₇ receptor. We also observed a high degree of co-localization between the 5-HT₇ receptor and synaptic marker, which may provide a physical basis for the functional effects on synaptogenesis. The functionality of these newly formed synapses was confirmed by a marked enhancement of spontaneous neuronal activity (e.g. EPSP and spike frequency) generated in networks formed by cultured hippocampal neurons. Notably the morphogenic functions of 5-HT₇ receptors were also preserved in organotypic preparations from the hippocampus of mice. Under such *in vivo* like conditions stimulation of 5-HT₇ receptor caused pronounced

elevation of spinogenesis. These structural changes were accompanied by an increase of both basal neuronal excitability (assessed by the analysis of fEPSPs) and mPSCs amplitudes. The last observation suggests that prolonged stimulation of the 5-HT₇ receptor may initiate the boosting of synaptic strength. The mechanisms responsible for the 5-HT mediated synaptic scaling were not addressed in this study. It is known that the total synaptic strength can be regulated through changes in number of functional synapses during development (Kirov et al., 2004; Turrigiano and Nelson, 2004; Takanishi et al., 2006; Turrigiano, 2008). The coordinated changes in synaptogenesis and synaptic scaling obtained here can therefore represent a mechanism responsible for the generation of initial synaptic connections and maturation of basal synaptic circuits during the early neuronal development. The mechanisms involved, however, seem to be different from these responsible for modulation of synaptic strength obtained either by activity blockade or by increased activity (Seeburg et al., 2008; Turrigiano, 2008; Peng et al., 2009).

Analysis of synaptic plasticity revealed that the induction of LTP at the Schaffer collateral synapses was reduced upon prolonged stimulation of the 5-HT₇ receptor. How can the 5-HT₇ receptor-mediated signaling lead to an increase in synaptic transmission and to decrease in synaptic plasticity? The most straightforward explanation of this observation is that the increased basal excitability, triggered by the activation of the 5-HT₇ receptor, leads to pre-potential of synaptic transmission and thus saturates LTP, preventing further potentiation (Saghatelian et al., 2001; Jedlicka et al., 2009).

What are the possible molecular downstream mechanisms underlying the structural and functional effects of the 5-HT₇ receptor in hippocampal neurons? The 5-HT₇ receptor is coupled to two different heterotrimeric G-proteins: G_s and G₁₂ (Vanhoenacker et al., 2000). It has also been shown that both the G_s- and G₁₂-proteins can regulate the cellular morphology by activating different signaling cascades. In case of G_s morphogenic effects are realized either by modulation of cAMP concentration (Corset et al., 2000) or by the direct binding of G α_s to the cytoskeleton (Yu et al., 2009). The downstream effectors of the G₁₂ protein mediating the changes in the actin cytoskeleton are the members of the Rho family of small GTPases, including RhoA, Rac1 and Cdc42 (Jaffe and Hall, 2005). Experiments

performed in hippocampal neuronal preparations from the $G\alpha_{12}$ deficient mouse verified that the morphological effects obtained upon stimulation of the 5-HT₇ receptor were mediated solely by the G₁₂ protein, demonstrating the critical role of 5-HT₇/G₁₂ signaling for formation of dendritic filopodia and new synapses. We have recently demonstrated that the small GTPases RhoA and Cdc42 represent the main down-stream effectors of the 5-HT₇/G₁₂ signaling. We also found that the major functional effects of this pathway, including actin reorganisation and formation of neurite-like protrusions, were mediated by the activation of Cdc42 (Kvachnina et al., 2005). The results of this study suggest that 5-HT₇ receptor-mediated activation of Cdc42 may also be responsible for the formation of dendritic filopodia and spines in hippocampal neurons.

The 5-HT mediated activation of Cdc42 has been shown to be major signaling pathways involved in formation of filopodia from presynaptic varicosities in sensory neurons of *Aplysia*, leading to long-term facilitation. In this case, however, the receptor responsible was not identified, although activation of PI3 kinase and PLC were discussed as possible signaling mechanism (Udo et al., 2005). Cdc42 also plays the central role in rapid conversion of early nonfunctional contacts between cultured hippocampal neurons into functional synapses after a brief train of presynaptic action potentials (Shen et al., 2006). Such activity-induced conversion of silent synapses occurred within minutes, suggesting involvement of different mechanisms as in the case of 5-HT₇ receptor-mediated effects, which required several hours.

Thus, 5-HT-induced activation of the 5-HT₇/G₁₂/Cdc42 signaling pathways and the consequent reorganization of the dendritic actin network appear to be a part of the initial molecular cascade required for the growth of new synapses which then become the subject of activity-dependent structural and functional plasticity (Citri and Malenka, 2008; Turrigiano, 2008).

4.1.2 Possible function of 5-HT7/G12 signaling during early postnatal development

Stimulatory effects of 5-HT7/G12 signaling on the dendritic morphology, synaptogenesis and synaptic plasticity obtained in hippocampal neurons were restricted to early postnatal development stages and abolished in adult mice. In accordance with this observation, we documented the decrease in the expression levels of both 5-HT7 receptor and G α 12 proteins in the hippocampus during the postnatal development. This suggests that serotonin, acting through the 5-HT7/G12/Cdc42 signaling pathway, promotes structural and functional changes in hippocampal neurons and, more importantly, that these effects may be regulated by the transient increase in expression of the 5-HT7 and G12 proteins during the early postnatal period. There is increasing evidence that in the central nervous system 5-HT is involved in regulation of different aspects of neuronal development before it acts as a neurotransmitter. The early actions of 5-HT include modulation of neuronal differentiation, synaptogenesis, axonal path-finding as well as effects on neurogenesis, cell migration and morphogenesis of the cortex (Okado et al., 1993; Bennett-Clarke et al., 1994; Lebrand et al., 1996; Mazer et al., 1997; Gould, 1999; Bonnin et al., 2007). Moreover, transient modifications of the serotonergic system, especially during the early postnatal development, appear to influence the brain morphology as well as cognitive and emotional behavior in adulthood (Mazer et al., 1997; Gross et al., 2002; Ansorge et al., 2004).

Molecular mechanisms underlying such developmental effects of 5-HT are poorly understood. The high variability of reported effects suggests, however, that different 5-HT actions during development may be defined by variable expression of the corresponding receptor subtypes and/or their downstream effectors. First experimental proof for that was recently provided by Bonnin and colleagues (Bonnin et al., 2006; Bonnin et al., 2007), who demonstrated that dynamic expression of 5-HT1 receptor subfamily members in the telencephalon of the prenatal mouse may be responsible for the serotonin-mediated modulation of responsiveness of embryonic thalamocortical axons to netrin-1. In the present study we also obtained the dynamic expression patterns of 5-HT7 receptor and G12 protein in hippocampus during postnatal development, which correlated with the morphogenic and functional effects mediated by the 5-HT7/G12 signaling.

What could be the possible function of regulated expression? We hypothesize that transient expression of 5-HT₇/G₁₂ signaling pathway can represent the mechanism, by which serotonin specifically modulates the formation of basal neuronal connections during the early postnatal development. This is supported by several observations. First, serotonergic system is one of the earliest neurotransmitter systems in the mammalian brain, with the final arborisation of serotonergic innervation occurring up to postnatal day 21 (Lidov and Molliver, 1982; Lauder, 1990). During this terminal serotonergic field development (E19 - P21), 5-HT reaches the highest concentration in the brain (Whitaker-Azmitia, 2005). It has been also shown that the physiological concentration of 5-HT both in and around the synaptic cleft can reach the millimolar range (1 - 10 mM) (Bruns et al., 2000). Therefore, the effective concentration of the released serotonin in hippocampus should be well within the range needed for the activation of 5-HT₇/G₁₂ signaling (100 nM). Moreover, we observed a high degree of co-localization between serotonin-containing varicosities and the 5-HT₇ receptor. This may provide a physical basis for the preferential activation of 5-HT₇/G₁₂ signaling at early postnatal stages.

4.2 Oligomerization of 5-HT1 receptor

During the last decade, a growing body of biochemical and biophysical evidence indicated that GPCRs can form oligomeric complexes. Although the existence of GPCR oligomers has now become generally accepted, their physiological incidence in native tissues as well as functional importance are still a matter of debate and in some cases remain even controversial (Hagan et al., 2000; Herrick-Davis et al., 2004; Herrick-Davis et al., 2005). It has been clearly documented that homo- and hetero-oligomerization of class C GPCRs such as metabotropic glutamate as well as GABA_B receptors is essential for the receptor trafficking to the cell surface, for ligand-induced receptor activation as well as for G-protein coupling (Maggio et al., 2005; Milligan, 2006). It has been clearly documented that homo- and hetero-oligomerization of class C GPCRs such as metabotropic glutamate as well as GABA_B receptors is essential for the receptor trafficking to the cell surface, for ligand-induced receptor activation as well as for G-protein coupling (Bouvier, 2001; Pin et al., 2003). In contrast, no general consensus is yet achieved for the functional importance of oligomerization for class A GPCRs. In the case of opioid receptor, heterodimers of kappa and delta receptors have been shown to form a distinct functional signaling unit in vivo (Waldhoer et al., 2005). Recent data on the heterodimerization between β 1A and β 2A receptors also demonstrated importance of oligomerization for the inhibition of agonist-promoted internalization of the β 2A and its ability to activate the ERK1/2MAPK signaling pathway (Lavoie et al., 2002). On the other hand, β 2A and rhodopsin receptors, which are often used as a model GPCRs for the homo-oligomerization analysis, can efficiently activate their G-proteins in monomeric conformation (Whorton et al., 2007). Similarly, oligomerization of the neurotensin NTS1 receptor is not required for G-protein activation, although it seems to alter the mode of the receptor-G protein interaction (White et al., 2007). These findings show that receptor oligomerization plays differing functional roles at different receptor-G-protein interfaces, suggesting that there is no common function applicable to all GPCRs. In the present study we verified the oligomerization state of the 5-HT1A receptor and also analyzed its oligomerization dynamics upon the agonist stimulation by using classical biochemical methods and different FRET-based approaches. In addition, we investigated the

possible interplay between palmitoylation and oligomerization of the 5-HT_{1A} receptor. A co-immunoprecipitation assay performed in neuroblastoma N1E-115 cells expressing receptor constructs containing different epitope tags revealed the presence of immunoreactive 5-HT_{1A} receptors only in co-transfected cells and not in individually transfected cells mixed before cell lysis. This strongly suggests that the 5-HT_{1A} receptor forms homo-oligomers. Homo-oligomerization of 5-HT_{1A} receptors has been also previously reported for recombinant 5-HT_{1A} receptor expressed in HEK-293 cells (Salim et al., 2002), suggesting that oligomerization is intrinsic to the 5-HT_{1A} itself. In addition, oligomerization experiments using a plasma membrane impermeable cross-linker BM[PEO]₃ applied to intact cells showed that the predominant receptor species on the plasma membrane are homodimers.

Biochemical methods used in this study represent the classical approaches used for the detection of GPCR oligomerization. However, these methods require solubilization and concentration of the membrane proteins, which could possibly result in artificial aggregation of receptors (Harrison and van der Graaf, 2006). In addition, these techniques do not allow an analysis of GPCR oligomerization dynamics in living cells. To overcome these limitations and to analyze the oligomerization behavior of the 5-HT_{1A} receptor in living cells, we applied different FRET-based approaches including the acceptor-photobleaching method (Bastiaens et al., 1996), the fluorescence lifetime-based FRET measurement as well as a novel lux-FRET approach (Wlodarczyk et al., 2008).

4.2.1 Verification of oligomerization specificity by a novel FRET-based approach

In addition to biochemical methods, we analyzed 5-HT_{1A} receptor oligomerization by FRET using receptors fused to enhanced CFP or YFP as donor and acceptor, respectively. It is notable that CFP- and YFP fused receptors demonstrated subcellular distribution, pharmacological profiles and signaling properties similar to that of their non-fluorescent wild-type or acylation-deficient counterparts (Renner et al., 2007) indicating that these fluorescent constructs can be used in functional studies. By using both acceptor-photobleaching and the fluorescence lifetime FRET methods, we measured FRET between CFP- and YFP tagged 5-

HT1A receptors expressed at the surface of N1E-115 cells. A valid interpretation of FRET data is, however, not trivial because the FRET signal depends on several factors such as interaction affinity and stoichiometry of fusion proteins, their folding probability and their mutual orientation, (Kenworthy and Edidin, 1998; Wallrabe et al., 2003). Moreover, positive FRET signals may result not only from specific protein interactions including receptor oligomerization, but also from randomly distributed proteins, as may be the case after overexpression of donors and acceptors (Meyer et al., 2006). Based on critical analysis of BRET data, it has been recently considered that the contribution of non-specific interactions measured by resonance energy transfer may be even larger than previously thought (James et al., 2006). Therefore, the analysis of FRET data over different donor to acceptor ratios and/or over different expression levels have been proposed as important prerequisite to discriminate between specific versus nonspecific interaction (James et al., 2006). Hence, using a novel lux-FRET approach, we obtained and analyzed apparent FRET efficiency as a function of the acceptor to donor ratio, $[A_i]/[D_i]$ with the aim to distinguish between these two cases (i.e. specific vs. non-specific interaction). By measuring the emission spectra at two different excitation wavelengths and applying linear unmixing, lux-FRET method allowed us to determine the stoichiometry of interacting fluorescently labeled receptors. Artifacts like bleed-through and cross-talk, which occur by using the filter channel based methods, do not affect such analysis. Moreover, this approach is more easily implemented than methods proposed previously (Hoppe et al., 2002; Zal and Gascoigne, 2004). Our data demonstrated that apparent FRET values obtained for different receptor combinations agreed with the model prediction for non-random interaction. In addition, the analysis of the energy transfer efficiency as a function of expression level at fixed donor to acceptor ratio demonstrates that FRET obtained for 5-HT1A receptors was largely independent of expression level. This observation further confirms specificity of oligomerization in case of the 5-HT1A receptor. Further evidence for the specificity of 5-HT1A receptor oligomerization was obtained from the analysis of recently published data on receptor pharmacology (Papoucheva et al., 2004). The Hill coefficient value calculated for HA-tagged 5-HT1A receptor was found to be 0.50 ± 0.17 , which indicates negative cooperativity. According to the theory (Abeliovich, 2005), the Hill coefficient value in negatively cooperating systems can be used to estimate the minimal

number of receptor subunits in complex, and the Hill slope of 0.5 indicates that 5-HT_{1A} exists as a dimer or higher order oligomer.

4.2.2 Regulation of oligomerization by agonist; role of lipid rafts and receptor palmitoylation

In several biophysical studies investigating the effect of agonists on receptor oligomerization, changes in the resonance energy transfer were obtained after receptor stimulation (Terrillon and Bouvier, 2004). This has often been interpreted as an agonist-induced change in oligomerization state. Since FRET efficiency highly depends on the relative distance and orientation between the donor and acceptor, such agonist-mediated changes in energy transfer may also reflect alterations in the pre-existing receptor conformation (Hoffmann et al., 2005). In the majority of studies, addition of agonist resulted in an increase of the FRET/BRET signal. However, agonist-dependent reduction of the signal has been reported for four GPCRs including cholecystokinin, neuropeptide Y₄, thyrotropin TSH and somatostatin SSTR2 receptors (Cheng and Miller, 2001; Kroeger et al., 2001; Berglund et al., 2003; Grant et al., 2003). Based on different tag combinations and positions (cholecystokinin receptor), on the FRAP technique (TSH receptor) as well as on biochemical analysis (neuropeptide Y₄ and SSTR2 receptors), authors proposed agonist-induced dissociation of oligomers rather than a conformational change as a possible reason for the decrease of the energy transfer efficiency. In the present study, we analyzed the time course of the apparent FRET efficiency for 5-HT_{1A} receptor oligomerization and found that receptor stimulation with agonist leads to significant decrease of the FRET signal. On the other hand, the amount of 5-HT_{1A} oligomers was not affected upon agonist stimulation as revealed by co-immunoprecipitation and cross-linking analysis. This result was in contrast to examples mentioned above and suggests that ligand mediated decrease of FRET obtained for the 5-HT_{1A} receptor does not arise from the dissociation of oligomers to monomers and is rather achieved by the conformational changes of pre-existing FRET-positive complexes to FRET-negative orientations. A more intriguing finding was the dependence of 5-HT_{1A} oligomerization efficiency and dynamics on the palmitoylation state of receptors. The results

of the biophysical studies revealed that the removal of palmitoylation sites resulted in increased FRET efficiency. On the other hand, agonist-mediated decrease of FRET signal obtained for the wild-type receptor was completely abolished in cells expressing of acylation-deficient mutants. Combined with the fact that agonist stimulation does not change the amount of oligomers composed by non-palmitoylated receptor, this suggests that lack of palmitoylation does not directly affect the extent of oligomerization rather influences orientation of C-terminal CFP and YFP leading to increased FRET efficiency.

What could be a possible mechanism by which palmitoylation may influence oligomerization and functions of the 5-HT_{1A} receptor? We have recently shown that a significant fraction of the 5-HT_{1A} receptor resides in lipid rafts, while the non-acylated mutants (which also do not couple to Gi-proteins) are excluded from these membrane microdomains (Papoucheva et al., 2004; Renner et al., 2007). Based on these data in combination with results presented here, we propose the existence of two populations of 5-HT_{1A} receptors. One population consists of receptor oligomers localized outside of lipid rafts. This population seems to be partly “non-functional” in terms of efficient signaling and needs raft localization to coincide with raft-resided Gi-proteins (Emerit et al., 1990). Another receptor population resides in lipid rafts and plays an important role in an efficient receptor-mediated signaling. This is also in line with the current view on the functional role of lipid rafts. Lipid rafts and caveolae have been shown to be involved in the regulation of various cell functions including the intracellular sorting of proteins and lipids (Sprong et al., 2001), the establishment of cell polarity (Sprong et al., 2001) and the fine tuning of signaling processes (Toomre et al., 2000). The detection of numerous signaling proteins within the detergent-resistant membrane fractions led to the assumption that lipid rafts represent scaffold platforms which facilitate signal transduction by spatially recruiting signaling components and by preventing an inappropriate cross-talk between pathways (Okamoto et al., 1998; Foster et al., 2003). Several members of the serotonin receptor family, including 5-HT_{2A} and 5-HT₇ receptors have also been shown to be highly enriched in lipid rafts and caveolae (Bhatnagar et al., 2004), suggesting general importance of this membrane subdomains for the serotonergic signaling. Similar enrichment in lipid rafts/caveolae has also been reported for other member of GPCR superfamily,

including GnRH, endothelin ETB and ETA and chemokine CCR5 receptors (Okamoto et al., 2000).

In the case of 5-HT_{1A} receptor, stimulation with agonist results in changing FRET-positive to FRET-negative orientation of oligomers residing in lipid rafts. This may originate from a more tight association of palmitoylated receptor C-terminus with raft-specific lipids (Melkonian et al., 1999; Percherancier et al., 2003) or from increased coupling of receptor with raft-resided G α_i proteins, particularly upon agonist stimulation. Both raft as well as non-raft populations seem to exist in dynamic equilibrium, which is important for fine tuning of receptor-mediated signaling. In this model palmitoylation does not directly modulate oligomerization of 5-HT_{1A}, but rather serves as a targeting signal responsible for the retention of the 5-HT_{1A} receptor in defined membrane microdomains. The fact that the FRET efficiency for the oligomers composed by wild-type receptors was lower than that for non-functional, acylation-deficient mutants is also in line with this model. Combined with the fact that cholesterol depletion resulted in the significant increase of FRET signal only in case of wild-type receptor, these data suggest that receptors residing in lipid rafts consist of oligomers in FRET-negative conformation. In addition, abolishing the agonist-mediated changes in the FRET efficiency obtained in cells expressing wild-type oligomers after cholesterol depletion further confirms the importance of lipid rafts in 5-HT_{1A}-mediated signaling. Further experimentation will be necessary to validate this model and elucidate molecular mechanisms regulating interplay between palmitoylation and oligomerization (Kobe et al, 2008).

5 SUMMARY

Role of 5-HT7/G12 signaling in morpho- and synaptogenesis. The neurotransmitter serotonin (5-hydroxytryptamine or 5-HT) modulates different aspects of early neuronal differentiation, including neurite outgrowth and synaptogenesis, before it acts as a neurotransmitter. Here we report that activation of the 5-HT7 serotonin receptor promotes dendritic branching, formation of the new synapses as well as spontaneous synaptic activity. The morphological effects obtained upon stimulation of the 5-HT7 receptor were mediated solely by the G12 protein, demonstrating the critical role of 5-HT7/G12 signaling for formation of dendritic filopodia and synaptogenesis. Analysis of organotypic preparation from the hippocampus of juvenile mice demonstrate that 5-HT7R/G12 signaling potentiates formation of dendritic spines, increases the basal neuronal excitability and leads to robust changes in long-term potentiation (LTP). We also found that the expression of both 5-HT7 receptor and $G\alpha_{12}$ protein was significantly reduced during development. Accordingly the effects of 5-HT7/G12 signaling in adult mice were abolished. Thus, regulated expression of both 5-HT7 receptor and $G\alpha_{12}$ protein may represent a molecular mechanisms by which serotonin specifically modulate the formation of basal neuronal connections during the early postnatal development.

Oligomerization of 5-HT1A receptor. In the present study we analyzed the oligomerization state of the serotonin 5-HT1A receptor and studied oligomerization dynamics in living cells. We also investigated the role of receptor palmitoylation in this process. Biochemical analysis performed in neuroblastoma N1E-115 cells demonstrated that both palmitoylated and non-palmitoylated 5-HT1A receptors form homo-oligomers and that the prevalent receptor species at the plasma membrane are dimers. A combination of an acceptor-photobleaching FRET approach with fluorescence lifetime measurements verified the interaction of CFP- and YFP-labeled wild-type as well as acylation-deficient 5-HT1A receptors at the plasma membrane of living cells. Using a novel FRET technique based on the spectral analysis we also confirmed the specific nature of receptor oligomerization. The analysis of

oligomerization dynamics revealed that apparent FRET efficiency measured for wild-type oligomers significantly decreased in response to agonist stimulation, and our combined results suggest that this decrease was mediated by accumulation of FRET-negative complexes rather than by dissociation of oligomers to monomers. In contrast, the agonist-mediated decrease of FRET signal was completely abolished in oligomers composed by non-palmitoylated receptor mutants, demonstrating the importance of palmitoylation in modulation of the structure of oligomers.

6 REFERENCES

- Abeliovich H (2005) An empirical extremum principle for the hill coefficient in ligand-protein interactions showing negative cooperativity. *Biophys J* 89:76-79.
- Adham N, Zgombick JM, Bard J, Branchek TA (1998) Functional characterization of the recombinant human 5-hydroxytryptamine_{7(a)} receptor isoform coupled to adenylate cyclase stimulation. *J Pharmacol Exp Ther* 287:508-514.
- Akgoz M, Azpiazu I, Kalyanaraman V, Gautam N (2002) Role of the G protein gamma subunit in beta gamma complex modulation of phospholipase C β function. *J Biol Chem* 277:19573-19578.
- Andrade R, Malenka RC, Nicoll RA (1986) A G protein couples serotonin and GABA_B receptors to the same channels in hippocampus. *Science* 234:1261-1265.
- Angers S, Salahpour A, Bouvier M (2001) Biochemical and biophysical demonstration of GPCR oligomerization in mammalian cells. *Life Sci* 68:2243-2250.
- Angers S, Salahpour A, Bouvier M (2002) Dimerization: an emerging concept for G protein-coupled receptor ontogeny and function. *Annu Rev Pharmacol Toxicol* 42:409-435.
- Ansorge MS, Zhou M, Lira A, Hen R, Gingrich JA (2004) Early-life blockade of the 5-HT transporter alters emotional behavior in adult mice. *Science* 306:879-881.
- Azmitia EC (2001) Modern views on an ancient chemical: serotonin effects on cell proliferation, maturation, and apoptosis. *Brain Res Bull* 56:413-424.
- Ballaz SJ, Akil H, Watson SJ (2007) Analysis of 5-HT₆ and 5-HT₇ receptor gene expression in rats showing differences in novelty-seeking behavior. *Neuroscience* 147:428-438.
- Barnes NM, Sharp T (1999) A review of central 5-HT receptors and their function. *Neuropharmacology* 38:1083-1152.
- Bartrup JT, Moorman JM, Newberry NR (1997) BDNF enhances neuronal growth and synaptic activity in hippocampal cell cultures. *Neuroreport* 8:3791-3794.
- Bastiaens PI, Majoul IV, Verveer PJ, Söling HD, Jovin TM (1996) Imaging the intracellular trafficking and state of the AB5 quaternary structure of cholera toxin. *EMBO J* 15:4246-4253.
- Beer MS, Stanton JA, Bevan Y, Chauhan NS, Middlemiss DN (1992) An investigation of the 5-HT_{1D} receptor binding affinity of 5-hydroxytryptamine, 5-carboxyamidotryptamine and sumatriptan in the central nervous system of seven species. *Eur J Pharmacol* 213:193-197.
- Bennett-Clarke CA, Leslie MJ, Lane RD, Rhoades RW (1994) Effect of serotonin depletion on vibrissa-related patterns of thalamic afferents in the rat's somatosensory cortex. *J Neurosci* 14:7594-7607.
- Berglund MM, Schober DA, Statnick MA, McDonald PH, Gehlert DR (2003) The use of bioluminescence resonance energy transfer 2 to study neuropeptide Y receptor agonist-induced beta-arrestin 2 interaction. *J Pharmacol Exp Ther* 306:147-156.
- Bhatnagar A, Sheffler DJ, Kroeze WK, Compton-Toth B, Roth BL (2004) Caveolin-1 interacts with 5-HT_{2A} serotonin receptors and profoundly modulates the signaling of selected G α q-coupled protein receptors. *J Biol Chem* 279:34614-34623.

- Bjorvatn B, Ursin R (1998) Changes in sleep and wakefulness following 5-HT_{1A} ligands given systemically and locally in different brain regions. *Reviews in the neurosciences* 9:265-273.
- Blank JL, Ross AH, Exton JH (1991) Purification and characterization of two G-proteins that activate the beta 1 isozyme of phosphoinositide-specific phospholipase C. Identification as members of the G_q class. *J Biol Chem* 266:18206-18216.
- Blier P, Bouchard C (1993) Functional characterization of a 5-HT₃ receptor which modulates the release of 5-HT in the guinea-pig brain. *Br J Pharmacol* 108:13-22.
- Bockaert J, Pin JP (1999) Molecular tinkering of G protein-coupled receptors: an evolutionary success. *EMBO J* 18:1723-1729.
- Bonnin A, Peng W, Hewlett W, Levitt P (2006) Expression mapping of 5-HT₁ serotonin receptor subtypes during fetal and early postnatal mouse forebrain development. *Neuroscience* 141:781-794.
- Bonnin A, Torii M, Wang L, Rakic P, Levitt P (2007) Serotonin modulates the response of embryonic thalamocortical axons to netrin-1. *Nat Neurosci* 10:588-597.
- Bouvier M (2001) Oligomerization of G-protein-coupled transmitter receptors. *Nature Reviews Neuroscience* 2:274-286.
- Brauner-Osborne H, Wellendorph P, Jensen AA (2007) Structure, pharmacology and therapeutic prospects of family C G-protein coupled receptors. *Current drug targets* 8:169-184.
- Brown DA, London E (1998) Functions of lipid rafts in biological membranes. *Annu Rev Cell Dev Biol* 14:111-136.
- Bruns D, Riedel D, Klingauf J, Jahn R (2000) Quantal release of serotonin. *Neuron* 28:205-220.
- Bulenger S, Marullo S, Bouvier M (2005) Emerging role of homo- and heterodimerization in G-protein-coupled receptor biosynthesis and maturation. *Trends Pharmacol Sci* 26:131-137.
- Burnet PW, Mefford IN, Smith CC, Gold PW, Sternberg EM (1996) Hippocampal 5-HT_{1A} receptor binding site densities, 5-HT_{1A} receptor messenger ribonucleic acid abundance and serotonin levels parallel the activity of the hypothalamo-pituitary-adrenal axis in rats. *Behav Brain Res* 73:365-368.
- Canton H, Emeson RB, Barker EL, Backstrom JR, Lu JT, Chang MS, Sanders-Bush E (1996) Identification, molecular cloning, and distribution of a short variant of the 5-hydroxytryptamine_{2C} receptor produced by alternative splicing. *Molecular pharmacology* 50:799-807.
- Chabre M, le Maire M (2005) Monomeric G-protein-coupled receptor as a functional unit. *Biochemistry* 44:9395-9403.
- Chandrashekar J, Mueller KL, Hoon MA, Adler E, Feng L, Guo W, Zuker CS, Ryba NJ (2000) T₂Rs function as bitter taste receptors. *Cell* 100:703-711.
- Cheng ZJ, Miller LJ (2001) Agonist-dependent dissociation of oligomeric complexes of G protein-coupled cholecystinin receptors demonstrated in living cells using bioluminescence resonance energy transfer. *J Biol Chem* 276:48040-48047.
- Citri A, Malenka RC (2008) Synaptic plasticity: multiple forms, functions, and mechanisms. *Neuropsychopharmacology* 33:18-41.

- Clarke WP, Yocca FD, Maayani S (1996) Lack of 5-hydroxytryptamine_{1A}-mediated inhibition of adenylyl cyclase in dorsal raphe of male and female rats. *J Pharmacol Exp Ther* 277:1259-1266.
- Corset V, Nguyen-Ba-Charvet KT, Forcet C, Moyse E, Chédotal A, Mehlen P (2000) Netrin-1-mediated axon outgrowth and cAMP production requires interaction with adenosine A_{2b} receptor. *Nature* 407:747-750.
- Coso OA, Teramoto H, Simonds WF, Gutkind JS (1996) Signaling from G protein-coupled receptors to c-Jun kinase involves beta gamma subunits of heterotrimeric G proteins acting on a Ras and Rac1-dependent pathway. *J Biol Chem* 271:3963-3966.
- Dawson LA, Hughes ZA, Starr KR, Storey JD, Bettelini L, Bacchi F, Arban R, Poffe A, Melotto S, Hagan JJ, Price GW (2006) Characterisation of the selective 5-HT_{1B} receptor antagonist SB-616234-A (1-[6-(cis-3,5-dimethylpiperazin-1-yl)-2,3-dihydro-5-methoxyindol-1-yl]-1-[2'-methyl-4'-(5-methyl-1,2,4-oxadiazol-3-yl)biphenyl-4-yl]methanone hydrochloride): in vivo neurochemical and behavioral evidence of anxiolytic/antidepressant activity. *Neuropharmacology* 50:975-983.
- De Paola V, Arber S, Caroni P (2003) AMPA receptors regulate dynamic equilibrium of presynaptic terminals in mature hippocampal networks. *Nature neuroscience* 6:491-500.
- De Ponti F, Tonini M (2001) Irritable bowel syndrome: new agents targeting serotonin receptor subtypes. *Drugs* 61:317-332.
- Delgado M, Caicoya AG, Greciano V, Benhamú B, López-Rodríguez ML, Fernández-Alfonso MS, Pozo MA, Manzanares J, Fuentes JA (2005) Anxiolytic-like effect of a serotonergic ligand with high affinity for 5-HT_{1A}, 5-HT_{2A} and 5-HT₃ receptors. *Eur J Pharmacol* 511:9-19.
- Devi LA (2001) Heterodimerization of G-protein-coupled receptors: pharmacology, signaling and trafficking. *Trends Pharmacol Sci* 22:532-537.
- Dityatev A, Dityateva G, Schachner M (2000) Synaptic strength as a function of post- versus presynaptic expression of the neural cell adhesion molecule NCAM. *Neuron* 26:207-217.
- Duncan MJ, Grear KE, Hoskins MA (2004) Aging and SB-269970-A, a selective 5-HT₇ receptor antagonist, attenuate circadian phase advances induced by microinjections of serotonergic drugs in the hamster dorsal raphe nucleus. *Brain Research* 1008:40-48.
- Dunphy JT, Linder ME (1998) Signalling functions of protein palmitoylation. *Biochim Biophys Acta* 1436:245-261.
- Emerit MB, el Mestikawy S, Gozlan H, Rouot B, Hamon M (1990) Physical evidence of the coupling of solubilized 5-HT_{1A} binding sites with G regulatory proteins. *Biochem Pharmacol* 39:7-18.
- Erspamer V, Asero B (1952) Identification of enteramine, the specific hormone of the enterochromaffin cell system, as 5-hydroxytryptamine. *Nature* 169:800-801.
- Fargin A, Raymond JR, Regan JW, Cotecchia S, Lefkowitz RJ, Caron MG (1989) Effector coupling mechanisms of the cloned 5-HT_{1A} receptor. *J Biol Chem* 264:14848-14852.
- Faure M, Voyno-Yasenetskaya TA, Bourne HR (1994) cAMP and beta gamma subunits of heterotrimeric G proteins stimulate the mitogen-activated protein kinase pathway in COS-7 cells. *J Biol Chem* 269:7851-7854.
- Filipek S, Stenkamp RE, Teller DC, Palczewski K (2003) G protein-coupled receptor rhodopsin: a prospectus. *Annu Rev Physiol* 65:851-879.

-
- Fiorica-Howells E, Maroteaux L, Gershon MD (2000) Serotonin and the 5-HT(2B) receptor in the development of enteric neurons. *J Neurosci* 20:294-305.
- Foster LJ, De Hoog CL, Mann M (2003) Unbiased quantitative proteomics of lipid rafts reveals high specificity for signaling factors. *Proc Natl Acad Sci U S A* 100:5813-5818.
- Forbes IT, Douglas S, Gribble AD, Ife RJ, Lightfoot AP, Garner AE, Riley GJ, Jeffrey P, Stevens AJ, Stean TO, Thomas DR (2002) SB-656104-A: a novel 5-HT(7) receptor antagonist with improved in vivo properties. *Bioorg Med Chem Lett* 12:3341-3344.
- Fredriksson R, Lagerström MC, Lundin L-G, Schiöth HB (2003) The G-protein-coupled receptors in the human genome form five main families. Phylogenetic analysis, paralogon groups, and fingerprints. *Mol Pharmacol* 63:1256-1272.
- Fricker AD, Rios C, Devi LA, Gomes I (2005) Serotonin receptor activation leads to neurite outgrowth and neuronal survival. *Brain Res Mol Brain Res* 138:228-235.
- Gähwiler BH, Capogna M, Debanne D, McKinney RA, Thompson SM (1997) Organotypic slice cultures: a technique has come of age. *Trends in Neurosciences* 20:471-477.
- Garnovskaya MN, van Biesen T, Hawe B, Casañas Ramos S, Lefkowitz RJ, Raymond JR (1996) Ras-dependent activation of fibroblast mitogen-activated protein kinase by 5-HT1A receptor via a G protein beta gamma-subunit-initiated pathway. *Biochemistry* 35:13716-13722.
- Gether U (2000) Uncovering molecular mechanisms involved in activation of G protein-coupled receptors. *Endocr Rev* 21:90-113.
- Gogolla N, Galimberti I, Depaola V, Caroni P (2006) Preparation of organotypic hippocampal slice cultures for long-term live imaging. *Nature protocols* 1:1165-1171.
- Gordon JA, Hen R (2004) The serotonergic system and anxiety. *Neuromolecular Med* 5:27-40.
- Gould E (1999) Serotonin and hippocampal neurogenesis. *Neuropsychopharmacology* 21:46S-51S.
- Grant GA, Hu Z, Xu XL (2003) Hybrid tetramers reveal elements of cooperativity in *Escherichia coli* D-3-phosphoglycerate dehydrogenase. *J Biol Chem* 278:18170-18176.
- Gross C, Zhuang X, Stark K, Ramboz S, Oosting R, Kirby L, Santarelli L, Beck S, Hen R (2002) Serotonin1A receptor acts during development to establish normal anxiety-like behavior in the adult. *Nature* 416:396-400.
- Gu JL, Müller S, Mancino V, Offermanns S, Simon MI (2002) Interaction of G alpha(12) with G alpha(13) and G alpha(q) signaling pathways. *Proc Natl Acad Sci U S A* 99:9352-9357.
- Hagan JJ, Price GW, Jeffrey P, Deeks NJ, Stean T, Piper D, Smith MI, Upton N, Medhurst AD, Middlemiss DN, Riley GJ, Lovell PJ, Bromidge SM, Thomas DR (2000) Characterization of SB-269970-A, a selective 5-HT(7) receptor antagonist. *Br J Pharmacol* 130:539-548.
- Hall A (1998) Rho GTPases and the actin cytoskeleton. *Science* 279:509-514.
- Harder T, Scheiffele P, Verkade P, Simons K (1998) Lipid domain structure of the plasma membrane revealed by patching of membrane components. *J Cell Biol* 141:929-942.
- Harhammer R, Gohla A, Schultz G (1996) Interaction of G protein Gbetagamma dimers with small GTP-binding proteins of the Rho family. *FEBS Letters* 399:211-214.

- Harrison C, van der Graaf PH (2006) Current methods used to investigate G protein coupled receptor oligomerisation. *Journal of pharmacological and toxicological methods* 54:26-35.
- Hedlund PB, Danielson PE, Thomas EA, Slanina K, Carson MJ, Sutcliffe JG (2003) No hypothermic response to serotonin in 5-HT₇ receptor knockout mice. *Proc Natl Acad Sci U S A* 100:1375-1380.
- Heidmann DE, Szot P, Kohen R, Hamblin MW (1998) Function and distribution of three rat 5-hydroxytryptamine₇ (5-HT₇) receptor isoforms produced by alternative splicing. *Neuropharmacology* 37:1621-1632.
- Herrick-Davis K, Grinde E, Mazurkiewicz JE (2004) Biochemical and biophysical characterization of serotonin 5-HT_{2C} receptor homodimers on the plasma membrane of living cells. *Biochemistry* 43:13963-13971.
- Herrick-Davis K, Grinde E, Harrigan TJ, Mazurkiewicz JE (2005) Inhibition of serotonin 5-hydroxytryptamine_{2c} receptor function through heterodimerization: receptor dimers bind two molecules of ligand and one G-protein. *J Biol Chem* 280:40144-40151.
- Herzog A, Krell G, Michaelis B, Ovtscharoff W, Braun K (2006) Detection of presynaptic terminals on dendritic spines in double labelin confocal images. In: ICPR pp 715-718. Hongkong.
- Hoffmann C, Gaietta G, Bünemann M, Adams SR, Oberdorff-Maass S, Behr B, Vilardaga J-P, Tsien RY, Ellisman MH, Lohse MJ (2005) A FIAsh-based FRET approach to determine G protein-coupled receptor activation in living cells. *Nat Methods* 2:171-176.
- Hoon MA, Adler E, Lindemeier J, Battey JF, Ryba NJ, Zuker CS (1999) Putative mammalian taste receptors: a class of taste-specific GPCRs with distinct topographic selectivity. *Cell* 96:541-551.
- Hoppe A, Christensen K, Swanson JA (2002) Fluorescence resonance energy transfer-based stoichiometry in living cells. *Biophys J* 83:3652-3664.
- Horn F, Bettler E, Oliveira L, Campagne F, Cohen F, Vriend G (2003) GPCRDB information system for G protein-coupled receptors. *Nucleic Acids Research* 31:294.
- Horn F, Weare J, Beukers MW, Hörsch S, Bairoch A, Chen W, Edvardsen O, Campagne F, Vriend G (1998) GPCRDB: an information system for G protein-coupled receptors. *Nucleic Acids Res* 26:275-279.
- Hoyer D, Hannon JP, Martin GR (2002) Molecular, pharmacological and functional diversity of 5-HT receptors. *Pharmacol Biochem Behav* 71:533-554.
- Hoyer D, Pazos A, Probst A, Palacios JM (1986) Serotonin receptors in the human brain. I. Characterization and autoradiographic localization of 5-HT_{1A} recognition sites. Apparent absence of 5-HT_{1B} recognition sites. *Brain Res* 376:85-96.
- Jaffe AB, Hall A (2005) Rho GTPases: biochemistry and biology. *Annu Rev Cell Dev Biol* 21:247-269.
- James JR, Oliveira MI, Carmo AM, Iaboni A, Davis SJ (2006) A rigorous experimental framework for detecting protein oligomerization using bioluminescence resonance energy transfer. *Nat Methods* 3:1001-1006.
- Javitch JA (2004) The ants go marching two by two: oligomeric structure of G-protein-coupled receptors. *Mol Pharmacol* 66:1077-1082.

- Jedlicka P, Papadopoulos T, Deller T, Betz H, Schwarzacher SW (2009) Increased network excitability and impaired induction of long-term potentiation in the dentate gyrus of collybistin-deficient mice in vivo. *Mol Cell Neurosci* 41:94-100.
- Jones KA, Borowsky B, Tamm JA, Craig DA, Durkin MM, Dai M, Yao WJ, Johnson M, Gunwaldsen C, Huang LY, Tang C, Shen Q, Salon JA, Morse K, Laz T, Smith KE, Nagarathnam D, Noble SA, Branchek TA, Gerald C (1998) GABA(B) receptors function as a heteromeric assembly of the subunits GABA(B)R1 and GABA(B)R2. *Nature* 396:674-679.
- Jontes JD, Smith SJ (2000) Filopodia, spines, and the generation of synaptic diversity. *Neuron* 27:11-14.
- Kamiyama D, Chiba A (2009) Endogenous activation patterns of Cdc42 GTPase within *Drosophila* embryos. *Science* 324:1338-1340.
- Katz LC, Shatz CJ (1996) Synaptic activity and the construction of cortical circuits. *Science* 274:1133-1138.
- Kaupmann K, Malitschek B, Schuler V, Heid J, Froestl W, Beck P, Mosbacher J, Bischoff S, Kulik A, Shigemoto R, Karschin A, Bettler B (1998) GABA(B)-receptor subtypes assemble into functional heteromeric complexes. *Nature* 396:683-687.
- Kenworthy AK, Edidin M (1998) Distribution of a glycosylphosphatidylinositol-anchored protein at the apical surface of MDCK cells examined at a resolution of <100 Å using imaging fluorescence resonance energy transfer. *J Cell Biol* 142:69-84.
- King MV, Marsden CA, Fone KCF (2008) A role for the 5-HT(1A), 5-HT4 and 5-HT6 receptors in learning and memory. *Trends in Pharmacological Sciences* 29:482-492.
- Kirov SA, Goddard CA, Harris KM (2004) Age-dependence in the homeostatic upregulation of hippocampal dendritic spine number during blocked synaptic transmission. *Neuropharmacology* 47:640-648.
- Kobe F, Renner U, Woehler A, Wlodarczyk J, Papusheva E, Bao G, Zeug A, Richter DW, Neher E, Ponimaskin E (2008) Stimulation- and palmitoylation-dependent changes in oligomeric conformation of serotonin 5-HT1A receptors. *Biochim Biophys Acta* 1783:1503-1516.
- Kroeger KM, Hanyaloglu AC, Seeber RM, Miles LE, Eidne KA (2001) Constitutive and agonist-dependent homo-oligomerization of the thyrotropin-releasing hormone receptor. Detection in living cells using bioluminescence resonance energy transfer. *J Biol Chem* 276:12736-12743.
- Kroeze WK, Kristiansen K, Roth BL (2002) Molecular biology of serotonin receptors structure and function at the molecular level. *Current topics in medicinal chemistry* 2:507-528.
- Kroeze WK, Sheffler DJ, Roth BL (2003) G-protein-coupled receptors at a glance. *J Cell Sci* 116:4867-4869.
- Kvachnina E, Liu G, Dityatev A, Renner U, Dumuis A, Richter DW, Dityateva G, Schachner M, Voyno-Yasenetskaya TA, Ponimaskin EG (2005) 5-HT7 receptor is coupled to G alpha subunits of heterotrimeric G12-protein to regulate gene transcription and neuronal morphology. *J Neurosci* 25:7821-7830.
- Lakowicz JR (2006) Principles of fluorescence spectroscopy, 3rd Edition. New York: Springer.

- Lander ES et al. (2001) Initial sequencing and analysis of the human genome. *Nature* 409:860-921.
- Laporte AM, Koscielniak T, Ponchant M, Vergé D, Hamon M, Gozlan H (1992) Quantitative autoradiographic mapping of 5-HT₃ receptors in the rat CNS using [¹²⁵I]iodozacopride and [³H]zacopride as radioligands. *Synapse* 10:271-281.
- Lauder JM (1990) Ontogeny of the serotonergic system in the rat: serotonin as a developmental signal. *Ann N Y Acad Sci* 600:297-313; discussion 314.
- Lavoie C, Mercier J-F, Salahpour A, Umapathy D, Breit A, Villeneuve L-R, Zhu W-Z, Xiao R-P, Lakatta EG, Bouvier M, Hébert TE (2002) Beta 1/beta 2-adrenergic receptor heterodimerization regulates beta 2-adrenergic receptor internalization and ERK signaling efficacy. *J Biol Chem* 277:35402-35410.
- Lebrand C, Cases O, Adelbrecht C, Doye A, Alvarez C, el Mestikawy S, Seif I, Gaspar P (1996) Transient uptake and storage of serotonin in developing thalamic neurons. *Neuron* 17:823-835.
- Lee T, Winter C, Marticke SS, Lee A, Luo L (2000) Essential roles of Drosophila RhoA in the regulation of neuroblast proliferation and dendritic but not axonal morphogenesis. *Neuron* 25:307-316.
- Li Z, Van Aelst L, Cline HT (2000) Rho GTPases regulate distinct aspects of dendritic arbor growth in *Xenopus* central neurons in vivo. *Nature neuroscience* 3:217-225.
- Liang Y, Fotiadis D, Filipek S, Saperstein DA, Palczewski K, Engel A (2003) Organization of the G protein-coupled receptors rhodopsin and opsin in native membranes. *J Biol Chem* 278:21655-21662.
- Lidov HG, Molliver ME (1982) Immunohistochemical study of the development of serotonergic neurons in the rat CNS. *Brain Res Bull* 9:559-604.
- Lindemann B (1996) Taste reception. *Physiol Rev* 76:718-766.
- Linder ME, Deschenes RJ (2003) New insights into the mechanisms of protein palmitoylation. *Biochemistry* 42:4311-4320.
- Logothetis DE, Kurachi Y, Galper J, Neer EJ, Clapham DE (1987) The beta gamma subunits of GTP-binding proteins activate the muscarinic K⁺ channel in heart. *Nature* 325:321-326.
- Lovenberg TW, Baron BM, de Lecea L, Miller JD, Prosser RA, Rea MA, Foye PE, Racke M, Slone AL, Siegel BW (1993) A novel adenylyl cyclase-activating serotonin receptor (5-HT₇) implicated in the regulation of mammalian circadian rhythms. *Neuron* 11:449-458.
- Lundstrom K (2005) Structural biology of G protein-coupled receptors. *Bioorg Med Chem Lett* 15:3654-3657.
- Maggio R, Vogel Z, Wess J (1993) Coexpression studies with mutant muscarinic/adrenergic receptors provide evidence for intermolecular "cross-talk" between G-protein-linked receptors. *Proc Natl Acad Sci U S A* 90:3103-3107.
- Maggio R, Novi F, Scarselli M, Corsini GU (2005) The impact of G-protein-coupled receptor hetero-oligomerization on function and pharmacology. *FEBS J* 272:2939-2946.
- Maletic-Savatic M, Malinow R, Svoboda K (1999) Rapid dendritic morphogenesis in CA1 hippocampal dendrites induced by synaptic activity. *Science* 283:1923-1927.
- Malgaroli A, Tsien RW (1992) Glutamate-induced long-term potentiation of the frequency of miniature synaptic currents in cultured hippocampal neurons. *Nature* 357:134-139.

- Manzke T, Guenther U, Ponimaskin EG, Haller M, Dutschmann M, Schwarzacher S, Richter DW (2003) 5-HT₄(a) receptors avert opioid-induced breathing depression without loss of analgesia. *Science* 301:226-229.
- Manzke T, Dutschmann M, Schlaf G, Mörschel M, Koch UR, Ponimaskin E, Bidon O, Lalley PM, Richter DW (2009) Serotonin targets inhibitory synapses to induce modulation of network functions. *Philos Trans R Soc Lond, B, Biol Sci* 364:2589-2602.
- Mattila PK, Lappalainen P (2008) Filopodia: molecular architecture and cellular functions. *Nat Rev Mol Cell Biol* 9:446-454.
- Mazer C, Muneyirci J, Taheny K, Raio N, Borella A, Whitaker-Azmitia P (1997) Serotonin depletion during synaptogenesis leads to decreased synaptic density and learning deficits in the adult rat: a possible model of neurodevelopmental disorders with cognitive deficits. *Brain Research* 760:68-73.
- McCudden CR, Hains MD, Kimple RJ, Siderovski DP, Willard FS (2005) G-protein signaling: back to the future. *Cell Mol Life Sci* 62:551-577.
- McIlwain KL, Merriweather MY, Yuva-Paylor LA, Paylor R (2001) The use of behavioral test batteries: effects of training history. *Physiol Behav* 73:705-717.
- Melkonian KA, Ostermeyer AG, Chen JZ, Roth MG, Brown DA (1999) Role of lipid modifications in targeting proteins to detergent-resistant membrane rafts. Many raft proteins are acylated, while few are prenylated. *J Biol Chem* 274:3910-3917.
- Meneses A (2008) Preface. Physiological, pathophysiological and therapeutic aspects of 5-HT mechanisms. *Behav Brain Res* 195:1.
- Meyer BH, Martinez KL, Segura J-M, Pascoal P, Hovius R, George N, Johnsson K, Vogel H (2006) Covalent labeling of cell-surface proteins for in-vivo FRET studies. *FEBS Letters* 580:1654-1658.
- Milligan G (2006) G-protein-coupled receptor heterodimers: pharmacology, function and relevance to drug discovery. *Drug Discov Today* 11:541-549.
- Monnot C, Bihoreau C, Conchon S, Curnow KM, Corvol P, Clauser E (1996) Polar residues in the transmembrane domains of the type 1 angiotensin II receptor are required for binding and coupling. Reconstitution of the binding site by co-expression of two deficient mutants. *J Biol Chem* 271:1507-1513.
- Morris R (1984) Developments of a water-maze procedure for studying spatial learning in the rat. *Journal of Neuroscience Methods* 11:47-60.
- Mulheron JG, Casañas SJ, Arthur JM, Garnovskaya MN, Gettys TW, Raymond JR (1994) Human 5-HT_{1A} receptor expressed in insect cells activates endogenous G(o)-like G protein(s). *J Biol Chem* 269:12954-12962.
- Müller M, Somjen GG (1998) Inhibition of major cationic inward currents prevents spreading depression-like hypoxic depolarization in rat hippocampal tissue slices. *Brain Research* 812:1-13.
- Mumby SM (1997) Reversible palmitoylation of signaling proteins. *Curr Opin Cell Biol* 9:148-154.
- Nelson G, Hoon MA, Chandrashekar J, Zhang Y, Ryba NJ, Zuker CS (2001) Mammalian sweet taste receptors. *Cell* 106:381-390.
- Newey SE, Velamoor V, Govek E-E, Van Aelst L (2005) Rho GTPases, dendritic structure, and mental retardation. *J Neurobiol* 64:58-74.
- Ng J, Nardine T, Harms M, Tzu J, Goldstein A, Sun Y, Dietzl G, Dickson BJ, Luo L (2002) Rac GTPases control axon growth, guidance and branching. *Nature* 416:442-447.

- Okado N, Cheng L, Tanatsugu Y, Hamada S, Hamaguchi K (1993) Synaptic loss following removal of serotonergic fibers in newly hatched and adult chickens. *J Neurobiol* 24:687-698.
- Okamoto T, Schlegel A, Scherer PE, Lisanti MP (1998) Caveolins, a family of scaffolding proteins for organizing "preassembled signaling complexes" at the plasma membrane. *J Biol Chem* 273:5419-5422.
- Okamoto Y, Ninomiya H, Miwa S, Masaki T (2000) Cholesterol oxidation switches the internalization pathway of endothelin receptor type A from caveolae to clathrin-coated pits in Chinese hamster ovary cells. *J Biol Chem* 275:6439-6446.
- Olenik C, Aktories K, Meyer DK (1999) Differential expression of the small GTP-binding proteins RhoA, RhoB, Cdc42u and Cdc42b in developing rat neocortex. *Brain Res Mol Brain Res* 70:9-17.
- Overstreet DH (2002) Behavioral characteristics of rat lines selected for differential hypothermic responses to cholinergic or serotonergic agonists. *Behav Genet* 32:335-348.
- Papoucheva E, Dumuis A, Sebben M, Richter DW, Ponimaskin EG (2004) The 5-hydroxytryptamine(1A) receptor is stably palmitoylated, and acylation is critical for communication of receptor with Gi protein. *J Biol Chem* 279:3280-3291.
- Parks CL, Robinson PS, Sibille E, Shenk T, Toth M (1998) Increased anxiety of mice lacking the serotonin1A receptor. *Proc Natl Acad Sci U S A* 95:10734-10739.
- Pazos A, Palacios JM (1985) Quantitative autoradiographic mapping of serotonin receptors in the rat brain. I. Serotonin-1 receptors. *Brain Research* 346:205-230.
- Peitzsch RM, McLaughlin S (1993) Binding of acylated peptides and fatty acids to phospholipid vesicles: pertinence to myristoylated proteins. *Biochemistry* 32:10436-10443.
- Peng Y-R, He S, Marie H, Zeng S-Y, Ma J, Tan Z-J, Lee SY, Malenka RC, Yu X (2009) Coordinated changes in dendritic arborization and synaptic strength during neural circuit development. *Neuron* 61:71-84.
- Percherancier Y, Lagane B, Planchenault T, Staropoli I, Altmeyer R, Virelizier J-L, Arenzana-Seisdedos F, Hoessli DC, Bachelier F (2003) HIV-1 entry into T-cells is not dependent on CD4 and CCR5 localization to sphingolipid-enriched, detergent-resistant, raft membrane domains. *J Biol Chem* 278:3153-3161.
- Pfleger KDG, Eidne KA (2005) Monitoring the formation of dynamic G-protein-coupled receptor-protein complexes in living cells. *Biochem J* 385:625-637.
- Pierce KL, Premont RT, Lefkowitz RJ (2002) Seven-transmembrane receptors. *Nature Reviews Molecular Cell Biology* 3:639-650.
- Pin J-P, Galvez T, Prézeau L (2003) Evolution, structure, and activation mechanism of family 3/C G-protein-coupled receptors. *Pharmacol Ther* 98:325-354.
- Ponimaskin E, Voyno-Yasenetskaya T, Richter DW, Schachner M, Dityatev A (2007) Morphogenic signaling in neurons via neurotransmitter receptors and small GTPases. *Molecular neurobiology* 35:278-287.
- Ponimaskin EG, Profirovic J, Vaiskunaite R, Richter DW, Voyno-Yasenetskaya TA (2002a) 5-Hydroxytryptamine 4(a) receptor is coupled to the Galpha subunit of heterotrimeric G13 protein. *J Biol Chem* 277:20812-20819.
- Ponimaskin EG, Heine M, Joubert L, Sebben M, Bickmeyer U, Richter DW, Dumuis A (2002b) The 5-hydroxytryptamine(4a) receptor is palmitoylated at two different sites,

- and acylation is critically involved in regulation of receptor constitutive activity. *J Biol Chem* 277:2534-2546.
- Radley JJ, Jacobs BL (2002) 5-HT_{1A} receptor antagonist administration decreases cell proliferation in the dentate gyrus. *Brain Res* 955:264-267.
- Radyushkin K, Anokhin K, Meyer BI, Jiang Q, Alvarez-Bolado G, Gruss P (2005) Genetic ablation of the mammillary bodies in the *Foxb1* mutant mouse leads to selective deficit of spatial working memory. *Eur J Neurosci* 21:219-229.
- Rapport MM, GREEN AA, PAGE IH (1948) Serum vasoconstrictor, serotonin; isolation and characterization. *J Biol Chem* 176:1243-1251.
- Renner U, Glebov K, Lang T, Papusheva E, Balakrishnan S, Keller B, Richter DW, Jahn R, Ponimaskin E (2007) Localization of the mouse 5-hydroxytryptamine(1A) receptor in lipid microdomains depends on its palmitoylation and is involved in receptor-mediated signaling. *Molecular pharmacology* 72:502-513.
- Reuter H (1995) Measurements of exocytosis from single presynaptic nerve terminals reveal heterogeneous inhibition by Ca(2+)-channel blockers. *Neuron* 14:773-779.
- Richter DW, Manzke T, Wilken B, Ponimaskin E (2003) Serotonin receptors: guardians of stable breathing. *Trends in molecular medicine* 9:542-548.
- Ross EM (1995) Protein modification. Palmitoylation in G-protein signaling pathways. *Curr Biol* 5:107-109.
- Saghatelian AK, Dityatev A, Schmidt S, Schuster T, Bartsch U, Schachner M (2001) Reduced perisomatic inhibition, increased excitatory transmission, and impaired long-term potentiation in mice deficient for the extracellular matrix glycoprotein tenascin-R. *Mol Cell Neurosci* 17:226-240.
- Salim K, Fenton T, Bacha J, Urien-Rodriguez H, Bonnert T, Skynner HA, Watts E, Kerby J, Heald A, Beer M, McAllister G, Guest PC (2002) Oligomerization of G-protein-coupled receptors shown by selective co-immunoprecipitation. *J Biol Chem* 277:15482-15485.
- Salom D, Le Trong I, Pohl E, Ballesteros JA, Stenkamp RE, Palczewski K, Lodowski DT (2006) Improvements in G protein-coupled receptor purification yield light stable rhodopsin crystals. *J Struct Biol* 156:497-504.
- Saxena PR, Villalón CM (1990) Brain 5-HT_{1A} receptor agonism: a novel mechanism for antihypertensive action. *Trends Pharmacol Sci* 11:95-96.
- Seeburg DP, Feliu-Mojer M, Gaiottino J, Pak DTS, Sheng M (2008) Critical role of CDK5 and Polo-like kinase 2 in homeostatic synaptic plasticity during elevated activity. *Neuron* 58:571-583.
- Shen W, Wu B, Zhang Z, Dou Y, Rao Z-R, Chen Y-R, Duan S (2006) Activity-induced rapid synaptic maturation mediated by presynaptic cdc42 signaling. *Neuron* 50:401-414.
- Smotrys JE, Linder ME (2004) Palmitoylation of intracellular signaling proteins: regulation and function. *Annu Rev Biochem* 73:559-587.
- Sprong H, van der Sluijs P, van Meer G (2001) How proteins move lipids and lipids move proteins. *Nat Rev Mol Cell Biol* 2:504-513.
- Stoppini L, Buchs PA, Muller D (1991) A simple method for organotypic cultures of nervous tissue. *Journal of Neuroscience Methods* 37:173-182.
- Strathmann MP, Simon MI (1991) G alpha 12 and G alpha 13 subunits define a fourth class of G protein alpha subunits. *Proc Natl Acad Sci U S A* 88:5582-5586.

-
- Sunahara RK, Taussig R (2002) Isoforms of mammalian adenylyl cyclase: multiplicities of signaling. *Mol Interv* 2:168-184.
- Sutherland EW, Rall TW (1958) Fractionation and characterization of a cyclic adenine ribonucleotide formed by tissue particles. *J Biol Chem* 232:1077-1091.
- Svenningsson P, Tzavara ET, Qi H, Carruthers R, Witkin JM, Nomikos GG, Greengard P (2007) Biochemical and behavioral evidence for antidepressant-like effects of 5-HT₆ receptor stimulation. *J Neurosci* 27:4201-4209.
- Takanishi CL, Bykova EA, Cheng W, Zheng J (2006) GFP-based FRET analysis in live cells. *Brain Research* 1091:132-139.
- Tang C-M, Insel PA (2005) Genetic variation in G-protein-coupled receptors--consequences for G-protein-coupled receptors as drug targets. *Expert Opin Ther Targets* 9:1247-1265.
- Terrillon S, Bouvier M (2004) Roles of G-protein-coupled receptor dimerization. *EMBO Reports* 5:30-34.
- Thomas DR, Melotto S, Massagrande M, Gribble AD, Jeffrey P, Stevens AJ, Deeks NJ, Eddershaw PJ, Fenwick SH, Riley G, Stean T, Scott CM, Hill MJ, Middlemiss DN, Hagan JJ, Price GW, Forbes IT (2003) SB-656104-A, a novel selective 5-HT₇ receptor antagonist, modulates REM sleep in rats. *Br J Pharmacol* 139:705-714.
- Thompson MD, Burnham WM, Cole DEC (2005) The G protein-coupled receptors: pharmacogenetics and disease. *Crit Rev Clin Lab Sci* 42:311-392.
- Thompson SM (2000) Synaptic plasticity: Building memories to last. *Curr Biol* 10:R218-221.
- Toomre D, Steyer JA, Keller P, Almers W, Simons K (2000) Fusion of constitutive membrane traffic with the cell surface observed by evanescent wave microscopy. *J Cell Biol* 149:33-40.
- Towler DA, Gordon JI, Adams SP, Glaser L (1988) The biology and enzymology of eukaryotic protein acylation. *Annu Rev Biochem* 57:69-99.
- Turrigiano GG (2008) The self-tuning neuron: synaptic scaling of excitatory synapses. *Cell* 135:422-435.
- Turrigiano GG, Nelson SB (2004) Homeostatic plasticity in the developing nervous system. *Nature Reviews Neuroscience* 5:97-107.
- Turrigiano GG, Leslie KR, Desai NS, Rutherford LC, Nelson SB (1998) Activity-dependent scaling of quantal amplitude in neocortical neurons. *Nature* 391:892-896.
- Udo H, Jin I, Kim J-H, Li H-L, Youn T, Hawkins RD, Kandel ER, Bailey CH (2005) Serotonin-induced regulation of the actin network for learning-related synaptic growth requires Cdc42, N-WASP, and PAK in Aplysia sensory neurons. *Neuron* 45:887-901.
- Vanhoenacker P, Haegeman G, Leysen JE (2000) 5-HT₇ receptors: current knowledge and future prospects. *Trends Pharmacol Sci* 21:70-77.
- Veatch W, Stryer L (1977) The dimeric nature of the gramicidin A transmembrane channel: conductance and fluorescence energy transfer studies of hybrid channels. *J Mol Biol* 113:89-102.
- Waldhoer M, Fong J, Jones RM, Lunzer MM, Sharma SK, Kostenis E, Portoghese PS, Whistler JL (2005) A heterodimer-selective agonist shows in vivo relevance of G protein-coupled receptor dimers. *Proc Natl Acad Sci U S A* 102:9050-9055.

- Wallrabe H, Elangovan M, Burchard A, Periasamy A, Barroso M (2003) Confocal FRET microscopy to measure clustering of ligand-receptor complexes in endocytic membranes. *Biophys J* 85:559-571.
- Wedegaertner PB, Wilson PT, Bourne HR (1995) Lipid modifications of trimeric G proteins. *J Biol Chem* 270:503-506.
- Wesołowska A, Nikiforuk A (2007) Effects of the brain-penetrant and selective 5-HT₆ receptor antagonist SB-399885 in animal models of anxiety and depression. *Neuropharmacology* 52:1274-1283.
- Whitaker-Azmitia PM (2005) Behavioral and cellular consequences of increasing serotonergic activity during brain development: a role in autism? *Int J Dev Neurosci* 23:75-83.
- White JH, Wise A, Main MJ, Green A, Fraser NJ, Disney GH, Barnes AA, Emson P, Foord SM, Marshall FH (1998) Heterodimerization is required for the formation of a functional GABA(B) receptor. *Nature* 396:679-682.
- Whorton MR, Bokoch MP, Rasmussen SGF, Huang B, Zare RN, Kobilka B, Sunahara RK (2007) A monomeric G protein-coupled receptor isolated in a high-density lipoprotein particle efficiently activates its G protein. *Proc Natl Acad Sci U S A* 104:7682-7687.
- Wlodarczyk J, Woehler A, Kobe F, Ponimaskin E, Zeug A, Neher E (2008) Analysis of FRET signals in the presence of free donors and acceptors. *Biophys J* 94:986-1000.
- Woehler A, Ponimaskin EG (2009) G protein--mediated signaling: same receptor, multiple effectors. *Curr Mol Pharmacol* 2:237-248.
- Wood M, Chaubey M, Atkinson P, Thomas DR (2000) Antagonist activity of meta-chlorophenylpiperazine and partial agonist activity of 8-OH-DPAT at the 5-HT(7) receptor. *Eur J Pharmacol* 396:1-8.
- Yamamoto K, Tanimoto T, Kim S, Kikuchi A, Takai Y (1989) Small molecular weight GTP-binding proteins and signal transduction. *Clin Chim Acta* 185:347-355.
- Yamazaki J, Katoh H, Yamaguchi Y, Negishi M (2005) Two G12 family G proteins, G α 12 and G α 13, show different subcellular localization. *Biochem Biophys Res Commun* 332:782-786.
- Yu J-Z, Dave RH, Allen JA, Sarma T, Rasenick MM (2009) Cytosolic G α s acts as an intracellular messenger to increase microtubule dynamics and promote neurite outgrowth. *J Biol Chem* 284:10462-10472.
- Zal T, Gascoigne NRJ (2004) Using live FRET imaging to reveal early protein-protein interactions during T cell activation. *Curr Opin Immunol* 16:418-427.
- Zipkin ID, Kindt RM, Kenyon CJ (1997) Role of a new Rho family member in cell migration and axon guidance in *C. elegans*. *Cell* 90:883-894.
- Zucker RS, Regehr WG (2002) Short-term synaptic plasticity. *Annu Rev Physiol* 64:355-405.

7 APPENDIX

7.1 Abbreviations

5-CT	5-carboxamidotryptamine
5-HT	5-hydroxytryptamine
ACSF	artificial cerebrospinal fluid
BRET	bioluminescence resonance energy transfer
cAMP	3'-5'-cyclic adenosine monophosphate
Cdc42	small GTPase of the Rho-subfamily
CFP	cyan fluorescent protein
CNS	Central nervous system
DIV	days in vitro
DMEM	Dulbecco's modified Eagle's medium
DRM	detergent resistant membrane
EPSC	excitatory postsynaptic synaptic currents
FCS	fetal calf serum
fEPSP	field excitatory postsynaptic potential
FRAP	fluorescence recovery after photobleaching
FRET	Förster resonance energy transfer
GABA	gamma-aminobutyric acid
GDP	guanosine 5'-diphosphate
GFP	green fluorescent protein
GI	gastrointestinal
GIRK	G-protein-activated inwardly rectifying potassium channels
GPCRs	G-protein coupled receptors
GTP	guanosine-5'-triphosphate
IP	intraperitoneal
LP	long dendritic protrusions
LTP	long-term potentiation (LTP)
lux-FRET	linear unmixing of FRET spectral components
MAPK	mitogen-activated protein kinase
MEM	minimal essential medium

mGlu	metabotropic glutamate
mPSCs	miniature postsynaptic currents
Mut	mutant, i.e. acylation-deficient receptor
P	postnatal
PAGE	polyacrylamide gel electrophoresis
PCR	polymerase chain reaction
PLC	phospholipase C
PNS	peripheral nervous system
PPF	paired pulse facilitation
Rac	small GTPase of the Rho-subfamily
RhoA	small GTPase of the Rho-subfamily
RNA	ribonucleic acid
SDS	sodiumdodecylsulfate
SEM	standard error of the mean
SP	short dendritic protrusions
TEMED	tetraaminethylendiamine
TM	transmembrane
TX-100	Triton X-100
WT	wild-type
YFP	yellow fluorescent protein
PBS	phosphate buffered saline
PKA	protein kinase A
PMSF	phenylmethylsulphonyl fluoride

7.2 Curriculum vitae

Persönliche Angaben

Name: Eberhard Fritz Kobe
 Geburtsdatum / -ort: 06. Oktober 1971 / Dresden
 Staatsangehörigkeit: deutsch

Promotion

seit 2005 Doktorarbeit am Institut für Neuro- und Sinnesphysiologie der Georg August Universität Göttingen bei Professor E. Ponimaskin
“Molecular Mechanisms of Serotonergic Signaling: Role for the Neuronal Outgrowth and Receptor Oligomerization”

Studium

07/2005 Abschluss als Diplom-Biologe
 Titel der Diplomarbeit:
„Die p21-aktivierbare Kinase1 (PAK1) moduliert die Plasminogen-Aktivator-Inhibitor-1 Expression über den Hypoxie-induzierbaren Faktor-1”
 (experimenteller Teil an der TU Kaiserslautern)

1998 - 2005 Studiengangwechsel Diplom-Biologie
 Georg-August-Universität Göttingen

1996 - 1997 Wechsel an die University of Bristol (UK) im Studiengang Humanmedizin

1994 - 1995 Erasmus Austauschprogramm University of Bristol (UK)

1992 - 1996 Studiengang Humanmedizin an der Humboldt-Universität zu Berlin

Praktika

1999 - 2003 Max Bergmann Center für Biomaterialien Dresden,
 (regelmäßig mehrmonatig) Leibniz Institut für Polymerforschung Dresden

in den Semesterferien)

05/05 – 07/05 2002

Max Planck Institut für experimentelle Medizin
Göttingen bei Prof. Dr. Dr. H. Ehrenreich

Freiwilliges Soziales Jahr

1991 - 1992

Betreuung körperlich behinderter Menschen in
London (UK)

Zivildienst

1990 - 1991

Intensivtherapiestation der Medizinischen Akademie
„Carl Gustav Carus“ Dresden

Schulbildung

1990

Allgemeine Hochschulreife (Abitur)

1988 - 1990

Erweiterte Oberschule Dresden-Plauen

1978 - 1988

68. Polytechnische Oberschule Dresden

Publikationen

- 2008 Kobe F, Renner U, Woehler A, Wlodarczyk J, Papusheva E, Bao G, Zeug A, Richter DW, Neher E, Ponimaskin E
Stimulation- and palmitoylation-dependent oligomerization of serotonin 5-HT1A receptors
Biochim Biophys Acta 2008 1783:1503-1516.
 Ponimaskin E, Dityateva G, Ruonala MO, Fukata M, Fukata Y, Kobe F, Wouters FS, Delling M, Bredt DS, Schachner M, Dityatev A
Fibroblast growth factor-regulated palmitoylation of the neural cell adhesion molecule determines neuronal morphogenesis.
J Neurosci 28:8897-8907
- Salonikidis PS, Zeug A, Kobe F, Ponimaskin E, Richter DW
Quantitative Measurement of cAMP Concentration Using an Epac Based FRET-Sensor
Biophys J 95:5412-5423.
- Wlodarczyk J, Woehler A, Kobe F, Ponimaskin E, Zeug A, Neher E.
Analysis of FRET-signals in the presence of free donors and acceptors.
Biophys J 94:986-1000.
- 2006 Tron K, Samoylenko A, Musikowski G, Kobe F, Immenschuh F, Schaper F, Ramadori G, Kietzmann T.
Regulation of rat heme oxygenase-1 gene expression by interleukin-6.
J Hepatol. 2006 Jul;45(1):72-80
- 2005 Fritz Kobe
Die p21-aktivierbare Kinase1 (PAK1) moduliert die Plasminogen-Aktivator-Inhibitor-1 Expression über den Hypoxie-induzierbaren Faktor-1
 Diplomarbeit im Fachbereich Biochemie der Georg-August-Universität, Göttingen, 2005
- 2004 Oswald J, Jörgensen B, Pompe T, Kobe F, Salchert K, Bornhäuser M, Ehninger G, Werner C.
Comparison of flow cytometry and laser scanning cytometry for the analysis of CD34+hematopoietic stem cells.
Cytometry A. 2004 Feb;57(2):100-7.
- 2003 Pompe T, Kobe F, Salchert K, Jörgensen B, Oswald J, Werner C.
Fibronectin anchorage to polymer substrates controls the initial phase of endothelial cell adhesion.
J Biomed Mater Res A. 2003 Nov 1;67(2):647-57.

